T.C.
ISTANBUL GEDİK UNIVERSITY
INSTITUTE OF GRADUATE STUDIES

ANALIYIZING THE EFFECT OF RAIN ON THE STABILITY OF A SLOPE IN IRAQ

MASTER'S THESIS

Sarah Galib Faraj AL-ISAWI

Civil Engineering Department

Master in Civil Engineering English Program

FEBRUARY 2024
ISTANBUL

T.C.
ISTANBUL GEDİK UNIVERSITY
INSTITUTE OF GRADUATE STUDIES

ANALIYIZING THE EFFECT OF RAIN ON THE STABILITY OF A SLOPE IN IRAQ

MASTER'S THESIS

Sarah Galib Faraj Al-Isawi
(211291021)

Civil Engineering Department

Master in Civil Engineering English Program

Thesis Advisor: Assoc. Prof. Dr. Mücahit NAMLI

Istanbul 2024

T.C.

İSTANBUL GEDİK ÜNİVERSİTESİ

Lisansüstü Eğitim Enstitüsü Müdürlüğü

Jüri Tez Onay Formu

15/02/2024

LİSANSÜSTÜ EĞİTİM ENSTİTÜSÜ MÜDÜRLÜĞÜ

Bu çalışma 15/02/2024 tarihinde aşağıdaki jüri tarafından İnşaat Mühendisliği Anabilim Dalı, İnşaat Mühendisliği (Tezli Yüksek Lisans) Programı Yüksek Lisans Tezi olarak kabul edilmiştir.

TEZ JÜRİSİ

Doç. Dr. Mücahit NAMLI
Danışman
İstanbul Medeniyet Üniversitesi

Doç. Dr. Redvan GHASEMLOUNIA
Üye (İmza)
İstanbul Gedik Üniversitesi

Doç. Dr. Hakkı Oral ÖZHAN
Üye (İmza)
İstanbul Yeditepe Üniversitesi

DECLARATION

I, Sarah Galib Faraj Al-ISAWI, hereby certify that this thesis entitled "Analiyizing the Effect of Rain on the Stability of A Slope in Iraq" is my original thesis for the award of a Master's Degree in Civil Engineering at the Faculty of Engineering. I certify that this thesis or any part thereof has not been submitted and presented for any other degree or research thesis at any other university or institution. (15.02.2024).

Sarah Galib Faraj Al-ISAWI

DEDICATION

I want to take the opportunity to thank God first for everything. I would also like to thank and praise my father, mother, Siblings and my son (Natheer) for their patience and support. I would also like to thank everyone who supported me and all my gratitude.

PREFACE

In conclusion, I want to express my sincere appreciation and indebtedness to my father and my family for their unwavering support. I express gratitude towards my pals for their diligent efforts and steadfast support. I therefore appreciate those who have provided valuable information, advice, or direction at any study phase. I thank my supervisor, Assoc. Prof. Dr. Mücahit NAMLI, for his invaluable guidance and ongoing instructions. I extend my gratitude to the head of the university, the head of the department, the department itself, and the esteemed members of the deliberation committee.

February 2024 Sarah Galib Faraj Al-ISAWI

TABLE OF CONTENT

Page

ABBREVIATIONS

FEA	: Finite Element Analysis
FEM	: Finite Element Method
FOS	: Safety Factor
HSM	: Hardening Soil Model
MCM	: Mohr-Coulomb model
PLAXIS	: Plane Strain and Axial Symmetry
SRF	: Strength-Reduction Factor
2D	: Two-Dimensional

LIST OF SYMBOLS

ψ : Angle of Dilatancy
ϕ : Angle of İnternal Friction
c : Cohesion of Soil
γ : Bulk Unit Weight.
υ : Poisson's Ratio.
γ_{sat} : Saturated Unit Weight
γ_{dry} : Dry unit weight
E : Young's Modulus
k : Coefficient of Permeability
Ie : Target Elements Size
E_{50}^{ref} : Secant Stiffness in Standard Drained Triaxial Test
E_{oed}^{ref} : Tangent Stiffness for Primary Oedometer Loading
E_{ur}^{ref} : Unloading / reloading stiffness
M : Power for Stress-Level Dependency of Stiffness
τ : Shear Strength
hr : Hour

LIST OF TABLES

Page

LIST OF FIGURES

Page

ANALIYIZING THE EFFECT OF RAIN ON THE STABILITY OF A SLOPE IN IRAQ

ABSTRACT

Rainfall-induced slope collapses are a destructive global natural hazard that occurs annually during rainy seasons worldwide. Recently, there has been a significant escalation in the intensity of rainfall in Iraq, resulting in floods that have caused slope collapses. The rainfall infiltration causes a decrease in the soil's matric suction and shear strength, ultimately leading to the instability of roadway slopes. The intensity and duration of rainfall mainly cause soil slope stability concerns. The behavior of unsaturated soil varies based on the soil type in response to different rainfall events. This research uses the finite element technique (PLAXIS 2D 2020) for slope stability analysis to examine the impact of various rainfall features on slope in Iraq. The soil in this study was simulated using the Mohr-Coulomb model, and the Hardening Soil model was also applied, and the resulting results were compared. The slope was chosen located in Najaf Governorate in southern Iraq. Rainfall events were identified from 1979 to 2014 and at return periods of (2, 15, 100) years. Based on published statistical studies of rainfall data. The model was analyzed under the influence of rainfall at different intensities with a constant time (12,21,28) mm/hr and different periods and constant intensity. The models' results showed that the affected by rainfall, safety factor decreased clearly by (15%). The study found that rainfall intensity significantly reduced the safety factor. Rainfall for a specific period and with variable intensity led to deformations in the slope soil. In contrast, an upward movement happened for the entire slope when exposed to rain with different temporal intensities. To compare the behavior of Hardening Soil model for simulating rainfall with the behavior of Mohr-Coulomb model, rainfall was simulated for the slope by applying the Hardening Soil model. The convergence of the safety factor was similar between the Mohr-Coulomb model and the application of the Hardening Soil model when the impact of rainfall was not included. There is a decrease in the safety factor for both Mohr-Coulomb model and Hardening Soil model under the influence of rainfall. However, the decrease in the safety factor for Hardening Soil model is more significant. When Hardening Soil model is applied to the model, the safety factor decreases by 35% for a rain intensity of 12 mm/hr and by approximately the same percentage for a 21 mm/hr rain intensity. The safety factor decreased by (40%) for a 28 mm/hr rainfall intensity. The behavior of the Hardening Soil model in analyzing the effect of rainfall with different rain intensities on the deformations is logical, as it showed the occurrence of settlement and upward movements in the slope. It is recommended to use the Hardening Soil model (HSM) to study the effect of rainfall on the factor of safety and displacement in PLAXIS 2D software.

Keywords: *Slope, Rainfall, İnfiltration, Stability, Hardening Soil model, Mohr-Coulomb model, PLAXIS 2D, Finite Element Analysis.*

IRAK'TA YAĞMURUN EĞİMİN STABİLİTESİ ÜZERİNDEKİ ETKİSİNİN ANALİZİ

ÖZET

Yağış kaynaklı şev çökmeleri, dünya genelinde her yıl yağışlı mevsimlerde meydana gelen yıkıcı bir küresel doğal tehlikedir. Son zamanlarda, Irak'ta yağış yoğunluğunda önemli bir artış olmuş ve bu da şev çökmelerine neden olan sellere yol açmıştır. Yağış infiltrasyonu, toprağın matrik emme ve kayma mukavemetinde bir azalmaya neden olmakta ve sonuçta karayolu şevlerinin dengesizliğine yol açmaktadır. Yağış yoğunluğu ve süresi esas olarak toprak şev stabilitesi endişelerine neden olmaktadır. Doymamış zeminin davranışı, farklı yağış olaylarına yanıt olarak zemin türüne göre değişir. Bu araştırma, Irak'ta çeşitli yağış özelliklerinin şev üzerindeki etkisini incelemek amacıyla şev stabilite analizi için sonlu elemanlar tekniğini (PLAXIS 2D 2020) kullanmaktadır. Bu çalışmada zemin Mohr-Coulomb model ve Hardening soil model kullanılarak simüle edilmiş ve elde edilen sonuçlar karşılaştırılmıştır. Eğim, Irak'ın güneyindeki Necef Valiliği'nde seçilmiştir. Yağış olayları 1979'dan 2014'e kadar ve (2, 15, 100) yıllık dönüş periyotlarında belirlenmiştir. Yağış verilerinin yayınlanmış istatistiksel çalışmalarına dayanmaktadır. Model, sabit zamanlı (12,21,28) mm/saat ve farklı periyotlarda ve sabit yoğunlukta farklı şiddetlerdeki yağışların etkisi altında analiz edilmiştir. Modellerin sonuçları, yağıştan etkilenen güvenlik faktörünün (%15) oranında net bir şekilde azaldığını göstermiştir. Çalışma, yağış yoğunluğunun güvenlik faktörünü önemli ölçüde azalttığını ortaya koymuştur. Belirli bir süre boyunca ve değişken yoğunlukta yağan yağmur, yamaç toprağında deformasyonlara yol açmıştır. Buna karşılık, farklı zamansal yoğunluklarda yağmura maruz kaldığında tüm yamaç için yukarı doğru bir hareket meydana gelmiştir. Yağış simülasyonu için Hardening soil model davranışını Mohr-Coulomb model davranışıyla karşılaştırmak için, Hardening soil model uygulanarak şev için yağış simülasyonu yapılmıştır. Yağış etkisi dahil edilmediğinde güvenlik faktörünün yakınsaması Mohr-Coulomb model, ile Hardening soil model uygulanması arasında benzerlik göstermiştir. Yağış etkisi altında hem Mohr-Coulomb model, hem de Hardening soil model için güvenlik faktöründe bir düşüş söz konusudur. Ancak, Hardening soil model için güvenlik faktöründeki düşüş daha belirgindir. Hardening soil model modele uygulandığında, güvenlik faktörü 12 mm/saat yağmur şiddeti için %35 oranında ve 21 mm/saat yağmur şiddeti için yaklaşık aynı oranda azalmaktadır. Güvenlik faktörü 28 mm/saat yağış yoğunluğu için (%40) oranında azalmıştır. Hardening soil model, farklı yağmur şiddetlerine sahip yağışların deformasyonlar üzerindeki etkisini analiz etmedeki davranışı, şevde oturma ve yukarı doğru hareketlerin meydana geldiğini gösterdiği için mantıklıdır. PLAXIS 2D yazılımında yağışın güvenlik faktörü ve yer değiştirme üzerindeki etkisini incelemek için Hardening soil model (HSM) kullanılması tavsiye edilir.

Anahtar Kelimeler: *Şev, Yağış, İnfiltrasyon, Stabilite, Hardening soil model, Mohr-Coulomb modeli, PLAXIS 2D, Sonlu Elemanlar Analizi*

1. INTRODUCTION

1.1 Background

Slope instability is a prominent issue in various parts of Iraq. Climate change is expected to exacerbate this problem by increasing the occurrence and severity of severe weather phenomena, such as intense precipitation and inundation, which can trigger landslides and slope failures. Slope stability is a significant issue in Iraq, and climate change is anticipated to worsen. this problem. The outcomes of the study will provide valuable information for those responsible for making decisions to plan and implement measures to improve the resilience of infrastructure and communities in Iraq against the risks of slope failures caused by climate change.

Slope stability refers to the capacity of sloped surfaces to withstand sliding or collapsing without failure. Landslides are an inherent occurrence in nature. United Nations data from 2014 indicate that natural catastrophes have resulted in around 2 trillion USD in worldwide damages and have impacted over 4 billion people since 1994[1].

1.2 Research Justification

Landslides occurred due to the recent increase in rainfall intensity in Iraq, and there are few studies on this topic in Iraq.

1.3 Objective of research

The primary objective of this study is to assess the impacts of different rainfall intensities with the constant of time and different rainfall duration with the constant of intensities on a natural slope in Iraq by using the software PLAXIS 2D 2020.

1.4 Research Limitations

Geographical restriction: Simulating the impact of rainfall on a slope in Iraq

1.5 Research Methodology

The project's goals were achieved by the following methodology:

i. Site was chosen to conduct the study, a slope located in the Najaf Governorate, south of Iraq.

ii. PLAXIS 2D is the FE program that was adopted in this study, the program was verified by matching the results of the 2D program with the results of the selected model, verification was used to design and simulate the slope using the software PLAXIS 2D 2020, calculate the safety factor. The purpose was to verify that the model worked adequately.

iii. Calculated the FOS and displacement for the slope by PLAXIS 2D with Mohr Coulomb Model.

iv. Examined the effect of various quantities of rainfall intensity constant of time and different rainfall duration with the constant of intensities on the above results.

v. The impact of precipitation was replicated by using the Harding Soil model, and subsequently, the outcomes were compared with Mohr Coulomb Model.

vi. Comparison effect of rainfall on safety factor between coarse, very fine mesh and fine mesh by using Hardening Soil Model (HSM).

2. LITERATURE REVIEW

2.1 Introduction to Slope Stability

A slope is a ground level with one extremity or lateral side higher than the other end or side. Sliding occurs when a large amount of soil fails to hold together at the base of a slope. All of the soil in the area moves downward and outward due to the collapse. Slope collapse arises mainly as a result of gravity and seepage pressures inside the soil gravity and seepage pressures inside the soil [2].

Along with earthquakes and volcanoes, slope instability is considered one of the three most severe geological catastrophes. Slope failures may occur as a result of gravitational and seepage forces within the soil, as well as other precipitating factors including the slope's geometry, height, excess pore water pressure, and the slope's orientation. The deterioration of shear strength due to weathering and liquefaction. In addition, geological occurrences such as earthquakes and volcanic eruptions can cause slope failure [3] [4].

A slope collapse transpires rapidly on a inclination of at least 20 degrees, and there are frequently no warning indications. Typically, this failure is caused due to rain that affects a limited, localized area. Conversely, a landslip involves a bigger area, a slope angle of twenty or less degrees, and a slow or gradual movement. If the mass's strength, which prevents its collapse, is the same as or higher than the gravitational force that causes the failure, then the soil mass is in equilibrium [5].**Hata! Başvuru kaynağı bulunamadı.**Table 2.1 summary providing an explanation of the most common varieties of failure [4].

Table 2.1: Types of Slope Failure

	Definition	**Figures**
Fall	It is the separation of rock and soil particles that leads to their descent of a slope.	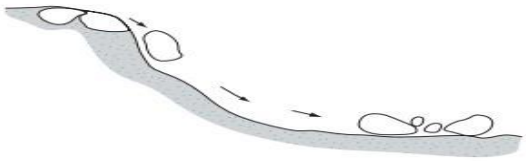 **Figure 2.1:** A Landslide of the "Fall" Type
Topple	The failure of a mass of soil or rock due to rotation. As the mass slides, it moves forward around a line below its center of mass.	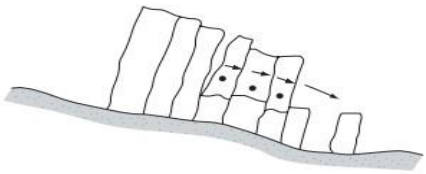 **Figure 2.2:** Toppling" Slope Failure
Slide	It's when a big part of the earth slides down a rippling surface.	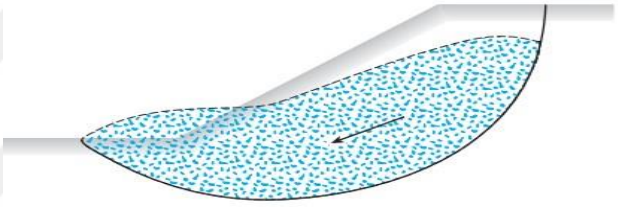 **Figure 2.3:** "Sliding" Failure of Slope
Spread	This failure type, a translational slide, occurs when clays or a heavy overburden give way to the horizontal displacement of water-bearing soil layers containing sand or silt.	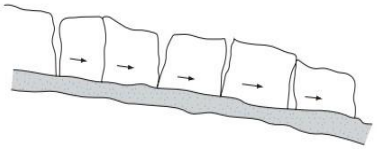 **Figure 2.4:** Spreading" Slope Failure
Flow	It looks like a thick liquid moving horizontally through the soil.	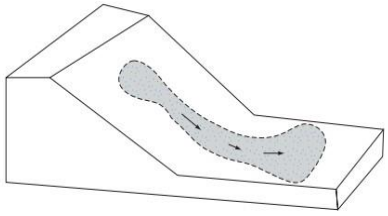 **Figure 2.5:** "Flowing" Slope Failure

Another significant form of slope failure is wedge failure. This is a failure mechanism that can be controlled by the structure that is typically observed on

competent rock inclines. Slopes are where wedge failures happen. They comprise intact rock slabs connected by unstable discontinuities such as intersections, beddings, defects, or shear zones. If discontinuities meet, how they are oriented, and whether they "daylight" emerges from the incline, decide if wedge failure will happen by moving across discontinuities as shown in **Hata! Başvuru kaynağı bulunamadı.** [6].

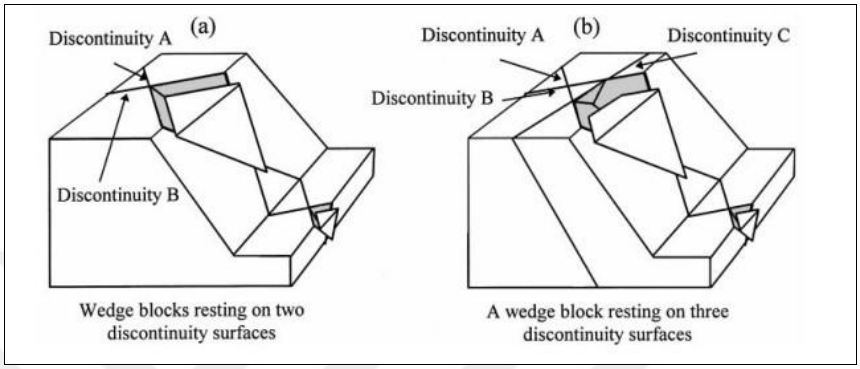

Figure 2.6: Classification of Wedge Failures

Source: (Kumsar et al., 2000)

Shallow and deep slides are two examples of failure mechanisms that might occur. A shallow failure is a failure that impacts shallow and superficial strata for the slope, generally due to erosion or flow caused by rainfall. The causes of profound failures penetrate a slope and surface at the subsurface level [7].

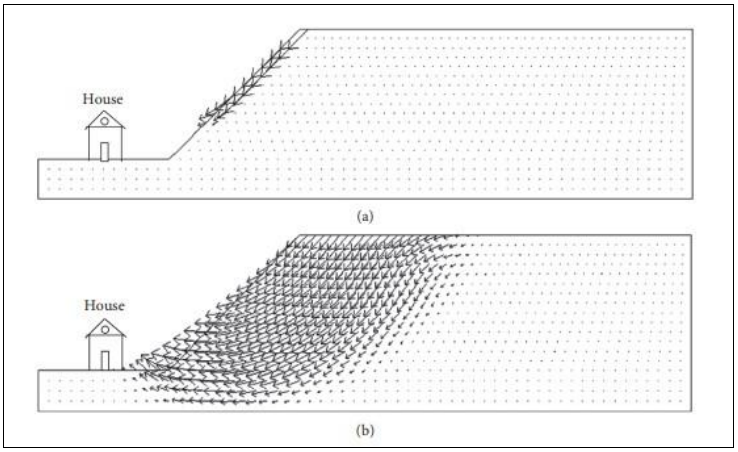

Figure 2.7: The Two Kinds of Soil Slope Mechanisms of Failure: (a) Shallow Slide and (b) Deep Slide

Source: (Li et al., 2019a).

Hata! Başvuru kaynağı bulunamadı. above shows the variation between failure consequences. While the consequences of failure might vary depending on the

location and the impact on human life and property, it is commonly observed that deep slides tend to result in more catastrophic outcomes compared to shallow slides[8][9].

Slope geometry, soil characteristics and behavior, shear strength, unit weight, rainfall intensity, hydraulic conductivity, degree of saturation, and even the existence of tension fractures or vegetation cover all have an impact on slope stability.

Despite extensive study on this topic over the years, several unknown slope collapses remain, and the causes of the geotechnical instability of a slope are not entirely understood [10] . Conducting a stability analysis of slopes is an essential element of engineering geotechnical[11] . Previously, analysis of slope stability was conducted manually using laborious and complex calculations. In stages, it has adjusted to more refined techniques that can be readily implemented using computer programs. This significant advancement has improved the accessibility and convenience of analysis of slope stability in geotechnical engineering for professionals, increasing their knowledge and skill on this field [12].

2.2 The Failure of a Slope as A Result of Rainfall

The greatest collapses in KwaZulu-Natal were identified as paleo-landslides by mapping and classification mass-movement deposits in the rugged terrain and precipitous slopes of the Drakensberg mountains and the main river basins. Thick deposits of colluvium sand developed from a bedrock of the Ordovician Natal Group made up the majority of these slopes [13] [14]. Another case is the Maya Place landslip, this took place in the same region and was underlain by the shale strata of the Pietermaritzburg Formation that sloped parallel to the hillslope [15] . Several catastrophic failures caused by the excessive rains in April 2019 are shown in **Hata! Başvuru kaynağı bulunamadı.**. Due to floods and slope failure, 32 lives were lost, and 42 were injured as a result of this rainstorm, even in the Durban area.

(a) (b)

Figure 2.8: a and b: showing a Selection of the Failures that Occurred During the Rains in April 2019

Source: (Floodlist, 2019).

Another case of catastrophic failures occurred in California, USA, because of the strong winds, snowfall, thunderstorms, and rain that fell on the area. Evacuation orders were issued for thousands of people; additionally, two deaths were due to the storm, which led to a landslide, as shown in **Hata! Başvuru kaynağı bulunamadı.** below.

Figure 2.9: Damage to Highway 1 in Monterey County, California, March 2023

Source: (Floodlist 2023)

A steep embankment made of soil that is wet collapsed in Kwazulu-Natal, which is yet another case of slope collapse caused by rains; the failing material was dumped 50m below, forcing the closure of a rail route. So, most landslides are localized, small-scale events triggered by intense rainfall mobilized by soil variability. Many studies have indicated that landslides are more common during the rainy season,

when they may cause significant damage to infrastructure and even human losses [16] [17] [18][19] [20] . Therefore, landslip hazard estimates need to consider the influence of precipitation on slope stability [21]. Slope failures caused by rainfall processes have significant implications for slope stability analyses. However, this area requires much more study. Slope soils are typically unsaturated, with saturation levels between 75% and 90%; hence, it is generally accepted that entering precipitation is the primary cause of landslides in unsaturated residual soils [15][16][17][18][19].

Soil not fully saturated with water contains three cases: solid, liquid, and air. It's important to remember that the soil porewater pressure is usually negative compared to pore-air pressure. The soil characteristics present at the site impact the overall slope stability concept [16].

How residual soils behave under shear stress has been shown to change significantly during periods of rainfall and wetness. Slope failure occurs when unsaturated soils become saturated, which causes the soil's structure to collapse and the pressure within its pores to rise [22][23].

Soil moisture is often classified as either saturated or unsaturated. The interplay between the water content of soil and soil features, such as saturation level and porewater pressure, establishes a distinction between the two conditions. The field of soil mechanics has significantly benefited from the insights provided by research into soil-water interactions. The highest soil layers frequently consist of unsaturated soil and have negative porewater pressure during the dry season. Matrix suction describes the negative pore water pressure that is thought to play a significant role in soils' shear strength and, by extension, slope stability. Several research studies have been done on simulating the effect of rain and related processes on the stability of natural slopes using a computer program called a rainfall simulator. It was hypothesized that precipitation seeped into a slope of unsaturated soil would weaken the slope's stability by reducing the matric suction inside the soil and, in turn, the slope's shear strength. In contrast, more extensive total runoff is more affected by precipitation than infiltration, concluding that less total rainfall might cause infiltration. The study concluded that a comprehensive evaluation of rainfall-induced slope collapse must account for every procedure associated with rainfall, including porewater pressure, infiltration, and runoff [24][25][26].

2.3 Saturated and Unsaturated Soil

Saturation of soil occurs when the interstitial spaces between particles are completely full with water. Soil is interpreted as unsaturated when a certain amount of the empty area is occupied by air. Saturated soil mechanics principles are applicable when the soil's degree of saturation exceeds 85%. Unsaturated soil mechanics principles are used when the degree of saturation is below 85%. [27].

In soil mechanics concepts, the phrase "water table" is used to denote the level at which water saturates the soil. Soil behavior under the water table is controlled by the effective stress principle (σ- u_w) however the unsaturated soil over the water table is controlled by two separate stress items : the net normal stress (σ- u_a) and matric suction ($u_a - u_w$) [28].

While saturated soil has a positive pore-water pressure, unsaturated soil is characterized by negative pore-water pressure, often known as "suction".

Due to variations in pore-water pressures, the stresses experienced by various soil zones also vary. The diagram shown below illustrates the distinction:

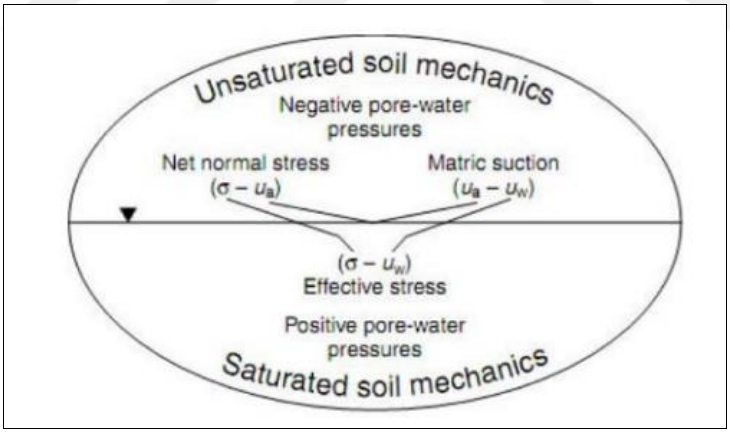

Figure 2.10: An Illustrative Tool for the Whole Realm of Soil Mechanics

Source: (D.G. Fredlund, 1996).

2.4 Shear Strength of Unsaturated Soil

The shear strength of soil is the highest level of shear stress that the soil can endure[29].

The Mohr-Coulomb failure criteria and the concept of effective stress may be used for explain the shear strength of saturated soil [30], using the formula in Equation (2.1).

$$\tau_f = c' + (\sigma - u_w) tan\, \phi' \quad (0.1)$$

Where, τ_f : shear stress on the plane of failure

Ć : effective cohesion

$\sigma - u_w$: Normal failure stress on the failure plane

σ : The total normal stress acting on the failure plane at the point of failure.

u_w : failure pore water pressure

ϕ': internal friction effective angle.

Figure 2.11 illustrates the failure envelope, which is defined by Equation (2.1).

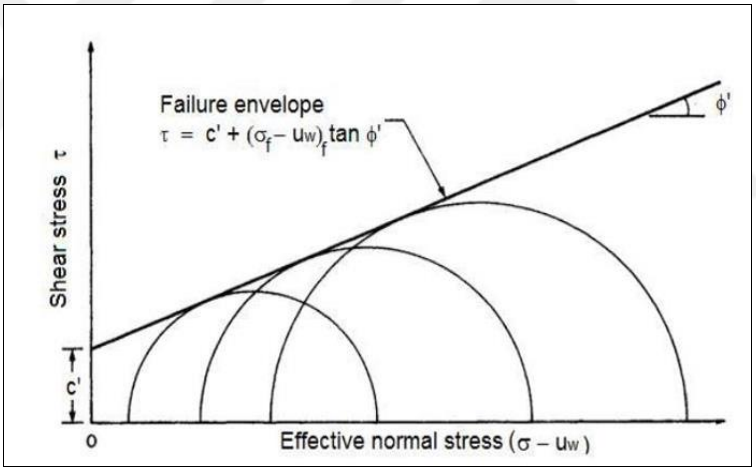

Figure 2.11: Mohr-Coulomb Saturated Soil Failure Envelope

Source: (Terzaghi, et. al., 1996)

Net normal stress $(\sigma - u_a)$ and matric suction $(u_a - u_w)$ are two independent stress-state variables that Fredlund and Rahardjo suggested as an equation to explain the shear strength of unsaturated soils [31], equation (2.2) expresses the shear strength using these variables:

$$\tau_f = c' + (\sigma - u_a) tan\, \phi' + (u_a - u_w) tan \phi^b \quad (0.2)$$

Where:

τ : failure-related shear stress plane

Ć: Intersection of the extended Mohr-Coulomb failure criterion

$(\sigma - u_a)$: typical failure plane stress at failure

u_a: air pressure on the failure plan when it fails

ϕ': is the angle of internal friction that goes with the variable for net normal stress.

$(u_a - u_w)$: The matric suction at the failure plane during failure

ϕb : The angle represents the increase in shear strength relative to matric suction.

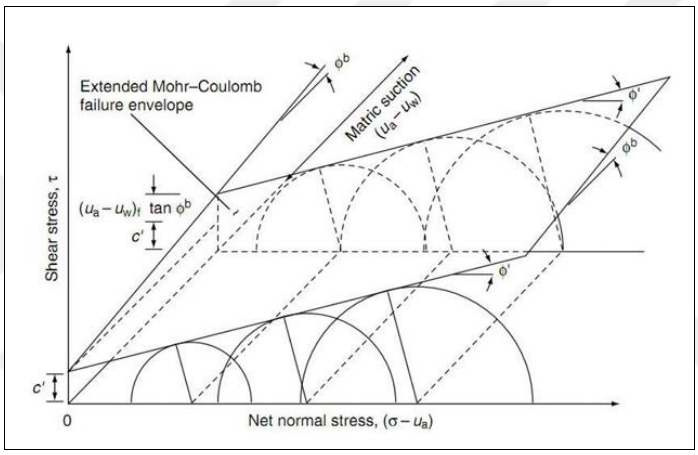

Figure 2.12: Graphically Illustrates the Expansion of the Mohr- Coulomb Failure Envelope for Unsaturated Soil

Source: (Fredlund and Rahardjo, 1993)

ϕ^b equivalent to ϕ' when the capillary zone of the soil is saturated however, the pore water pressure is under tension. ϕ^bexhibits a direct relationship with the degree of saturation, indicating that ϕ^b decreases as the soil becomes less saturated [32]. Once all empty spaces are filled with water, the values of ua, uw, and u will become equal. This will transition the state from unsaturated to saturated, and Equation 2.2 will be transformed into Equation 2.1.

2.5 Methods of Slope Stability Analysis

The three most used approaches to analyzing slope stability are limit equilibrium, finite element, and probabilistic methods. The traditional limit equilibrium approach is widely used by geotechnical engineers (LEM) [33] . The finite element method

(FEM) is an advanced method that allows engineering professionals to accurately evaluate slopes in two or three dimensions while also considering variations in soil properties. The probabilistic technique is used to quantify unknown elements and is primarily employed in formulating slope reliability indices [34].

2.5.1 Finite element method (FEM)

Finite element technique solves numerically. The flow zone is divided into discrete components using a grid pattern (which need not be rectangular) to generate N equations with N unknowns. Boundary conditions (heads and flow rates) and material parameters (such as permeability) are provided for each element. The finite element strategy is better for more complicated permeability situations than the finite difference method [35].

2.5.1.1 Finite element formulation

The idea behind the finite element approach is to estimate the unknown function of the field variable by dividing the issue region into subdomains (Finite Elements) linked at their common nodal points. Each element's approximate solution is represented as a continuous function, like the one below:

$$H=\sum_{e=1}^{noe}[N_i^e]\{H_i^e\} \quad (0.3)$$

Where H_i^e= nodal value of (H) for i^{th} node in element (e), noe = total number of elements and N_i^e = shape function of element (e).

The problem's approximate answer may be formulated in a variety of ways. Adjusting the phreatic surface's position and the mesh size of the finite elements iteratively until the appropriate degree of convergence for the nodal head H is reached is necessary for solving the seepage issue with a phreatic surface. All iterative approaches begin with an educated estimate for the unknown phreatic surface and ultimately solve by repeatedly solving the system of equations using recurrence relations to update the previous values until the solution converges to the actual values within a specified error bound [36].

2.5.1.2 FEM advantages

The FEM has become more popular for application in slope stability analysis as technology has progressed. There are some advantages to the FEM: The analysis can

be done relatively rapidly. It's a straightforward method that can analyze soil collapse all the way to the FOS. It allows for a variety of slope issues and geometries. The zone of the slope where the driving forces are more potent than the resisting forces is where the collapse takes place. Therefore, there is no need to make any guesses about the position or direction of the slip surface models, and they can determine slope deformation, stresses, and pore pressures[37].

2.5.1.3 FEM disadvantages

Although the finite element method is regarded as a helpful and dependable methodology for evaluating slope stability, analyzing deformations, and addressing other geotechnical issues. It is not as common as using usual limit equilibrium procedures [38][39].Theoretically, traditional LEM is easier to employ due to its fast and somewhat precise FOS calculations, and practically, Traditional LEM Software is more readily available than finite element method (FEM) software. It takes a lot of time and complicated calculations and theory to conduct assessments using finite element models, and many input parameters need to be obtained [12].

2.5.1.4 Calculating safety factor using FEM

The shear strength reduction technique is added to FEM to determine FOS. Therefore, the factored parameters of shear strength $\boldsymbol{C'f}$ & $\boldsymbol{\theta' f}$ are given by:

$$f' = \frac{c'}{SRF} \tag{2.4}$$

$$\theta f' = arctan\left(\frac{tan\theta'}{SFR}\right) \tag{0.4}$$

SRF: Strength reduction factor

SRF that is acceptable for both terms are determined via a methodical iterative process. At the point of first failure, the SRF and FoS are equal. $FoS = SRF$ [40].

2.5.2 Limit equilibrium method (LEM)

The LEM requires the plastic Mohr-Coulomb criterion when a combination of the maximal normal and shear stresses causes the material's failure. The LEM determines needed slope geometry and soil properties, then calculates the slope's stability using the Mohr-Coulomb criterion by doing a comparative analysis of the causes leading to failure and the forces that resist failure. During this process, the

equations of static equilibrium are applied to calculate the FOS. " The main idea is that something fails when a mass or block moves along a slip surface''. To determine the proper Factor of Safety (FOS), it is necessary to assume many slip surfaces to determine the crucial slip surface [41] [42][43].

The LEM requires the assumption of the following: the soil shows Mohr-Coulomb behavior; for all concerned soils, the factor of safety (FOS) for the cohesive strength component and the frictional strength component exhibit similarities; each object on the slide surface contains a similar FOS and assuming inter-slice forces, the problem is considered determinate[44].

2.5.2.1 LEM advantages

The LEM, or the Limit Equilibrium Method, presents several advantages when analyzing slope stability. Firstly, it is a simplistic strategy that is easy to understand and apply. Moreover, it requires minimal information about the soil characteristics and slope geometry, which makes it a cost-effective approach. One of the critical aspects of using LEM is to design an optimum slope that is based on the calculated Factor of Safety (FOS), which should prevent any movement along the slide surface and with its many advantages, the LEM can prove to be an effective tool in the field of geotechnical engineering [45].

2.5.2.2 LEM Limitations

The Limit Equilibrium Method (LEM) has some disadvantages. Firstly, numerical inconsistencies can lead to inaccurate results. Secondly, the same analysis technique is applied to all scenarios, including newly constructed embankments, recent excavations, and existing natural slopes. This approach restricts the method's applicability to specific slope conditions. Additionally, the stress-strain is not taken into account by the LEM behavior for the material, but it may impact the precision of the analysis. Moreover, effective use of the LEM requires a comprehensive knowledge of the concepts behind slope stability and geotechnical engineering, including the orientation of the slide surface. Lastly, the LEM cannot represent the surface's gradual breakdown and deformation without making assumptions about the surface's behavior, which may impact the accuracy of results. Despite these limitations, the LEM remains a valuable equipment in analysis of slope stability, but

it is crucial to recognize its capabilities and limitations before using it in any scenario[46].

2.5.2.3 Calculating factor of safety using LEM

The Factor of Safety (FOS) is a numerical measure of slope stability. A calculated FOS value equal to 1 represents the forces on the slope being in equilibrium. This means that the resisting forces inside the slope contribute to its stability and are balanced with the driving forces that make the slope unstable. A determined factor of safety (FOS) number beyond 1.0 indicates that the slope is stable under the specified circumstances, with resisting forces surpassing driving forces. Conversely, a FOS value below 1.0 signifies slope instability, where driving forces outweigh resisting forces.[47].

FOS is the amount the soil's ultimate shear strength has to be decreased for failure to occur [48] . As mentioned by Duncan and Wright (2005), The most common explanation of FOS in terms of slope stability is as follows:

$$FOS=\frac{shear\ strength\ of\ the\ soil}{shear\ stres\ required\ for\ equilibrium}=\frac{s}{\tau} \quad (0.5)$$

2.5.3 Method of slices

This Procedure for analyzing stability is predicated on the friction block working on an inclination level. The same friction principles govern stability for a piece or block of soil one unit wide or more above a slippery surface. Still, soil cohesion and water pressure also play a role in determining the effective stresses [49].

The safety factor is calculated using the slicing technique, which assumes a circular slip surface with radius R. Several slices that are vertical and have a width of b and a height of h are cut from the soil mass located above the arc **Hata! Başvuru kaynağı bulunamadı.**. Each slice's base is considered a linear line, leaning at an angle so that the data may be shown and analyzed quickly. It is believed that the total body, containing all of its components, rotates clockwise around the center of the circle O. This requires the presence of forces between the slices, called interslice forces [49].

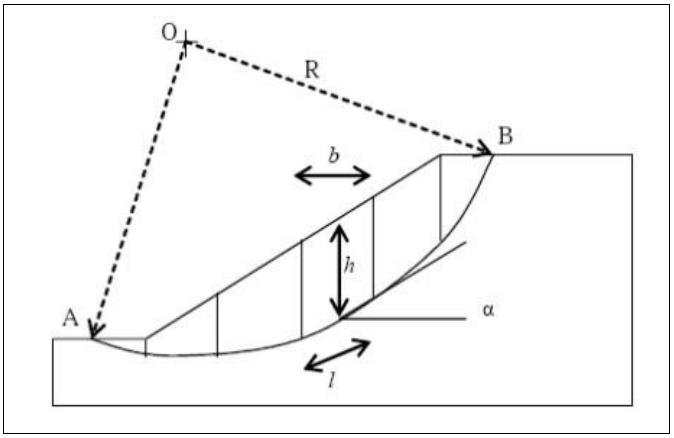

Figure 2.13: Slip Surface That Is Circular with A Radius of R and A Center at O Has Its Endpoints on the Ground at a and b

Source: (Joanne et al. 2008)

The forces influencing a slice **Hata! Başvuru kaynağı bulunamadı.** are:

- $W = bh\gamma$, where γ: the bulk unit weight of the soil, which is the formula for the total weight of the slice.
- Every slice creates a shear stress next to its foundation, $S = w\sin\propto$
- the overall force that is usually acting on the foundation, $N = \sigma l$
- the overall force that is equal to normal levels of stress, the normal force that is effective

$N' = \sigma' l$, and the force of water $U = ul$ where u is the pore pressure of water.

- The force of shear τl.
- The forces between slices are accounted for by normal E1 and E2 overall and tangential shear forces X1 and X2 [49].

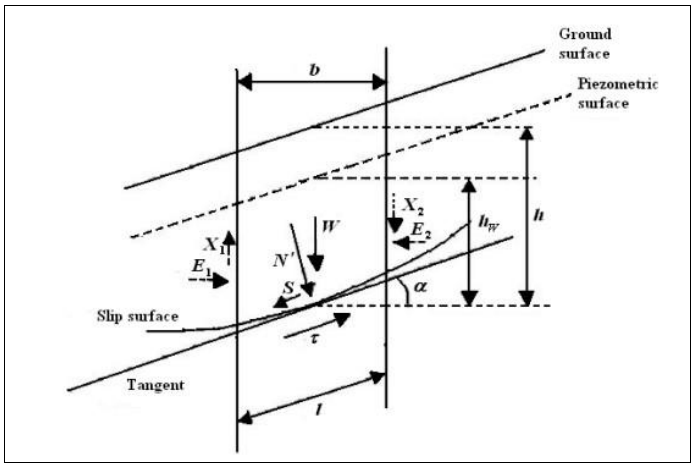

Figure 2.14: Forces Acting on a Slice

Source: (Joanne et al. 2008)

Using the Mohr-Coulomb relation for strength, which : $\tau = c' + \sigma_n' tan\ \phi'$ where τ : possible shear stress, c' = effective cohesion, σ' = effective normal stress [49] .On the shear level and ϕ' = the slip surface's effective angle of friction. One possible form of the new equation is:

$$FoS = \frac{c' l + N' tan\theta'}{W sin\alpha} \quad (0.6)$$

2.5.3.1 Ordinary or fellenius method

This technique disregards all interslice forces and fails to achieve equilibrium of forces for the side mass and Particular individual slices. Even though this is among the most basic. Procedures applying the slices method. The water surface and the slide surface are parallel, i.e., $(X2 - X1)\ cos\ \alpha - (E2 - E1)\ sin\ \alpha = 0$. When a combination of high base angles and high water pressures is applied to the slice, notable errors occur [49] (Joanne et al. 2008).

$$FoS = \frac{\sum [c' l + (W cos\alpha - ul)\ tan\varphi']}{\sum W\ sin\alpha} \quad (0.7)$$

2.5.3.2 Bishop method

Equal and opposite tangential interslice forces exist $(X1 = X2)$, whereas regular forces between slices are unequal $(E1 > E2)$. The magnitude of a factor of safety appears on all sides of the statement; therefore, an approximate value for the factor of safety it has to be selected in the direction of the right to calculate the value of the factor of safety in the direction of the left. During a series of iterations, getting closer to the actual value of the factor of safety is achieved [49][50].

$$FOS = \frac{\sum \left[\frac{(c' b + (W - ub) tan\varphi') sec\alpha}{(1 + (1/FoS_m) tan\varphi' tan\alpha)} \right]}{\sum W sin\alpha} \quad (0.8)$$

2.5.3.3 Janbu method

Similar to Bishop except that the equation is expressed in terms of horizontal force equilibrium and a compensation factor (f_0 = 1.05) is added. Moreover, Janbu assumes zero shear stresses between adjacent slices, minimizing the number of variables to $(4n - 1)$, where n is the amount of slices [51] .

$$FoS = \frac{\sum \left[\frac{(c' b + (W - ub) tan\varphi') sec\alpha}{\left(1 + \left(1/Fos_f\right) tan\varphi' tan\alpha\right) cos\alpha} \right]}{\sum W tan\ \alpha} x f_o \quad (0.9)$$

2.5.3.4 Method by morgenstern-price

Morgenstern and Price proposed a method comparable to Spencer's method, with the assumption that the inclination of the interslice resultant force varies according to a portion of an arbitrary function. This extra portion of a chosen function introduces a new unknown, leaving 4n unknowns and 4n equations, where n is the number of slices [52].

2.5.4 Response surface methods (RSM)

There are a variety of approaches of doing experiments using computers. Sampling methods belong to the first category. This category includes the likes of the Monte Carlo technique, the Latin Hypercube, and the importance sampling. To determine output characteristics, these strategies include drawing samples from distributions of parameters and then using computer analysis (or doing physical tests). When the event of interest has a low probability, he says, multiple simulations may be necessary. The second set of techniques is called "response surface methods," including spatial methods, reliability methods, and the traditional response surface approach. Using fewer computational/physical operations to probe the response space is a benefit shared by all response surface approaches. To explain and assess challenges when several variables impact response of interest, and the goal is to design, refine, and improve related processes, response surface methodology (RSM) has been developed [53] [54].

To effectively describe all potential points in a design space with a small number of points, the design of experiments and response surface methods (RSM) are pretty helpful. Although several designs have been presented, they all vary concerning the points picked to represent the whole Factorial set (the outputs resulting from combining all input parameters at all possible stages). Any design cannot achieve a perfect fit unless it considers every potential variable. The design will limit the model's shape that may be installed. When fitting polynomials, additional data points allow for a higher order model to be used. The "aliasing" or mingling of higher order effects is a major drawback of response surface technique models. Designs with a few things could be used to match surfaces with more orders, but this should be done with caution since the more prominent effects are going to be confused, or aliased,

with additional impacts, making it difficult to determine what the "true" impact is[54].

First, let's consider what a response surface model looks like. In functional terms, a response surface is a way to translate multiple inputs to one output characteristic. Here it takes the form of a polynomial function.

$$z = Ax + By + Cxy + Dx^2 + \cdots + \varepsilon \quad (0.10)$$

Where in this case:

z : feature of output of interest

x & y : input parameters

ε : error term.

A, B, C, D : regression coefficients, determined using the least squares technique.

The number of input parameters may be unlimited; here only two are considered because visualization is easier. Order of the model is determined by the number of points used to "train" it. Typically, model properties of interest are those that characterize model fit quality, contribution of an individual variable to total model variance, parameter aliasing properties (how much one parameter gets "mixed up" with other parameters), and model resolution. When performing response surface analysis, it is customary to use normalized or "coded" input parameter values. Also, if power transformations of the model output feature result in a better fit, they are commonly employed [54].

2.6 Previous Studies

Slope stability failure is a severe issue on both natural and artificial slopes. It may result in landslides, rockfalls, and other slope instability scenarios that cause property damage, fatalities, and environmental harm. Over the years, extensive research has been done to comprehend the mechanisms underlying slope failure and create efficient defenses against it. Numerous aspects of slope stability have been studied, such as soil characteristics, slope geometry, groundwater conditions, and environmental factors like seismic activity and rainfall. This research has shed important light on the origins and effects of slope instability, inspiring the creation of

cutting-edge techniques for risk assessment and stabilizing slopes. The main conclusions of earlier research on will be summed up in this introduction:

Wen Nie and colleagues (2017) compared various models for evaluating slope stability over time in their investigation. The study concluded that the dynamic Bayesian network (DBN) method offers more accurate slope stability assessments over time than the deterministic model, although it lacks in conveying physical meaning. In contrast, despite its stronger physical interpretation, the deterministic model exhibits a relatively lower estimation capability due to parameter uncertainties. Meanwhile, the logistic regression model demonstrated the highest accuracy, contingent on the number of statistical samples used; however, it falls short in conveying physical meaning compared to the DBN and deterministic models. The study posits that the DBN method holds promise for evaluating slope stability, particularly when integrated with actual monitoring data. Simultaneously, the deterministic model offers a more profound understanding of the physical processes involved. Nonetheless, the research underscores the need for further investigation to overcome the limitations inherent in each method and enhance their utility in assessing slope stability [55].

In this research, demonstrate the application of ANSYS 11.0 for modeling and analyzing a levee, focusing specifically on seepage and slope stability. The study addresses the critical issue of how seepage forces, which intensify during flooding events, can contribute to the failure of levees. To analyze this hydraulic challenge, the study employs ANSYS/THERMAL. This choice is informed by the recognized analogy between the mechanisms of seepage and heat diffusion, allowing for a more nuanced understanding of the hydraulic problems associated with levee integrity. The analysis of slope stability is conducted with the Strength Reduction Finite Element Method. The findings demonstrate that ANSYS/APDL is a very effective instrument for analyzing seepage and slope stability. The safety factors for cohesionless soil under all situations with a slope of 1:1 is found to be much less than one. Similarly, with a slope of 1:1.5, the safety factor is less than the needed value of 1.2. This is also seen in sandy clay soil under high and low flood conditions for a slope of 1:1. The safety factor for slope stability significantly falls when seismic force is applied to the segment, particularly for a 1:1 slope. A clay core may effectively reduce pore water pressures and maintain sufficient slope stability in the dam part. This study

highlights the importance of proper modeling and analysis of levee structures for seepage and slope stability under different flood and soil conditions [56]

D. Bhattacharjee's et al, 2019 study found that slope instability is caused by rapid loss of matric suction, causing safety factors to fall below 1.0. To address this, the researchers suggested using dual-function hybrid geosynthetics as reinforcement and drainage aids. The study found that these materials-maintained soil suction after rainfall events and improved stability, likely due to their efficient dispersion of excess pore water pressure and reinforcement properties. The study used the finite-element software SEEP/W to conduct hydro-mechanical infiltration analysis. The resulting pore water pressure values collected amidst rainfall were then integrated into the limit equilibrium-based program SLOPE/W to monitor the factors of safety [57].

Lindung Zalbuin Mase's 2020 study examined the environmental impact of rising water levels in the Semarang Segment of the Muara Bangkahulu Sub-watershed in Bengkulu City, Indonesia. The study found widespread erosion and sedimentation, highlighting the need for water conservation measures to mitigate flood inundation risks. The study also highlighted the impact of rising water levels on slope stability, particularly in residential zones. The research recommends the implementation of slope protection strategies and water conservation practices to mitigate potential slope failures. The study provides valuable insights for stakeholders, emphasizing the need to anticipate and prepare for future effects of extreme weather variations in the region [58].

Hsin-Fu Yeh and Yi-Jin Tsai's 2018 study examined the impact of climate change on rainfall patterns and slope stability in the Zengwen reservoir catchment area. They analyzed daily rainfall data from 1990 to 2016, using the Mann-Kendall test and Theil-Sen estimator. The results showed a significant increase in rainfall intensity, with projections suggesting that by 2050, the region could surpass the limit for prolonged extreme events. The study also found that increased rainfall intensity reduced slope safety factors, increasing the risk of slope instability and related disasters. The study recommends slope protection measures, such as improving drainage systems, to counteract future rainfall intensity trends. However, the study's trend analyses were not conclusive, highlighting the need for more comprehensive hydrological analysis [59].

Soumia Merat and her team conducted a study in 2018 to assess the impact of rainfall on slope stability in a natural setting. They used the PLAXIS2D software to analyze multiple variables, including rainfall intensity, duration, slope geometry, soil properties, and hydraulic conductivity. The study found that slopes with superior soil qualities generally maintained stability during rainfall events. However, the safety factor decreased and total displacement increased. Steeper and higher slopes were more prone to failure under these conditions. The study also found that slope response to rainfall is influenced by soil permeability. Lower permeability soils showed a delayed reaction to rainfall, while highly permeable slopes exhibited quicker infiltration and a rapid onset of failure. The study underscores the importance of incorporating climatic factors in geotechnical evaluations [60] .

This research investigates the influence of both the height and angle of slopes on the stability of loose granular soil slopes, using the finite element method and the non-linear hardening soil model. Twelve numerical analyses are conducted, and surcharge load is also examined. Results show that slope height and slope angle significantly affect the safety factor of the slope, with circular failure surfaces classified as face slope failure. Increasing slope height and slope angle decreases the safety factor, and curves and charts are proposed for easy estimation. The study also provides a simulation method for analyzing rainfall-induced rock weakening, considering water infiltration and fractured rock mass properties [61].

A study in Yunnan, China, aimed to understand the stability and failure mechanisms of a red bed slope, particularly in the context of rainfall-induced geological hazards. Researchers used GeoStudio software to create a numerical model based on observations of a small-scale landslide along the XiaoMo highway. Historical rainfall data from Mengla County was used to analyze seepage variations and assess slope stability during the rainy season. Key findings revealed that variation in pore water pressure was primarily concentrated in shallower regions during rainfall periods. Cracks significantly impacted the slope's stability, acting as conduits for rainwater infiltration. The study emphasizes the need for careful consideration of these aspects in geotechnical engineering and hazard mitigation strategies[62].

Jin Qian and colleagues conducted a 2021 study on the impact of rainfall on slope stability. They identified Qianfeng-type rainfall as having the lowest safety factor, typically occurring towards the end of summer. The study also found that pore water

pressure within the slope increased in response to rainfall. The impact of rainfall intensity and permeability coefficient on slope stability was more complex than a linear relationship of addition and subtraction. The study found that the direct effects and interactions between factors had a relatively low impact on slope stability when considered individually. Understanding these relationships can help engineers and geologists develop effective measures for slope stabilization and hazard mitigation [63] .

In research conducted in 2022, Jeffery Nazrien and his colleagues investigated the influence of intense precipitation on the stability of slopes in the Sg Langat area of Malaysia. The study used historical precipitation data, slope attributes, and flow boundary conditions to investigate the impact of intense rainfall episodes on slope dynamics. The investigation revealed that the slopes in all analyzed channels exhibited instability as a consequence of substantial fluctuations in negative porewater pressure, leading to a decrease in soil strength and subsequent slope collapse. The research also found that the configuration of slopes and the intensity of rainfall were factors that influenced the stability of slopes. Utilizing numerical modeling, the assessment of slope stability was conducted with precision, particularly in the face of intense rainfall events. The results have significant implications for forecasting the possible consequences of intense precipitation on the stability of slopes, as well as for mitigating accidents and tragedies [64] .

Tamara and her colleagues conducted a 2022 study on a landslide in Slovenia caused by heavy rain in 2021. They found that net water penetration is crucial for slope stability and suggested strategies to decrease it, such as selective planting and controlling runoff from surfaces. The study also highlighted the importance of water permeability and groundwater flow on slope stability. The research suggests that future climate change impacts should be considered, requiring a comprehensive study to accurately measure water penetration rates and consider land-climate interactions. It also recommends further research on the impact of higher soil water content on soil cohesiveness. The findings offer insights for controlling slope stability in response to climate changes [65] .

Research conducted in the Shengzhou region, which is close to the Hangzhou-Taizhou high-speed railway, revealed unfavorable hydrophysical characteristics and susceptibility to cracking when subjected to alternating dry and wet circumstances.

The research also used a high-speed railway slope fake rainfall simulation system to examine variations in soil slope characteristics. The research suggests implementing adequate safeguards for diatomaceous earth slopes to ensure safety during the building of high-speed railways. Subsequent investigations should include a three-year observation of diatomite slopes and the execution of on-site fissure diatomite strength assessments [66] .

The study investigates real-time slope stability in Meghalaya, India, prone to monsoon landslides. It uses field data and finite element analysis to understand rainfall-induced slope collapse. Results show significant displacement during monsoons, groundwater table changes, and unsaturated soil characteristics impact slope stability. Tensiometer placement helps explain matric suction, which causes slope instability. The study also provides a local warning system for landslide mitigation [67].

3. FINITE ELEMENT MODELING

3.1 Introduction

The following chapter includes two major components. Part, one includes a present the program and finite element model. The last part explains the verification of the program by finding convergence between PLAXIS 2D result and for the result 2D Finite Element Method for the slope in a study (Z. Alsharifi, 2021).

3.2 PLAXIS 2D Program

PLAXIS 2D is a solid and easy-to-use software for analyzing deformation and stability in geotechnical engineering and rock mechanics using finite element methods. Top engineering businesses and institutes in the civil engineering and geotechnical engineering sectors worldwide utilize it. The applications include excavation, embankment construction, foundation work, tunneling, mining, and reservoir geo-mechanics. PLAXIS is equipped with a wide array of sophisticated features that may be used to simulate various geotechnical issues. These features are all included in a single integrated software package[68]. Because the software was made to deal with geotechnical engineering issues, there are standard ways to set up common geotechnical issues like the slopes that were looked at in this study. Based on the PLAXIS manuals[69].

3.3 Finite Element Formulation

When it comes to studying complex engineering issues, the Finite Element Method (FEM) is a strong instrument. One approximation method that estimates the distribution of stresses and strains throughout a continuum is the finite element method (FEM), which is based on the concept of virtual work. This research uses PLAXIS 2D (2020), a geotechnical application-specific two-dimensional finite element software. The soil's behavior is simulated using sophisticated constitutive models detailed in the following sections:

3.3.1 Finite elements and nodes

The PLAXIS tool has many elements and nodes that can be used to solve geotechnical problems correctly; the following sections include the classifications used in the present study.

3.3.1.1 Soil element

PLAXIS 2D includes two separate elements for soil modeling. These elements are triangular and feature 6 and 15 nodes, respectively. Additionally, they have 3 and 12 stress points, respectively. As shown in the **Hata! Başvuru kaynağı bulunamadı.**. In this study, 15 nodes were used.

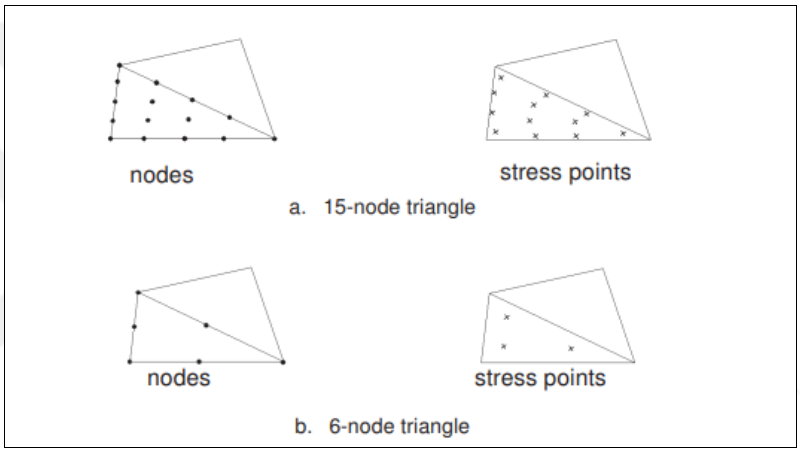

Figure 3.1: Soil Nodes and Stress Locations

Source: PLAXIS 2D Reference manual)

Based on the chosen material model, the characteristics are given to each cluster, which defines a soil element. When modeling soil, material model's fundamental.

3.3.2 Modeling of soil behavior

Soils exhibit significant non-linear behavior when subjected to a load. The non-linear stress-strain behavior may be represented using various degrees of complexity. The quantity of the model's parameters rises proportionately to the amount of development. PLAXIS offers many models for simulating soil behavior and other continuous materials. The Mohr-Coulomb model and Hardening Soil model utilized in this study is explained in the following section.

3.3.2.1 Mohr-coulomb model

The model is of first-order that simplifies soil by treating it as an elastic-perfectly plastic substance. For the Mohr-Coulomb model, five parameters are required. These parameters consist of two stiffness and three strength parameters, which are well-known to the majority of geotechnical engineers and may be acquired from fundamental sources [69].

The model of Mohr-Coulomb stiffness parameters (drained behavior):

E': the effective Young's modulus [KN/m2].

v': the effective Poisson's ratio

Other stiffness parameters may be used instead of Young's modulus. Listed below are these relations, parameters, and the units that are standard for each:

G: the modulus of shear, where $G = \frac{E'}{2(1+v')}$ [KN/m²]

E_{oed}: Modulus of an odometer, where $E_{0ed} = \frac{E'(1-v')}{(1+v')(1-2v')}$ [KN/m²]

The Mohr-Coulomb model's strength parameters are:

c'_{ref} : Effective cohesion [KN/m²]

$\emptyset'$: Angle of effective friction (Degree)

ψ: The angle of dilatancy (Degree)

Under drained circumstances, the Mohr-Coulomb model accurately describes soil failure behavior. Still, when yielding occurs, it assumes continuous dilatation, leading to overestimating the undrained shear strength [70].

3.3.2.2 Hardening soil model (HSM)

This model is designed to simulate soil behavior at an advanced level. The Hardening Soil model is an elastoplastic hyperbolic model that is constructed within the paradigm of shear hardening plasticity. Additionally, the model incorporates compression hardening to replicate the irreversible compaction of soil during initial compression. The second-order model is applicable for simulating the behavior of several kinds of soil, including sands, gravel, clays, and silts.

Parameters for hardening the soil model

HSM encompasses two distinct groups of input parameters: Failure parameters and stiffness parameters. Each category will be described as follows:

Failure parameters

The Hardening soil Model has the same strength parameters as the non-hardening Mohr-Coulomb model, which Consists of three parameters:

c`: Effective cohesion (KN/m²)

φ `: Effective angle of internal friction (Degrees)

ψ : Angle of dilatancy (Degrees)

Stiffness parameters

Consists of four parameters:

E_{50}^{ref} : Secant stiffness in a standard triaxial test with drainage (KN/m²)

E_{oed}^{ref}: Tangent stiffness for the main odometer load (KN/m²)

E_{ur}^{ref}: Stiffness as unloading and reloading (KN/m²)

m: Power for stress-level-dependent stiffness (-)

3.3.3 Mesh generating

Once the geometry model is entirely generated, it must be partitioned into finite elements to streamline finite element computations. Meshing is the term used to denote a collection of limited components. Mesh mode is utilized to produce the mesh. The mesh must possess a high level of fineness to provide precise numerical outcomes. However, avoiding using very small meshes is advisable since this may result in longer computation times. The PLAXIS 2D software employs a completely programmed method for generating finite element models. A reliable triangulation procedure creates this mesh. The mesh-generating procedure considers the soil stratigraphy and any structural items, loads, and boundary conditions.

PLAXIS 2D employs an unstructured mesh, automatically creating and offering global and local mesh modification options. PLAXIS 2D provides five options for mesh density, ranging from a very coarse mesh to a very tiny mesh. Mesh generator

requires a global parameter for meshing, denoted as I_e, which signifies the desired dimension of the elements. The PLAXIS software derives this value from the measurements of the outside shape elements' distributions ($x_{minimum}$, $x_{maximum}$, $y_{minimum}$, $y_{maximum}$) chosen in the mesh settings box. The dimensions of the chosen element are computed using the equation shown below:

$$I_e = r_e \times 0.06 \times \sqrt{(x_{max} - x_{min})^2 + (y_{max} - y_{min})^2} \quad (0.1)$$

The Element distribution calculates the proportionate factor of element size. There are five levels in the globe. Medium is the default setting for the Element distribution; however, whoever uses it can choose a different level to adjust the mesh to be finer or coarser on a global scale. The relative element size factor values vary based on the coarseness of the element, as shown in **Hata! Başvuru kaynağı bulunamadı.**.

Table 3.1: The Relative Element Size Factor Values Based On the Coarseness of the Elements

Element Coarseness	The Related Factor For Element Size
Very coarse	2
Coarse	1.33
Medium	1
Fine	0.67
Very fine	0.50

3.3.4 Initial condition

In PLAXIS, it is necessary to establish the starting state of the soil before doing the significant computations. This involves determining the soil's initial stress level and the first water pressure inside it.

3.3.5 Effective stress

Vertical and horizontal stress determine the initial stress state in 2D analysis. Vertical stress is caused by external loads or soil self-weight. In contrast, it is possible to calculate the horizontal stress using the coefficient K. PLAXIS computes these stresses at each stress point inside the model given a starting condition. The absence of external loads in the initial state necessitates the calculation of vertical stresses based on the unit weight of the soil. The first situation also indicates that the soil is in a state of rest.

3.3.6 Types of calculations

The main FEM calculation could be done once the shape is set and the starting conditions are known. Three categories of calculations apply to this subject: plastic, fully coupled flow-deformation and safety. Including considerable displacements (with an updated mesh) and dynamic analyses using an extension application in different computations are feasible. Various computation methods are shown here.

3.3.6.1 Plastic calculation

Plastic computation calculates elastic-plastic deformation. They were used to analyze item failure and stability. The plastic computation approach fails to decrease excess pressure in pores time-dependently. This form of computation is suitable for the majority of real geotechnical applications.

3.3.6.2 Fully coupled flow-deformation analysis

A fully linked flow-deformation study is performed when it is important to examine the simultaneous evolution of deformations and pore pressures in saturated and partly saturated soils due to time-dependent variations in the hydraulic boundary conditions. Soil permeabilities need to be entered in this stage, use non-zero-time interval.

A comprehensive flow-deformation investigation considers the behavior of unsaturated soil and the suction in the unsaturated zone above the phreatic level. This study is characterized by its high level of sophistication and accuracy since it considers the lower permeability and degree of saturation in the unsaturated zone. The ignore suction option is unavailable in fully coupled flow-deformation analysis for this reason.

Rain is simulated at this stage, The parameters used to define precipitation are: the unit of length per unit of time for infiltration(q), maximum pore pressure head (Ψ_{max}) , minimum pore pressure head ($\Psi_{\min}$).

3.3.6.3 Safety analysis (PHI-C reduction)

All soil layers and interfaces are automatically included for safety calculations. Using improved safety analysis makes decreasing strength in buildings and soil clusters feasible. In addition, the enhanced safety analysis allows for

excluding specific soil clusters or buildings from the strength reduction operation. The strength reduction multiplier, ΣMsf, governs safety calculations. The objectives of Enhanced safety may include the following:

- Removing surface soil clusters situated along a slope while reducing strength to prevent shallow failure mechanisms is feasible. If the structures exhibit elastoplastic behavior and have limited strength, they may be chosen for strength reduction in addition to the soil clusters.
- Manually selecting soil clusters or buildings at various stages may improve safety analysis.

3.3.7 Staged construction

Construction happens in phases. PLAXIS divides its computation method into calculation phases to emulate this. This primarily aims to prevent potential failures during the building phase and accurately reproduce the excavation procedures.

The starting condition set earlier is always the first step in the calculation. Following the intended building procedure, one could include several stages regarding the structural aspect elements, loads, and soil groups that are successively activated or deactivated. Additionally, it is feasible to modify the material properties and water conditions and apply pre-stress to anchors.

3.4 Finite Element Verification

The PLAXIS 2D program will be used for this study, but before using the program, the program will be matched with the results of previous researcher. Verification will be done through slope model. This section used verification model to show the convergence the PLAXIS 2D solution. The model compared the safety factor results using PLAXIS 2D with the result 2D Finite Element Method for the slope in a study (Z. Alsharifi, 2021).

3.4.1 Verification of slope

3.4.1.1 The research area's description

The research location is situated within the slope next to the historic city of Al-Najaf and close to the shrine of Imam Ali in the southwestern region of Iraq, as shown in **Hata! Başvuru kaynağı bulunamadı.** this area has had recent growth, and more expansion is anticipated due to the city's religious appeal. Construction is a key element of growth, and it is necessary to examine the city's slope instability resulting from the additional weight induced by rainfall. The soil of the slope is sand [71].

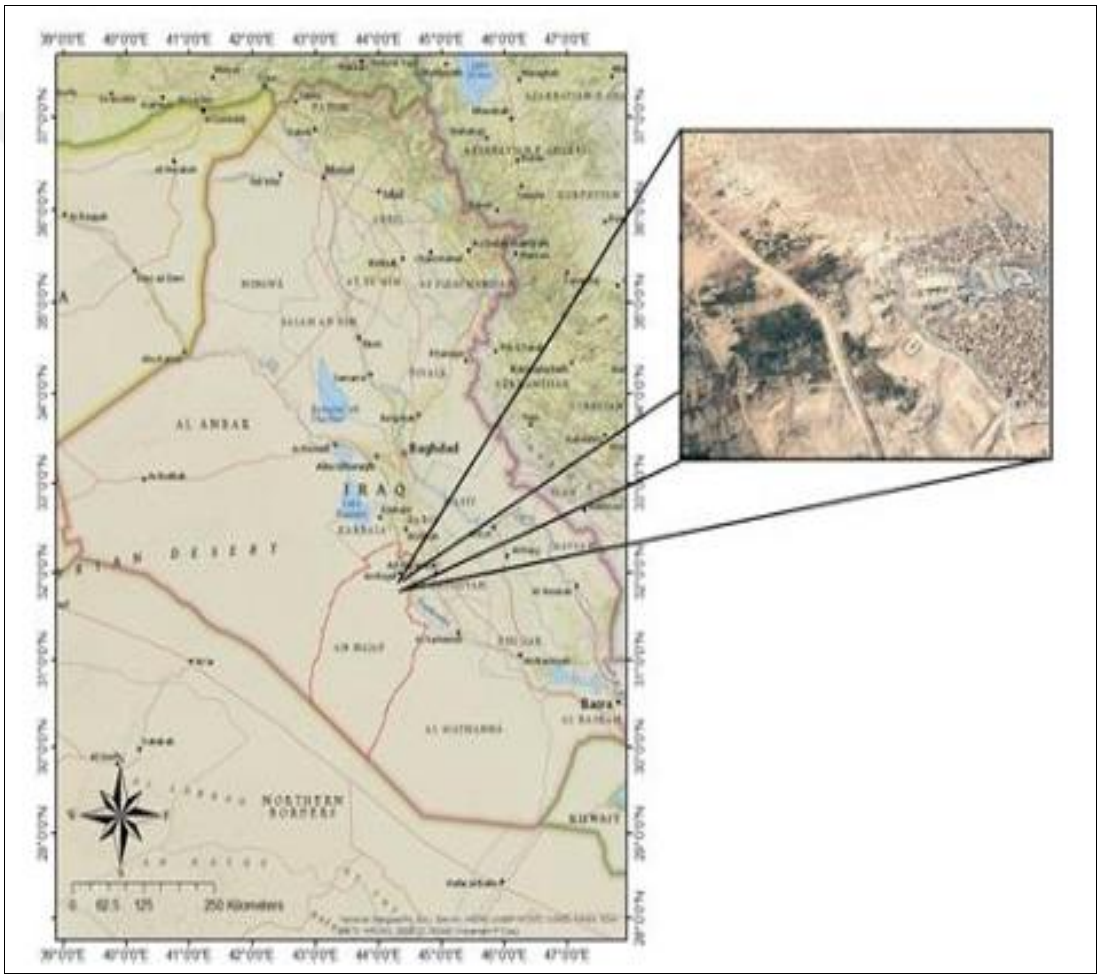

Figure 3.2: Site of the Slope

Source: (Z. Alsharifi et al.,2021).

3.4.1.2 Simulation of slope with PLAXIS 2D

The slope was simulated with PLAXIS 2D. The soil in the slope was modeled using the Mohr-Coulomb model. The soil's finite element model parameters are outlined in **Hata! Başvuru kaynağı bulunamadı.**. The mesh properties were set to 2495 nodes

and 295 elements, a fine mesh was used. **Hata! Başvuru kaynağı bulunamadı. Hata! Başvuru kaynağı bulunamadı.**shows the total displacement for the slope and show the slip surface without effects of rainfall. the permeability ($k_{x,y}$) of soil is 2m/d according to (Budhu, 2011) [72].

Table 3.2: Summarizes the Characteristics of the Soil

Parameter	Value
Permeability (K_X)(m/day)	2
Permeability (K_y)(m/day)	2
Unit Weight ($KN/m3$)	19
Young's Modulus (KPa)	20125
Poisson's Ratio,V	0.35
Cohesion, C (Kpa)	0
Friction Angle, ϕ, (degree)	35
Dilatancy Angle, Ψ (degree)	0

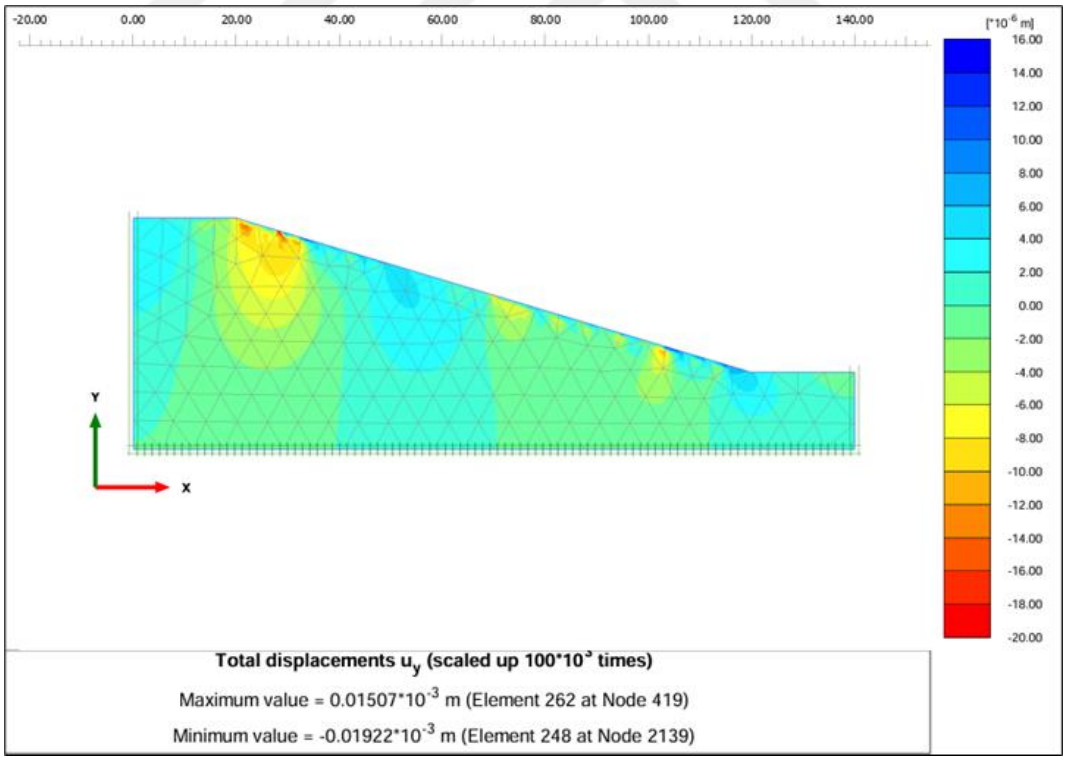

Figure 3.3: Total Displacement of the slope Without Rainfall

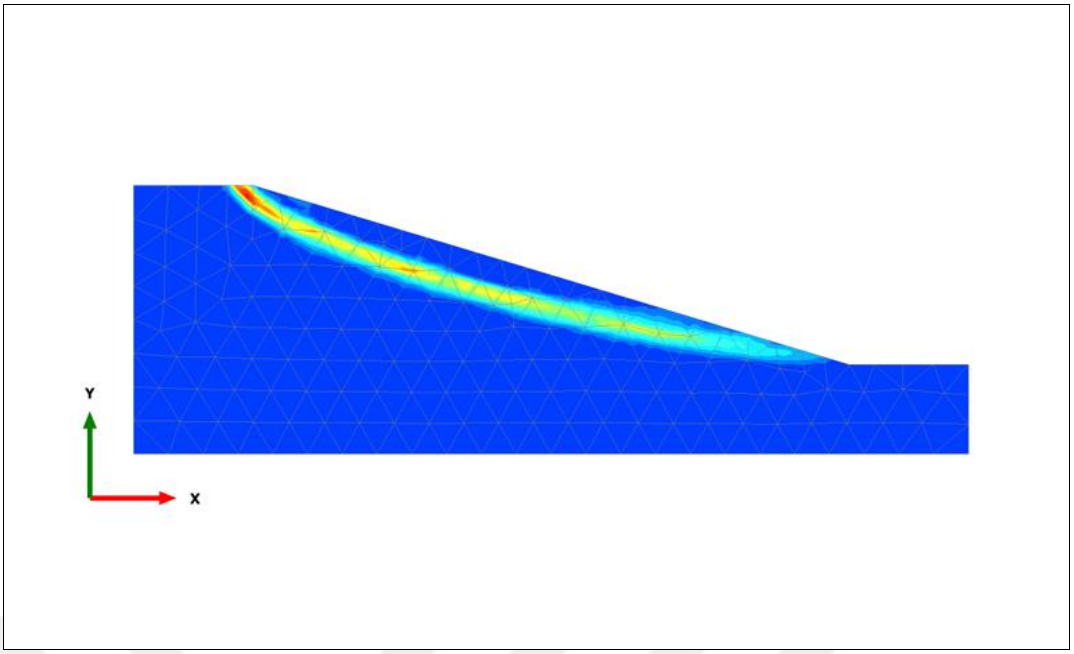

Figure 3.4: Slip Surface of the Slope Without Rainfall

Hata! Başvuru kaynağı bulunamadı. shows the safety factor curve in PLAXIS 2D. It was noticed that the 2D finite element results match the measured data compared to study (Z. Alsharifi, 2021).

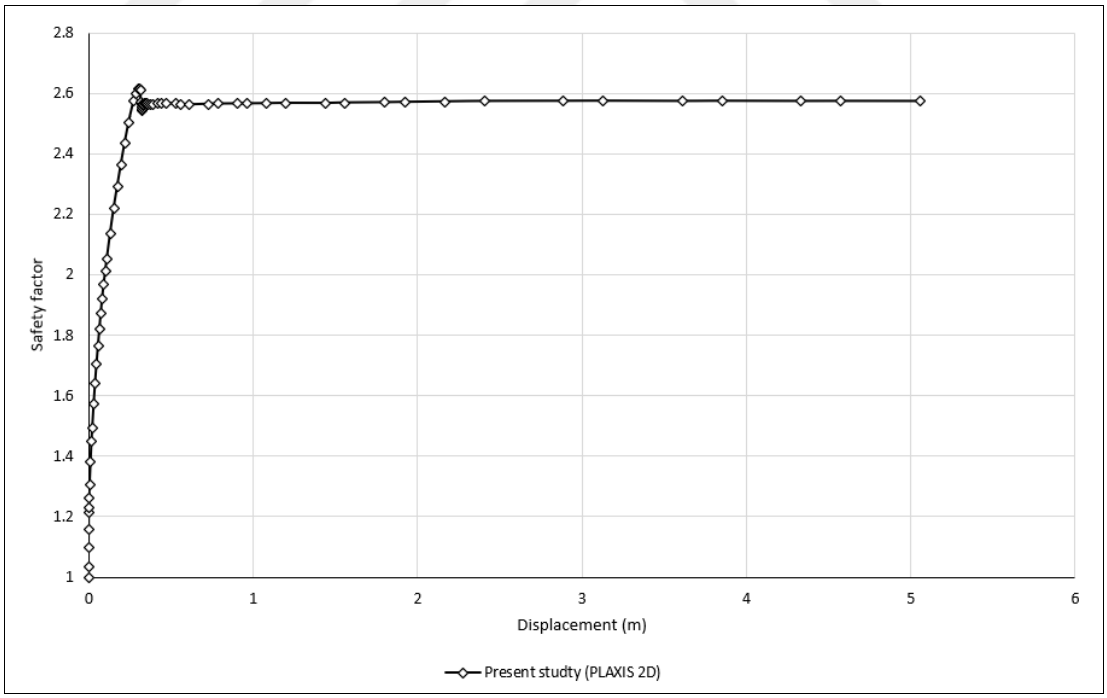

Figure 3.5: Factor of Safety of Slope without Rainfall

4. RESULTS AND DISCUSSION

4.1 Introduction

The Slope was simulated using FEA to determine the value of the maximum displacement, the potential sliding surface, and safety factors for slope using the PLAXIS 2D 2020. The primary aim of this research is to identify the effects of varying rainfall intensities on the FOS, maximum displacement, and potential slip surface for slope. This chapter will cover all the output related to this research.

As previously stated, heavy precipitation often causes landslides. Nevertheless, soils on slopes exhibit diverse reactions to precipitation, contingent upon the attributes of both rainfall and soil qualities. The interaction between rainfall and soil is crucial in determining water infiltration into the top layer of slope soils. To cause a critical state, it is necessary for the rainfall to not only have sufficient intensity but also to last for a significant amount of time, allowing the infiltrating water to lower shear strength adequately. The variability of rainfall, especially during severe periods, significantly impacts infiltration, making the resolution of rainfall crucial. Furthermore, rainfall distribution is an additional component that substantially affects landslide vulnerability. However, soil qualities, particularly hydraulic properties about the intensity of rainfall, can contribute significantly to landslides triggered by rainfall.

4.2 Rainfall Data

Rainfall data directly measured for design purposes are seldom used. Instead, statistical data for estimated rainfall, generally represented in the Intensity-Duration relationship diagram, is employed. Rainfall data was recorded in the northern part of Iraq in Kirkuk governorate (the nearest station to the research area). The relationship between rainfall intensity during a rainstorm and the storm's duration at a specific return period is shown in **Hata! Başvuru kaynağı bulunamadı.**. The maximum hourly precipitation at the station was calculated for each year from 1979 to 2014

and at return periods of (2, 5, 10, 15, 25, 50, 100) years.[73] This research used three sets of rainfall data (12,21,28) mm/hr and at return periods of (2, 15, 100) years and a fixed rain intensity of 21mm/ hr (1,4,8,16,24) hr.

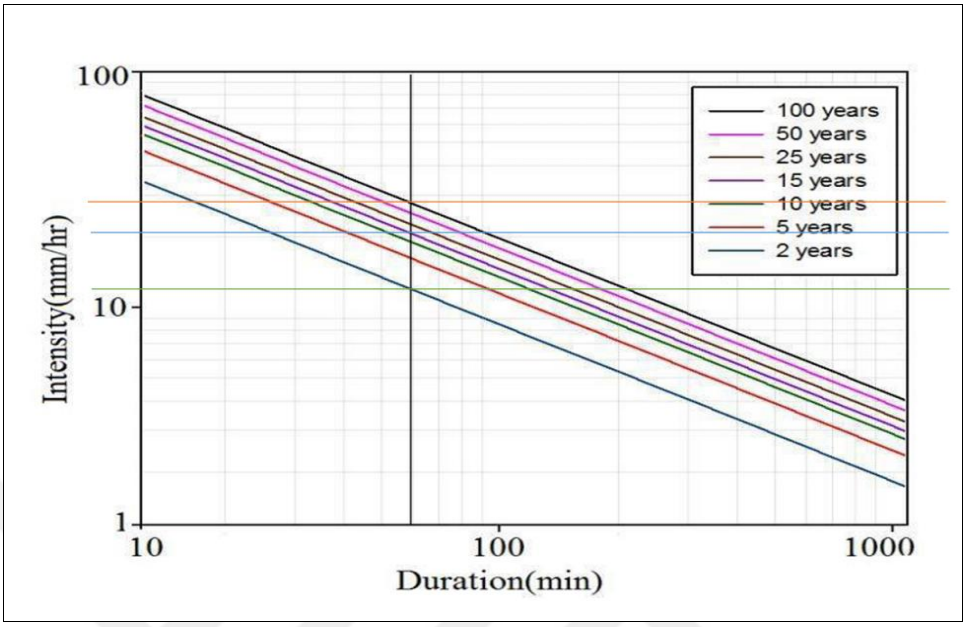

Figure 4.1: Relationship Diagram between Intensity Rainfall and Duration

4.3 Problem Modeling

The Finite Element Analysis (FEA) was conducted using the PLAXIS 2D code to examine the effect of rainfall on slope stability. Finite element analyses were carried out on all layers of the soil of the slope to evaluate the impact of rainfall on the soil. rainfall data are the variables examined in this study, and they were used to calculate the displacement and safety factors.

4.3.1 Initial phase

First, an initial phase is created to calculate the soil's primary stresses according to its volumetric weight in its inclined, non-horizontal state based on the Gravity Loading calculation type. In this case, the Mohr-Coulomb soil model was used.

4.3.2 Plastic calculation

A plastic computation was used to calculate an elastic-plastic deformation with Calculate the pore pressure using a type of calculation, phreatic levels depending on hydraulic circumstances. Input of soil permeability required.

4.3.3 Safety analysis

Strength reduction method: Phi/c reduction and reduction of strength parameters until failure is reached. The process of calculation was applied in this analysis. The primary input parameters are unit weight (γ), effective cohesion (c'), internal friction angle (ϕ'), and pore-water pressures. These parameters are automatically entered into the slope stability assessments using the software's linked function. The primary output parameter coming out of this process is the factor of safety (FOS), which indicates the stability of slopes.

a. Phi/c reduction:

b. Progressive weakening of strength parameters till reaching the point of failure.

Making use of effective strength

$$\sum Msf = \frac{(tan\varphi)_{input}}{(tan\varphi)_{reduced}} = \frac{c}{c_{reduced}}$$

Employing undrained shear strength

$$\sum Msf = \frac{s_{U,input}}{s_{U,reduced}}$$

ΣMsf = strength-reduction coefficient

4.3.4 Safety analysis in PLAXIS – calculation

The safety factor in the program is calculated using calculation type safety. Analysis and calculation of effective stress based on Gravity loading (it is not counted within the initial phase). It takes into account areas of inclination.

Strength reduction with a predefined factor (Target ΣMsf)

1- Create a Safety phase:

a. Set Loading input to Target ΣMsf

b. Specify a target reduction factor

2- Calculate

Safety analysis was used in two places: the first position was used to determine the safety factor for the typical case without the effect of rain, and it was used in another position to calculate the safety factor with the effect of rain.

4.3.5 Fully coupled flow deformation analysis

During this phase, the analysis focused on the concurrent development of deformations and pore pressures in both saturated and partly saturated soils. This was in response to time-dependent variations, namely changes in rainfall, in the hydraulic boundary conditions. Rainfall was simulated at this stage by activating the Precipitation option to use infiltration (q) due to rainfall. Two types of rain analysis were used: the first type was with a fixed time. It used a time of one hour with a rain intensity of (12, 21, and 28) mm; the other analysis was to know the time that causes an apparent effect on the safety factor. This was further achieved using different times with a fixed rain intensity of 21mm/hr for (1,4,8,16,24) hr.

4.4 Hydraulic Boundary Conditions

The boundary condition was chosen to represent the water entering the soil. The boundaries of the model were determined by setting the behavior of the slope aspects as seepage. Boundaries set as Seepage will not be immediately converted to Offside Boundaries when rainfall is indicated. Percolation was chosen for the slope surface (precipitation infiltrates the soil from the outside environment). **Hata! Başvuru kaynağı bulunamadı.** shows the hydraulic boundary conditions for the slope.

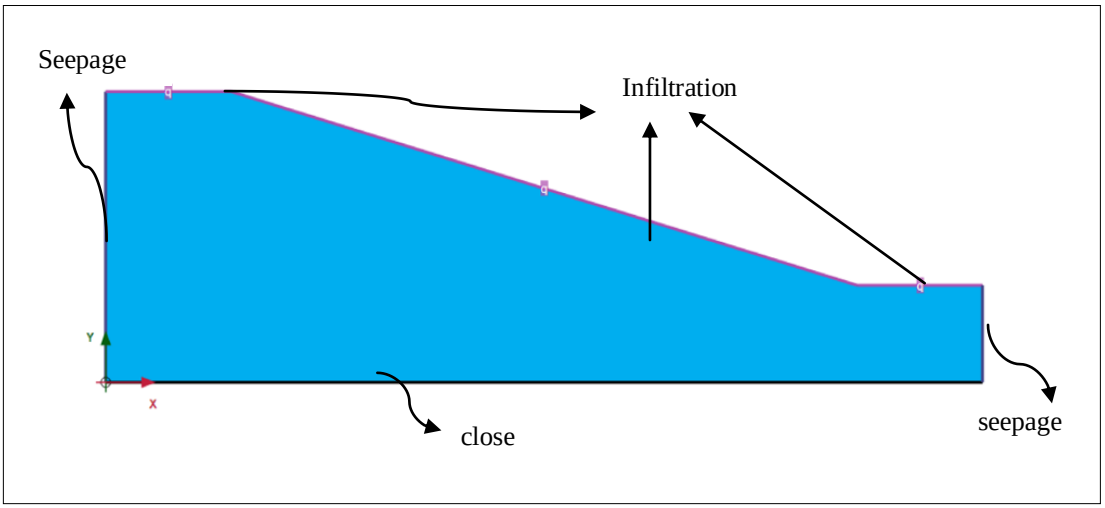

Figure 4.2: Hydraulic Boundary Conditions for the Slope

4.5 Effect of Rainfall on FOS by using MCM

The factor of safety (FOS) is a dimensionless parameter used to assess the overall stability of the soil under different climatic loading conditions. Rainfall analysis was

conducted with constant time and varied rain intensity and constant intensity and time variation.

4.5.1 Effect of rainfall intensities on FOS by using MCM

The effect of rainfall intensity on the safety factor for different rainfall intensities and a fixed time (12,21,28) mm/hr for the slope is shown in **Hata! Başvuru kaynağı bulunamadı.**.

It can notice an apparent decrease in the safety factor for the slope under the influence of rainfall (12,21,28) mm\ hr in the rate of (15%), it can be noted that there is no noticeable difference in the safety factors between different rain intensities because the work done by the program is to saturate the area or convert the unsaturated area within the failure zone to saturated, it will lose its unsaturated properties. The intensity of rainfall (12, 21, 28) mm is equal in affecting the safety factor because the three rain intensities saturate the failure zone in the same period.

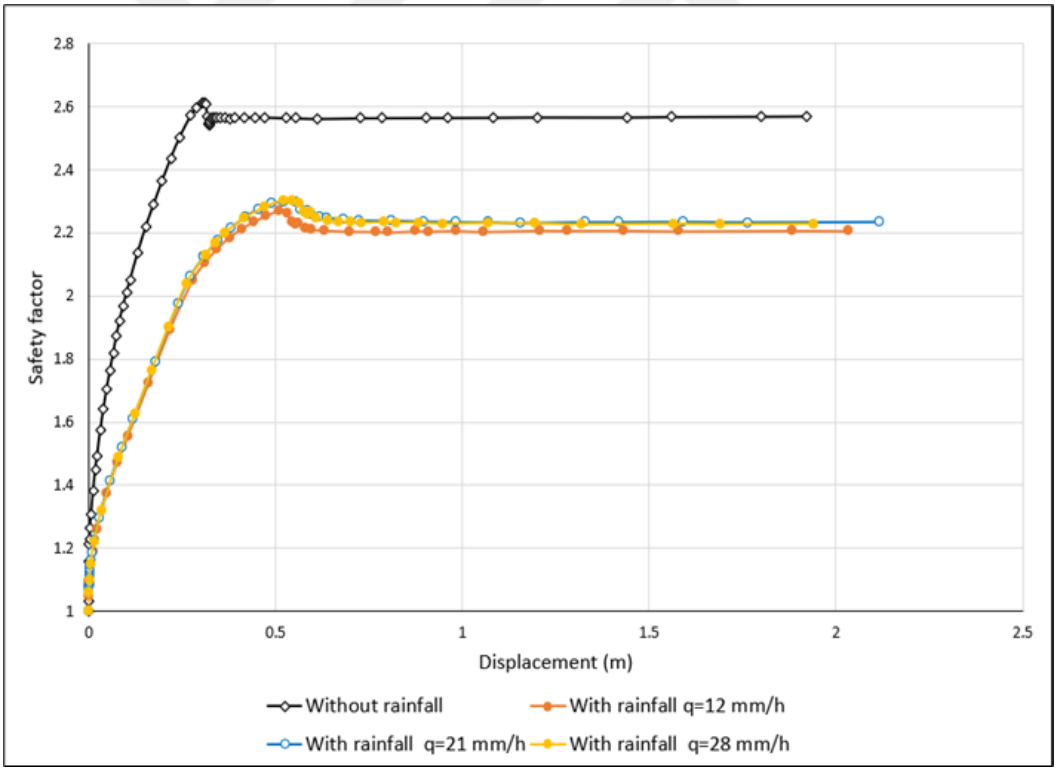

Figure 4.3: Safety Factors of the Slope under the Effect of Rainfall (MCM)

4.5.2 Effect of rainfall duration on FOS by using MCM

The effect of rainfall intensity on the safety factor for different durations of rainfall (1,4,8,16,24) hours and fixed intensities of rainfall (21 mm/hr). The effect of rainfall intensity on the safety factor for different durations of rainfall for slope is shown in

Hata! Başvuru kaynağı bulunamadı.. It can be noticed that for a higher duration of rainfall (24 hr), a massive decrease in FOS occurred. On the other hand, for lower-duration rainfall (1 hr), the FOS decreased less, leading to a reduction in the safety factor by (12%) when it rained for one hour (28%) when it rained for 4 hours and by (37%) when rain falls within 8 hours, and (42%) when rain falls for 16 and 24 hours.

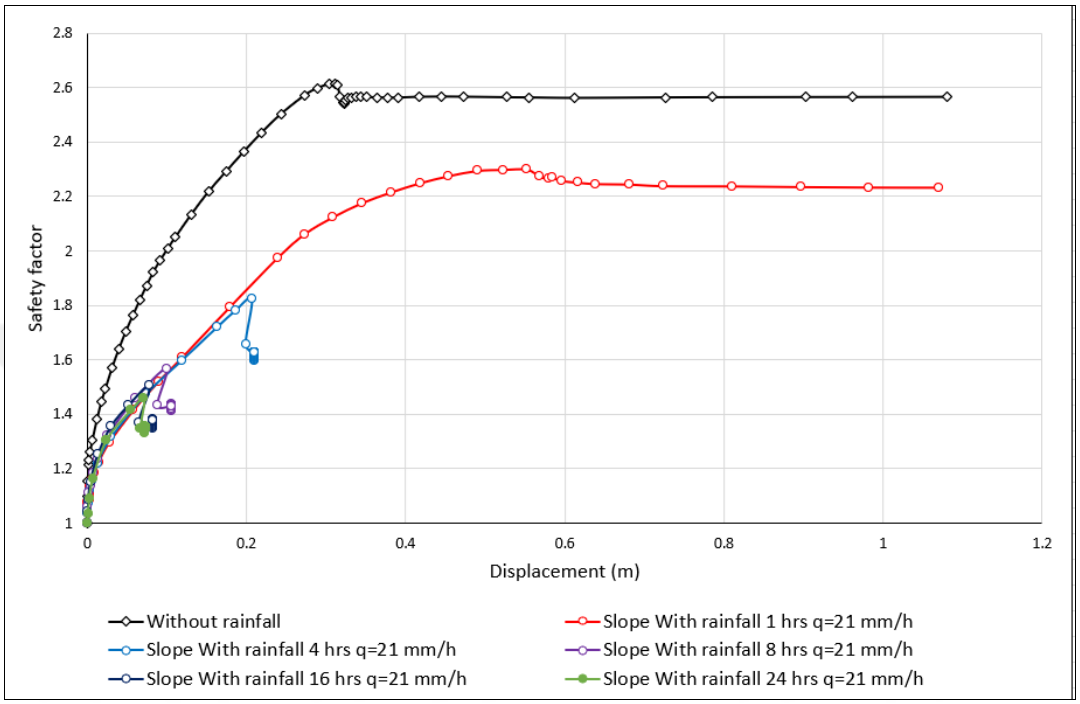

Figure 4.4: Safety Factors of the Slope under the Effect of Different Rainfall Duration (MCM)

4.6 Effect of Rainfall on Deformation for Slope by using MCM

4.6.1 Effect of Rainfall Intensities on Deformation

The effect of rainfall (12, 21, and 28) mm\hr was applied to the slope model, and the Mohr-Coulomb model was applied to the slope soil, and the point was chosen at the top edge to know the values of deformations and to know the deformation's locations of the slope. Observed occurrence of the settlement in the crest of the slope (the horizontal area at the top of the slope) (a counterclockwise movement occurred from the top of slope to the below), and the upward movement emerged in the slope area (mid of the slope). The findings suggest that the values of the most significant deformation occurred in the slope region (mid of the slope) for three rainfall intensities (12,21and 28) mm/hr, and it can be seen that there is no noticeable difference in deformation in the crest of the slope. **Hata! Başvuru kaynağı**

bulunamadı. shows the impact of rainfall on the total values of deformations. **Hata! Başvuru kaynağı bulunamadı.** shows the total displacement of the slope without the effects of rainfall. The impact of rainfall on total displacement is shown in **Hata! Başvuru kaynağı bulunamadı.** to **Hata! Başvuru kaynağı bulunamadı.**. figure 4-12 shows the slip surface of the slope.

Table 4.1: Slope Deformations with Different Rainfall Intensities for MCM

Rainfall intensity (mm/hr)	**Maximum displacement at the crest of a slope (mm)**	**Maximum heave (upward movement) at a mid of slope (mm)**
0	-0.02	0.015
12	-0.29	41
21	-0.108	41
28	-0.142	40

* Negative sign means settlement, and the positive is upward movement (heave)

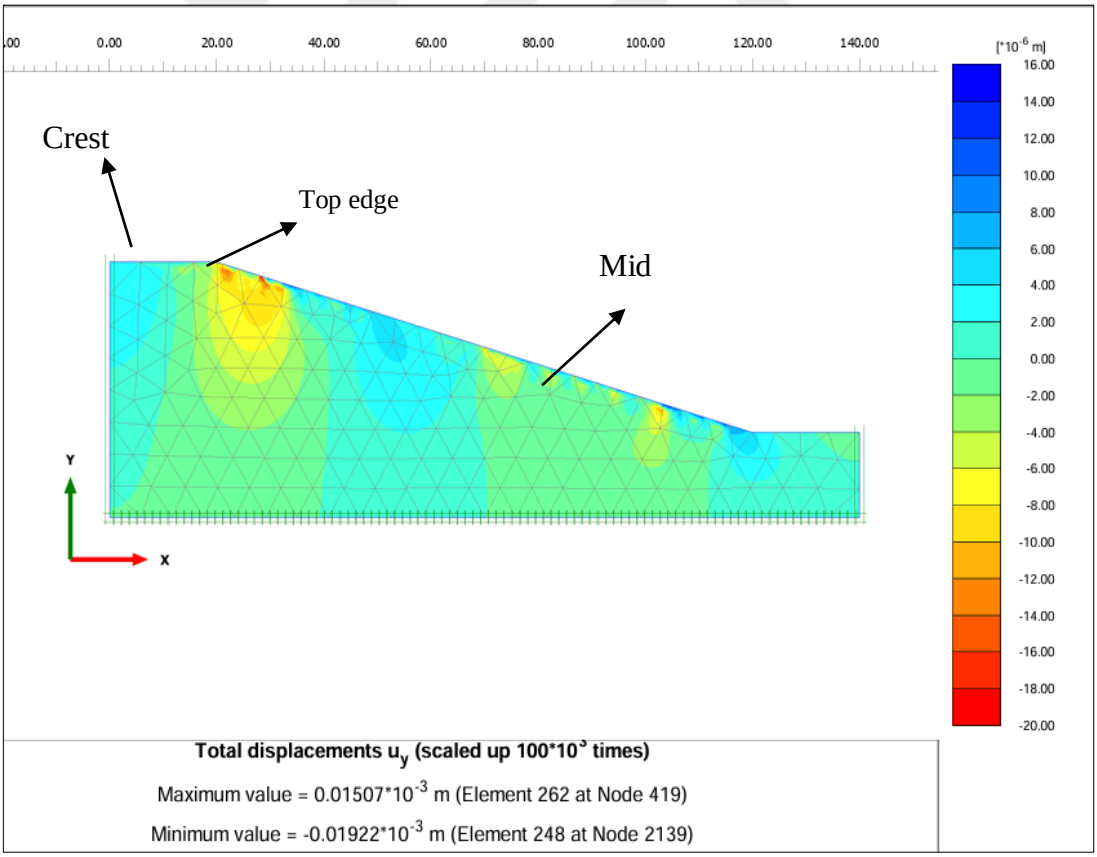

Figure 4.5: Total Displacement of the Slope without Rainfall for MCM

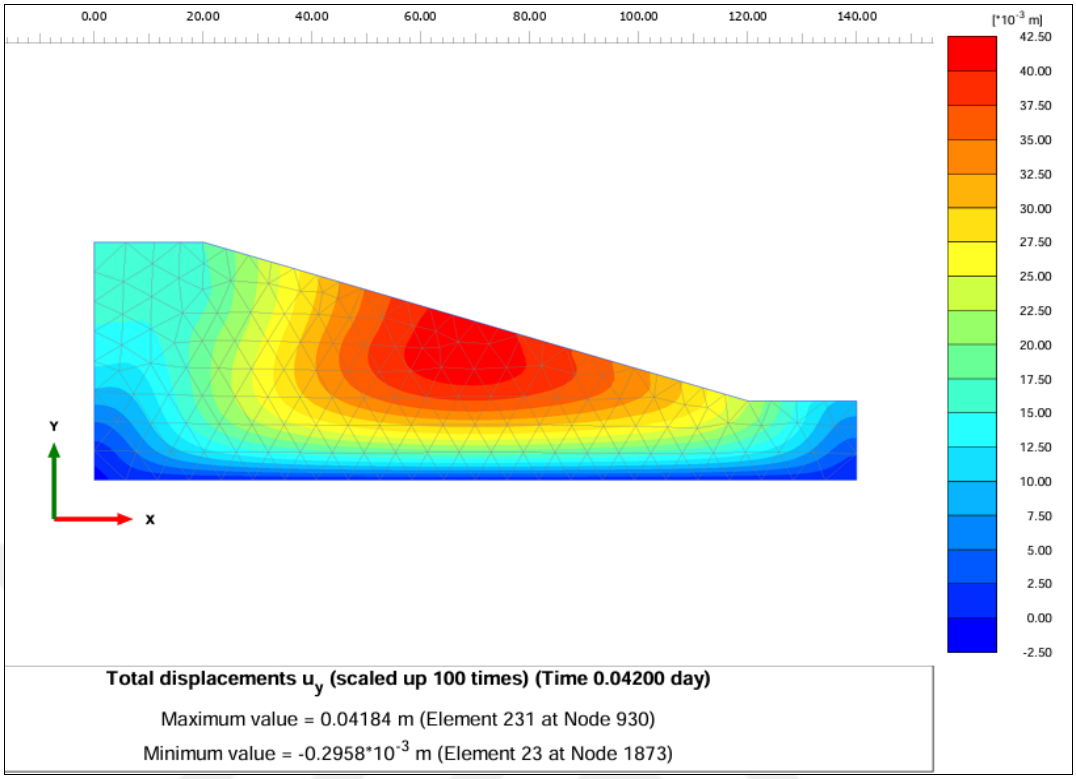

Figure 4.6: Total Displacement of the Slope with Rainfall q= 12mm/hr for MCM

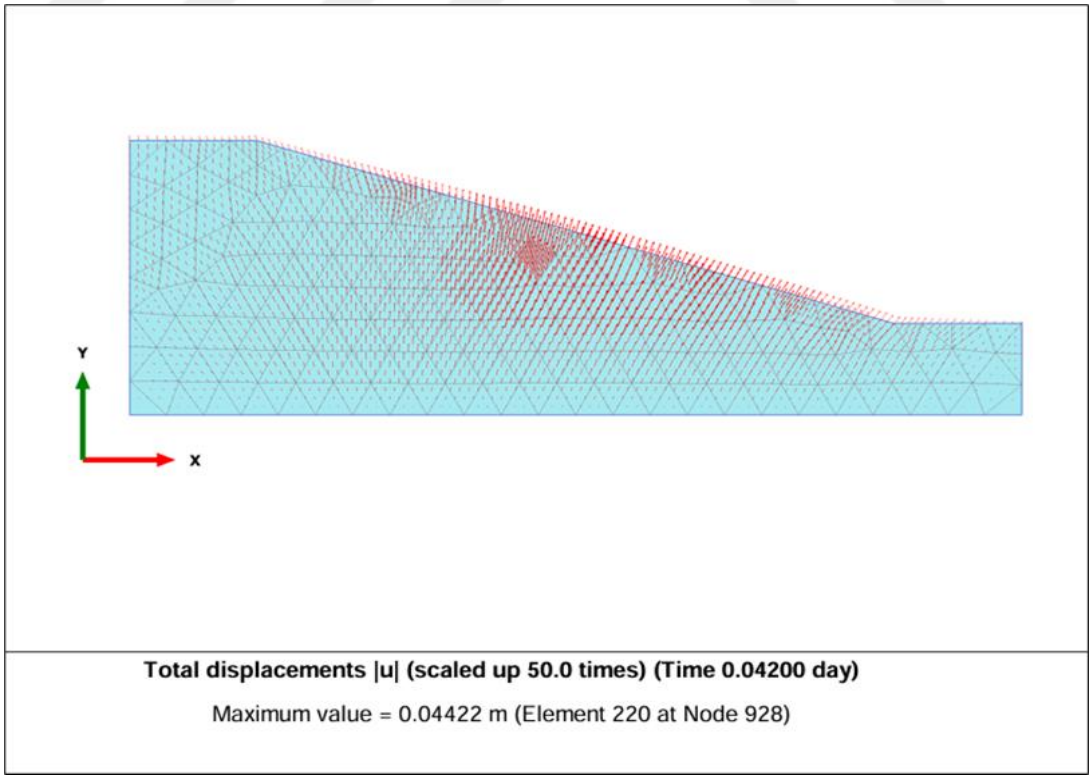

Figure 4.7: Total Displacement Arrows Presentation q=12 mm/hr for MCM

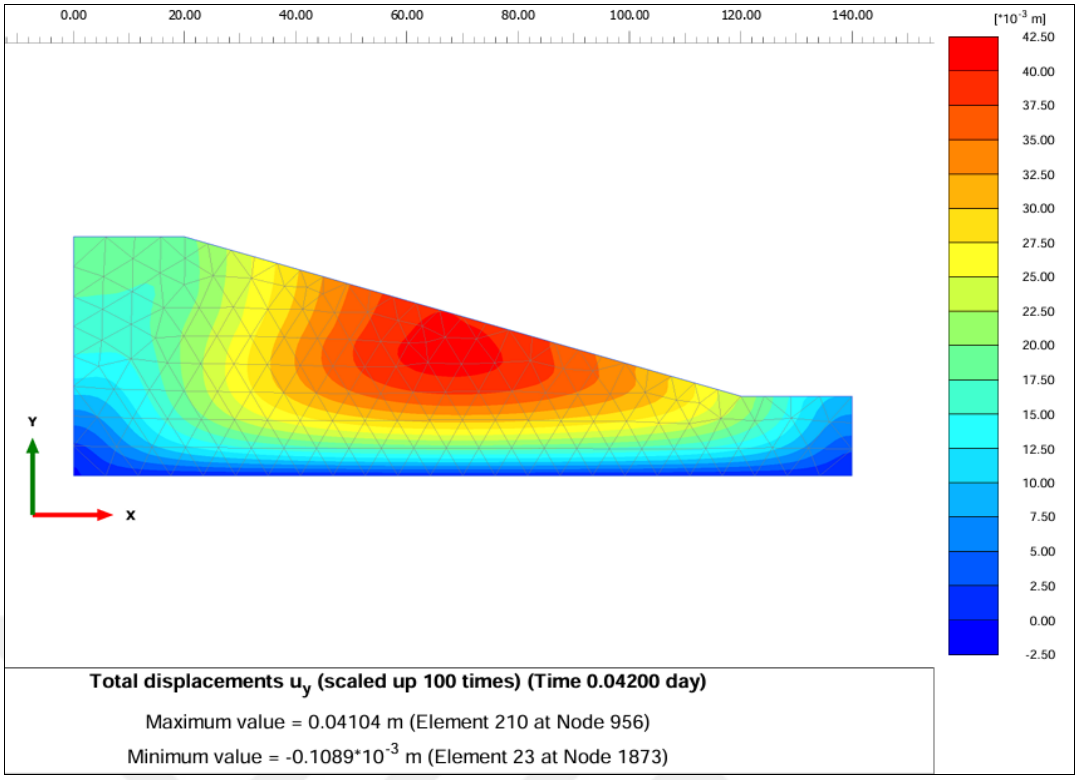

Figure 4.8: Total Displacement of the Slope with Rainfall q= 21mm/hr for MCM

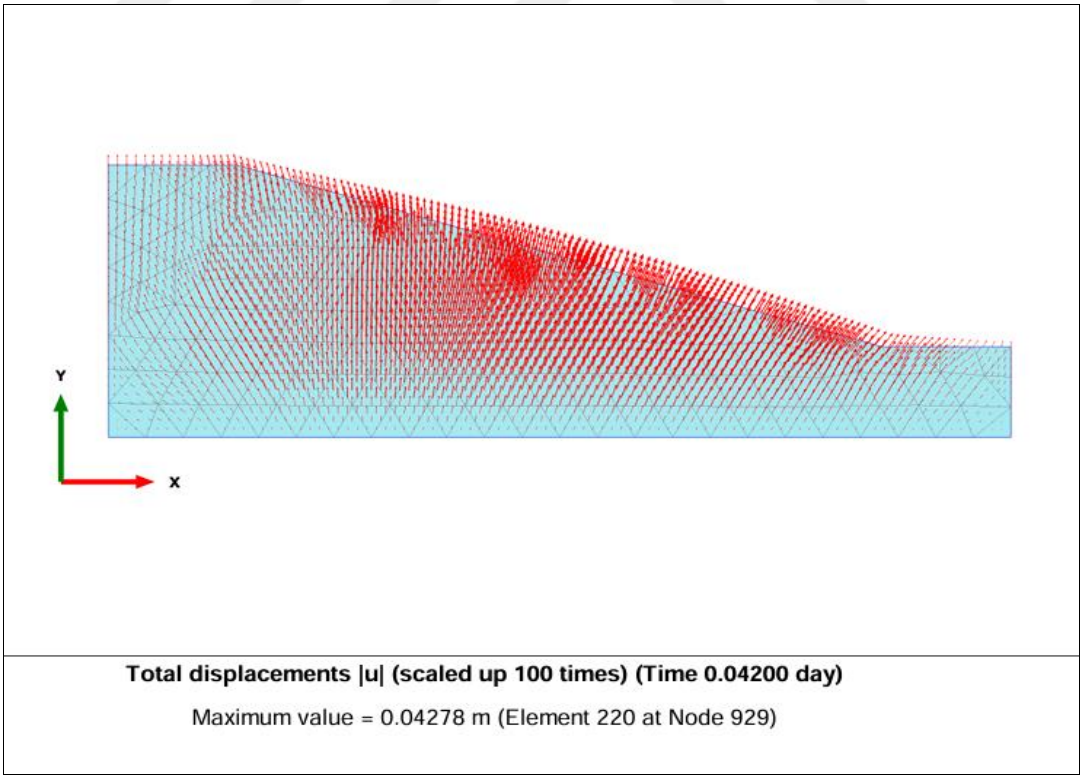

Figure 4.9: Total Displacement Arrows Presentation q=21 mm/hr for MCM

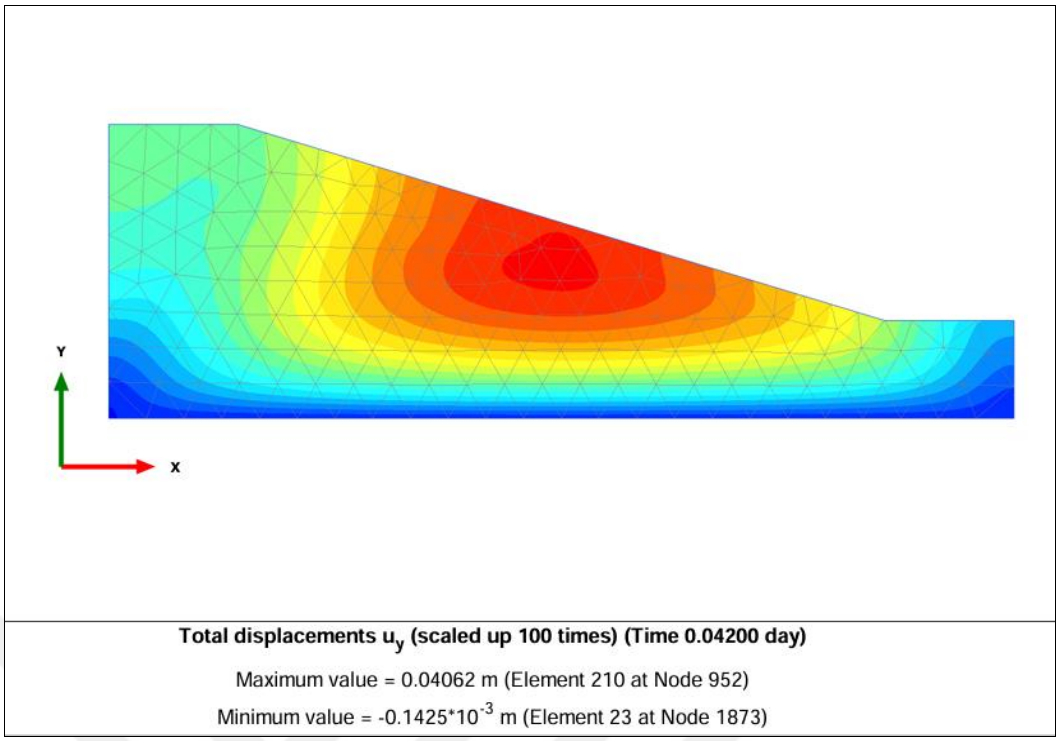

Figure 4.10: Total Displacement of the Slope with Rainfall q= 28 mm/hr for MCM

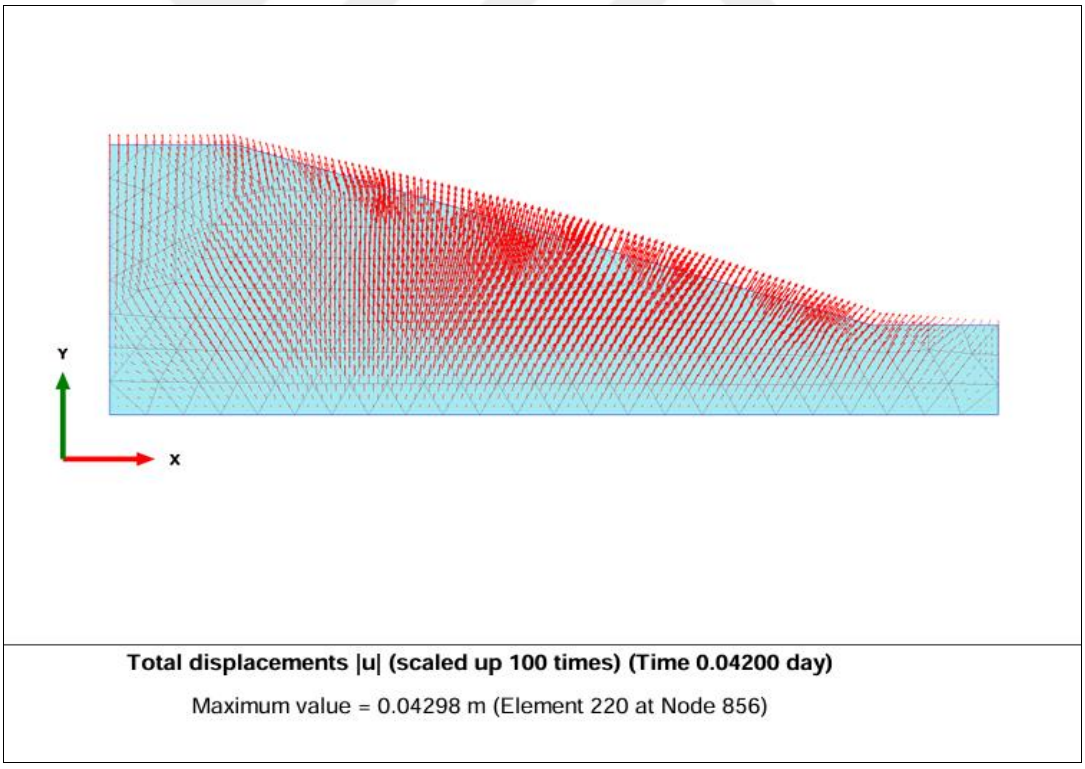

Figure 4.11: Total Displacement Arrows Presentation q=28 mm/hr for MCM

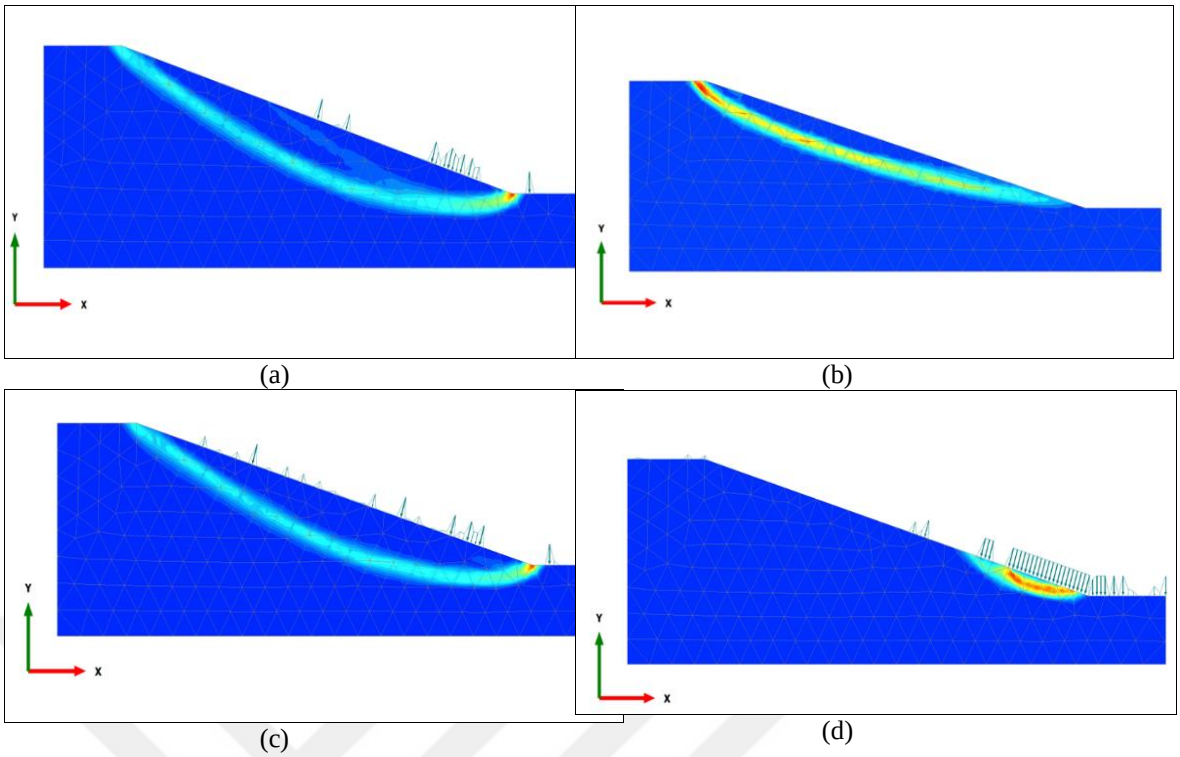

Figure 4.12: Slip Surface for Slope (a) Without Effect of Rainfall (b) With Rainfall q=12mm/hr (c) with Rainfall q= 21mm/hr (d) with Rainfall q=28mm/hr for MCM

4.6.2 Effect of rainfall duration on deformation by using MCM

The simulation of the effect of rainfall throughout (1,4,8,16,24) hours with a constant rainfall intensity of 21mm/hr led to an upward movement in the slope. It is evident that the more hours of rain, the greater the value of the upward movement.

shows the effects of rainfall deformation values in the slope.

Table 4.2: Slope Deformations with Different Rainfall Times (MCM)

Rainfall time (h)	Maximum displacement at the crest of the slope (mm)(MCM)	Maximum heave (upward movement) at a slope (mm)
0	-0.02	0.015
1	-0.108	41
4	44	69
8	44	72
16	50	80
24	55	85

4.7 Comparison between Behavior of Mohr-Coulomb Model (MCM) and Hardening Soil Model (HSM)

The slope was modeled by applying the Hardening soil model to the slope soil, to know the difference in the model's behavior under the influence of rain from the Mohr-Coulomb model behavior. **Hata! Başvuru kaynağı bulunamadı.** below shows the HSM coefficients that were used.

Table 4.3: Slope Soil Parameters

Parameters	Slope soil
E_{50}^{ref}	20,000
E_{ode}^{ref}	20,000
E_{ur}^{ref}	60,000
Power (m)	0.5

4.7.1 Effect of rainfall on safety factor by using HSM

4.7.1.1 Effect of rainfall intensities on safety factor by using HSM

The effect of rainfall was simulated by applying the Hardening soil model for rainfall intensity 12, 21, and 28 mm/ hr over a one-hour rain time. Figure 4-13 shows the results of the safety factor obtained. Figure 4-14 shows Comparing the safety factor results for the MCM and HSM. Noted the convergence of the safety factor without the influence of rainfall between the Mohr-Coulomb model and the applying the Hardening soil model. There is an MCM response under the influence of rainfall, where the safety factor decreased by (15 %) for all rain intensities by the same percentage. Still, it is less than the HSM response, where the safety factor by application of HSM on the model decreased by (35%) for the rain intensity of 12 mm/hr. Approximately the same percentage for the rain intensity of 21 mm/hr, and the safety factor decreased by 40% for rainfall intensity of 28 mm/hr. We conclude from this that the soil model affects the values of the safety factor under the influence of rain, as it was shown that the HSM affects the response and behavior in the event of rain.

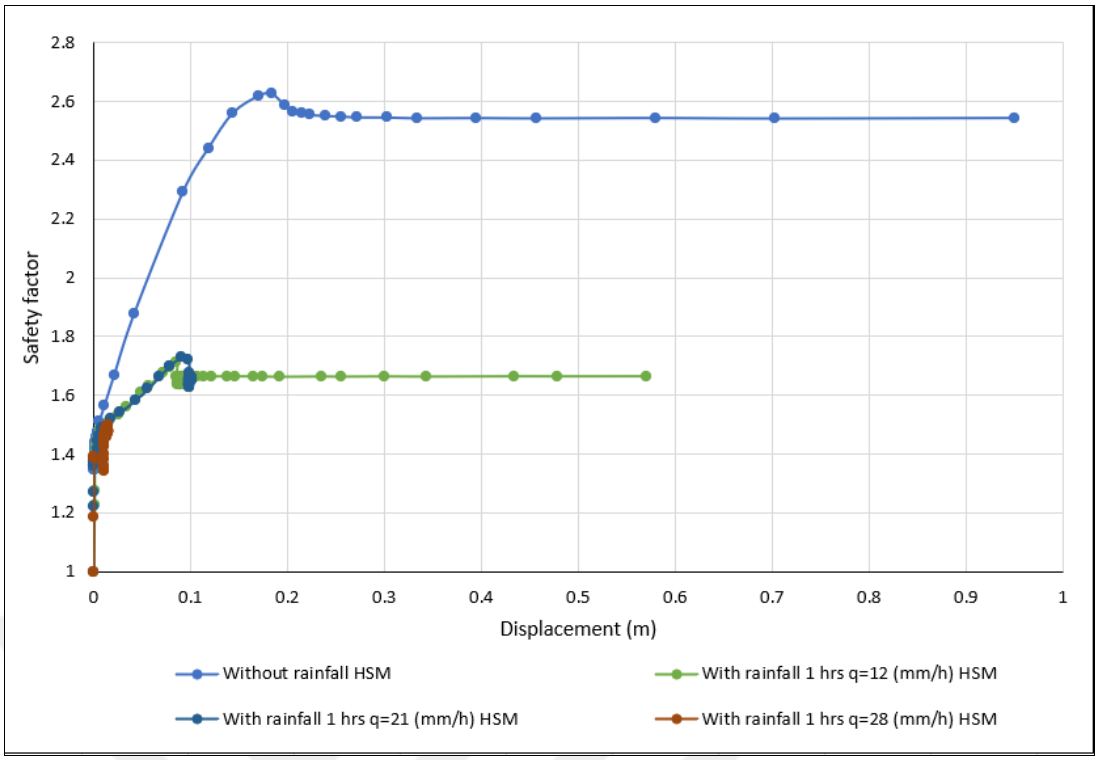

Figure 4.13: Safety Factor of Slope for Fine Mesh MCM and HSM

4.7.1.2 Effect of Rainfall Duration on safety factor by using HSM

The effect of rainfall was simulated by applying the Hardening soil model for different durations of rainfall (1,4,8,16,24) hours and fixed intensities of rainfall (21 mm/hr). The effect of rainfall intensity on the safety factor for different durations of rainfall for slope is shown in Figure 4 -15 A significant reduction in Factor of Safety (FOS) was seen with longer rainfall durations, namely (4,8,16,24) hours. Conversely, with shorter-duration rainfall (1 hour), the FOS decreased less, leading to a reduction in the safety factor by (42%) when it rained for one-hour (46%) when it rained for (4,8,16,24) hours.

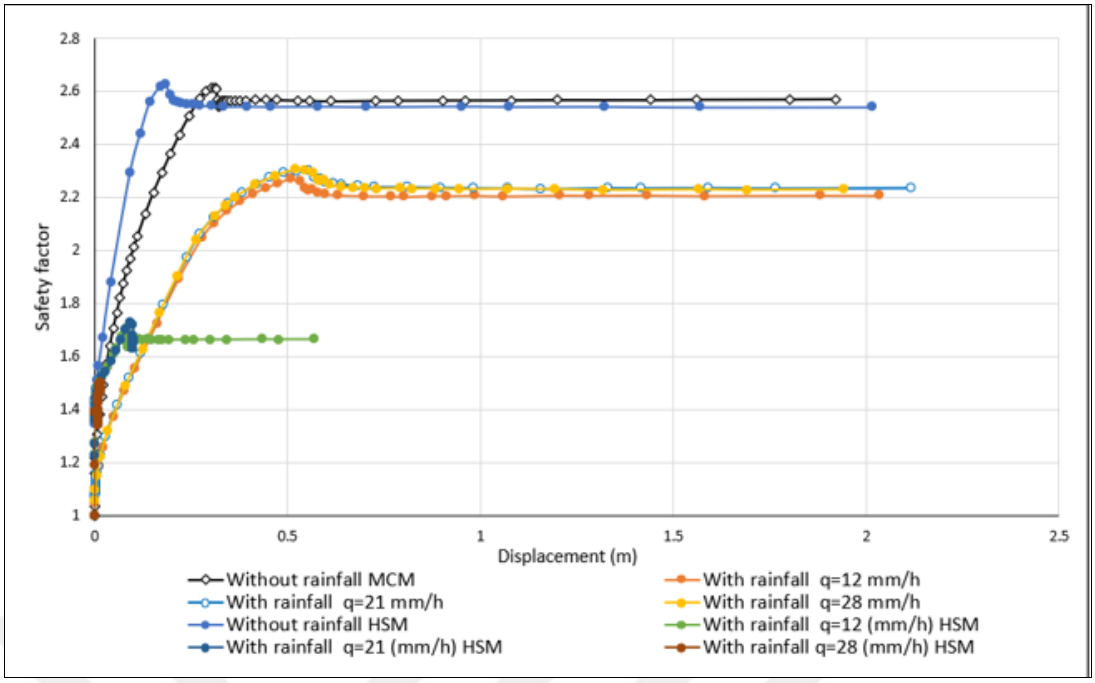

Figure 4.14: Safety Factor of Slope for fine Mesh MCM and HSM

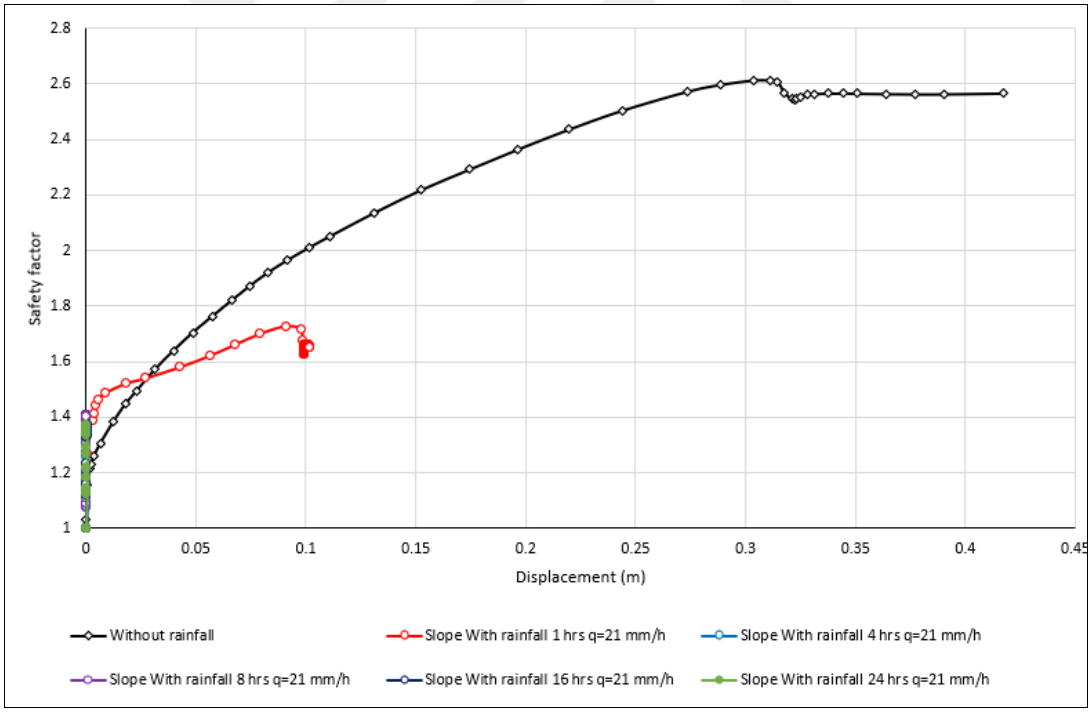

Figure 4.15: Safety Factor of Slope for Different Rainfall Duration for Fine Mesh (HSM)

4.7.2 Effect of rainfall on deformation by using HSM

4.7.2.1 Effect of rainfall intensities on Deformation by using HSM

Rainfall 12, 21, and 28 mm/ hr was simulated on the slope model. The slope soil was modeled using the Hardening soil model. A point was selected at the top edge of the slope to measure deformation values and determine their positions. Table 4.4: Slope Deformations with Different Rainfall Intensities HSMshows the impact of rainfall on the total values of deformations. There was a noticeable settlement in the crest of the slope and a heave in the mid-slope. The findings obtained by modeling rainfall using the Mohr-Coulomb Model, as shown in **Hata! Başvuru kaynağı bulunamadı.**, show no noteworthy settlement was seen in the crest area, but there is an upward movement occurred in the mid of the slope with values greater than the values obtained for the Hardening Soil Model. show the displacement of slope under rainfall effects by using the Hardening soil model. Figures 4- 16 to 4 -21 show the displacement of slope under rainfall effects by using the Hardening soil model.

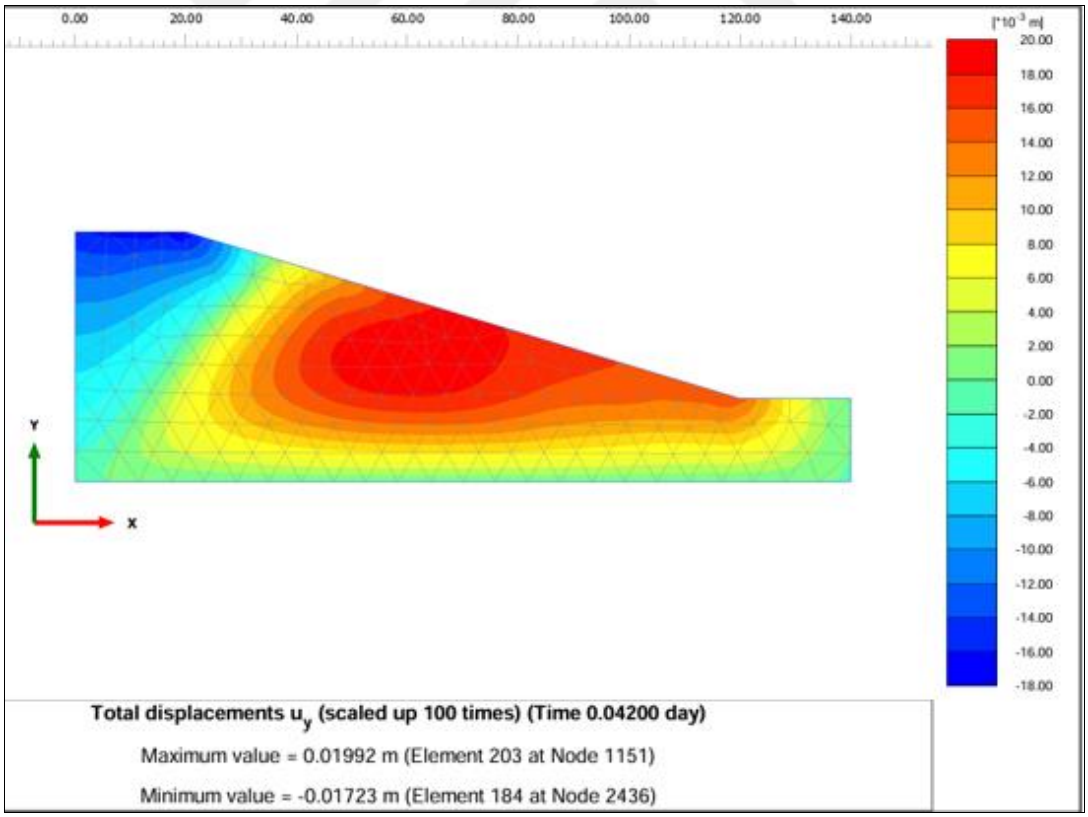

Figure 4.16: Total Displacement of the Slope with Rainfall q=12 mm/hr for HSM

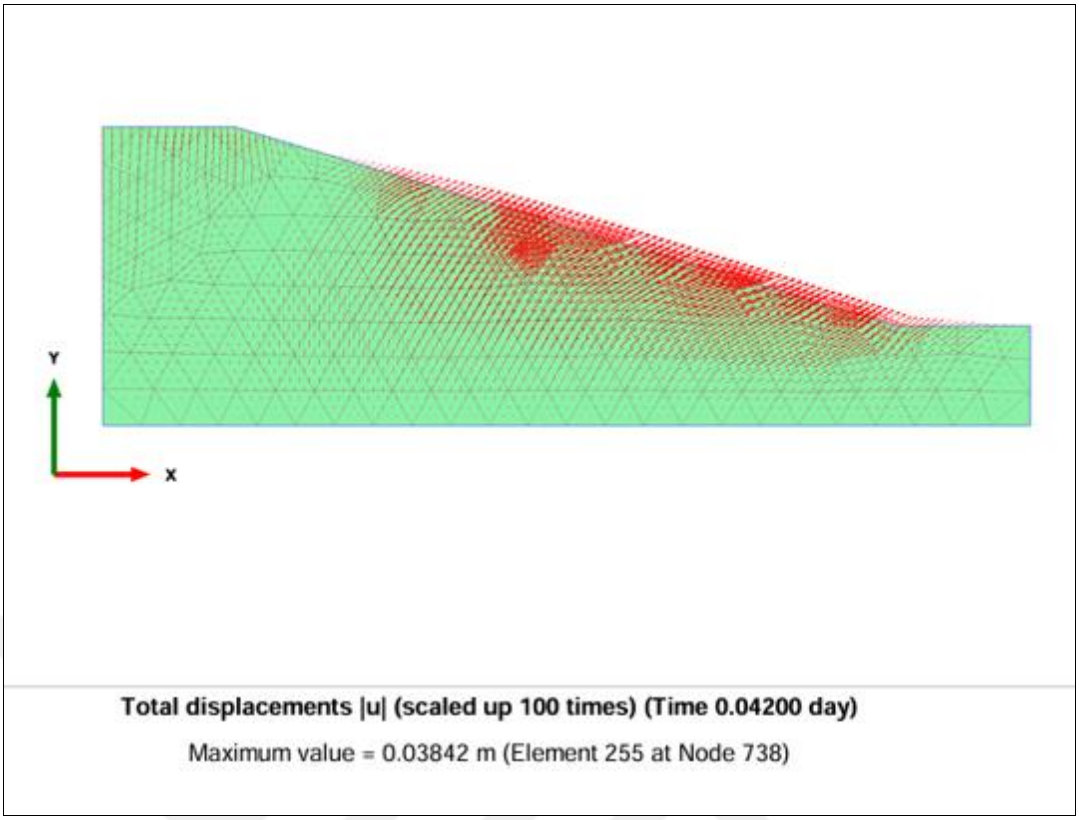

Figure 4.17: Total Displacement Arrows Presentation q=12 mm/hr for HSM

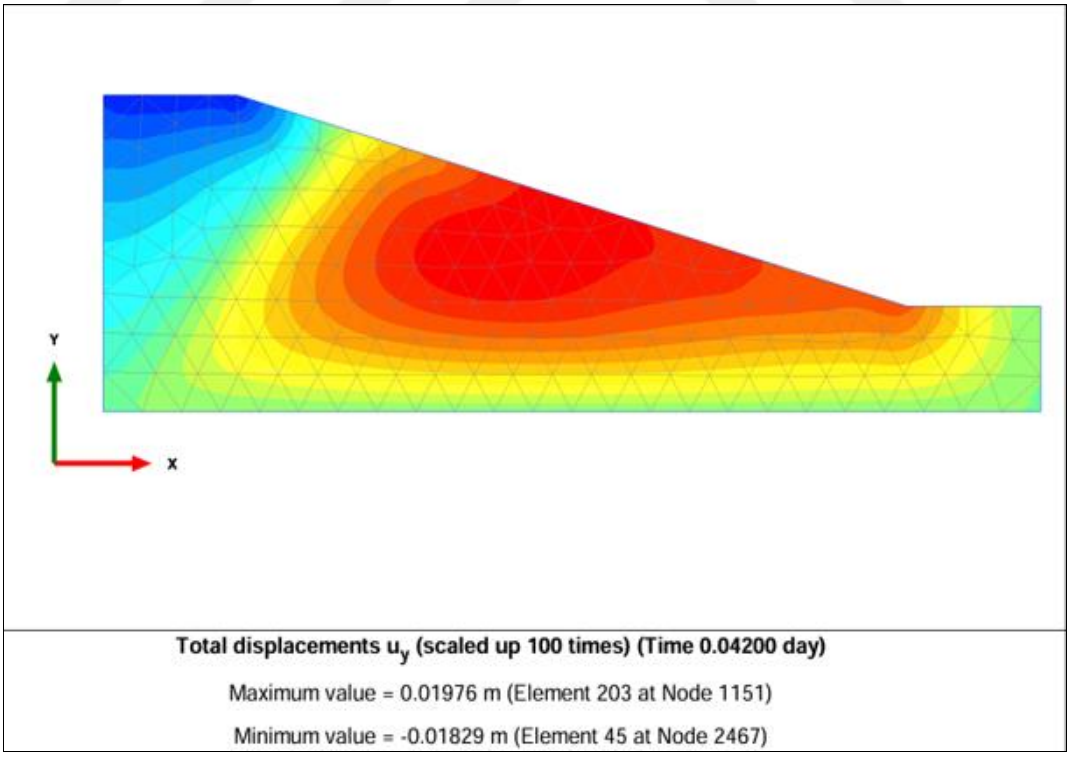

Figure 4.18: Total Displacement of the Slope with Rainfall q=21 mm/hr for HSM

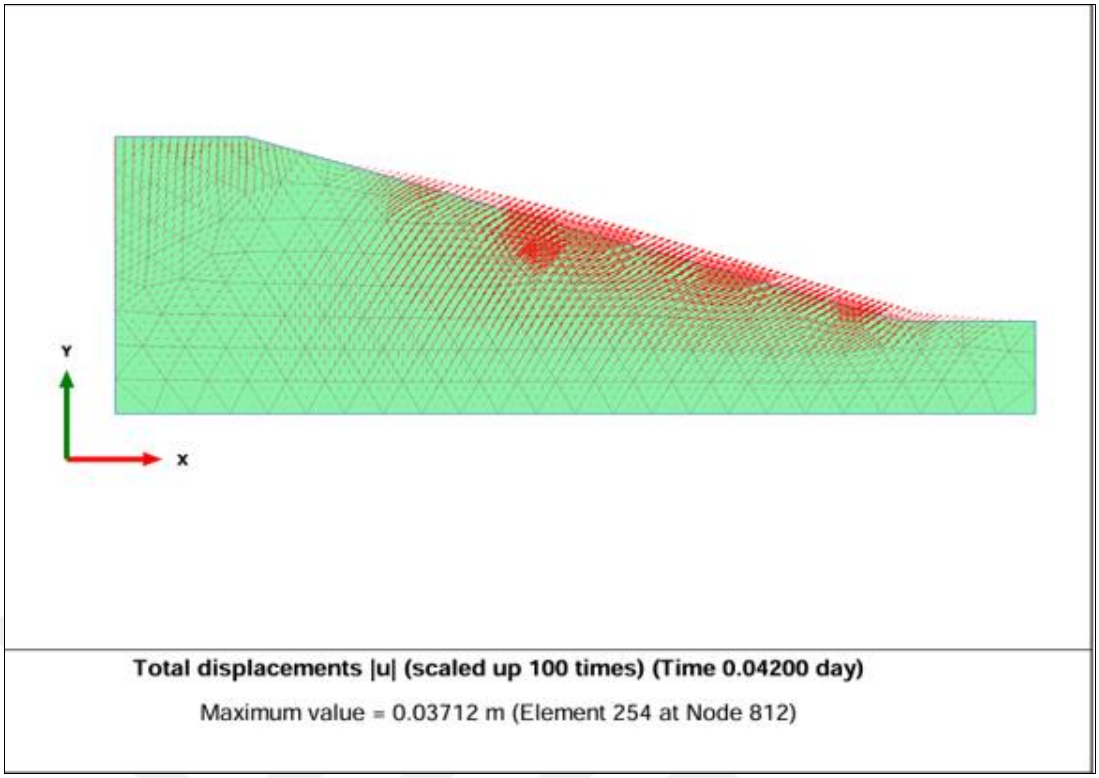

Figure 4.19: Total Displacement Arrows Presentation q= 21 mm/hr for HSM

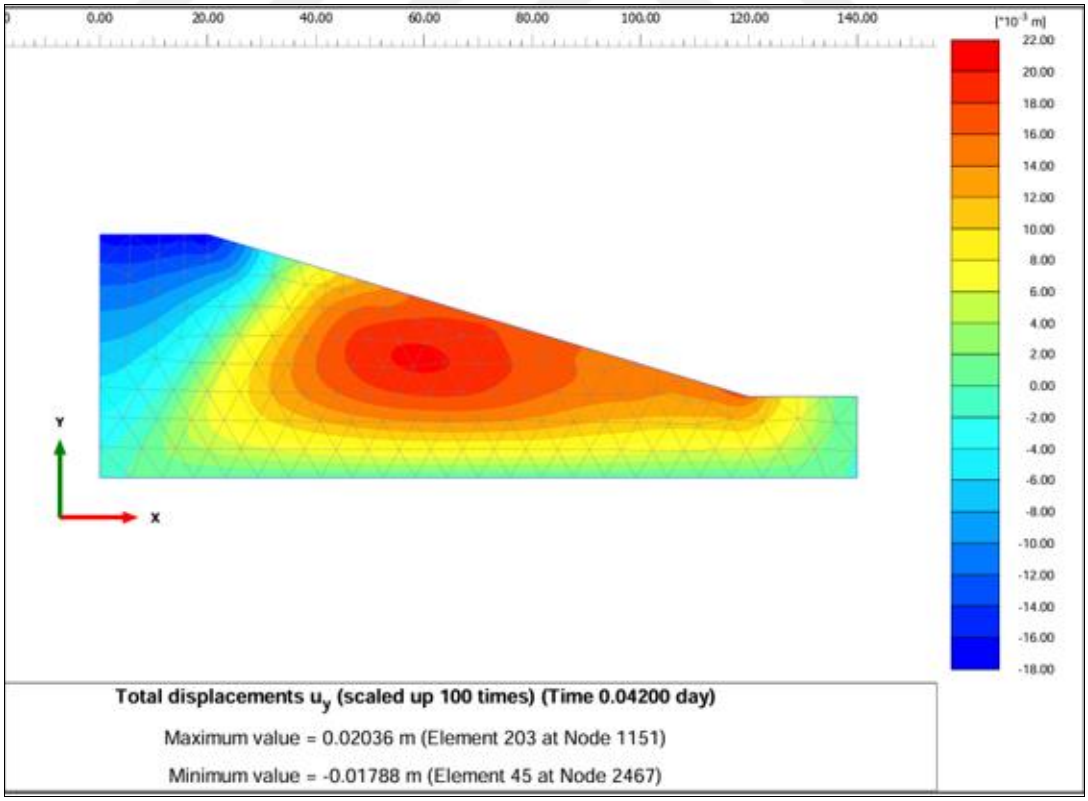

Figure 4.20: Total Displacement of the Slope with Rainfall q=28 mm/hr for HSM

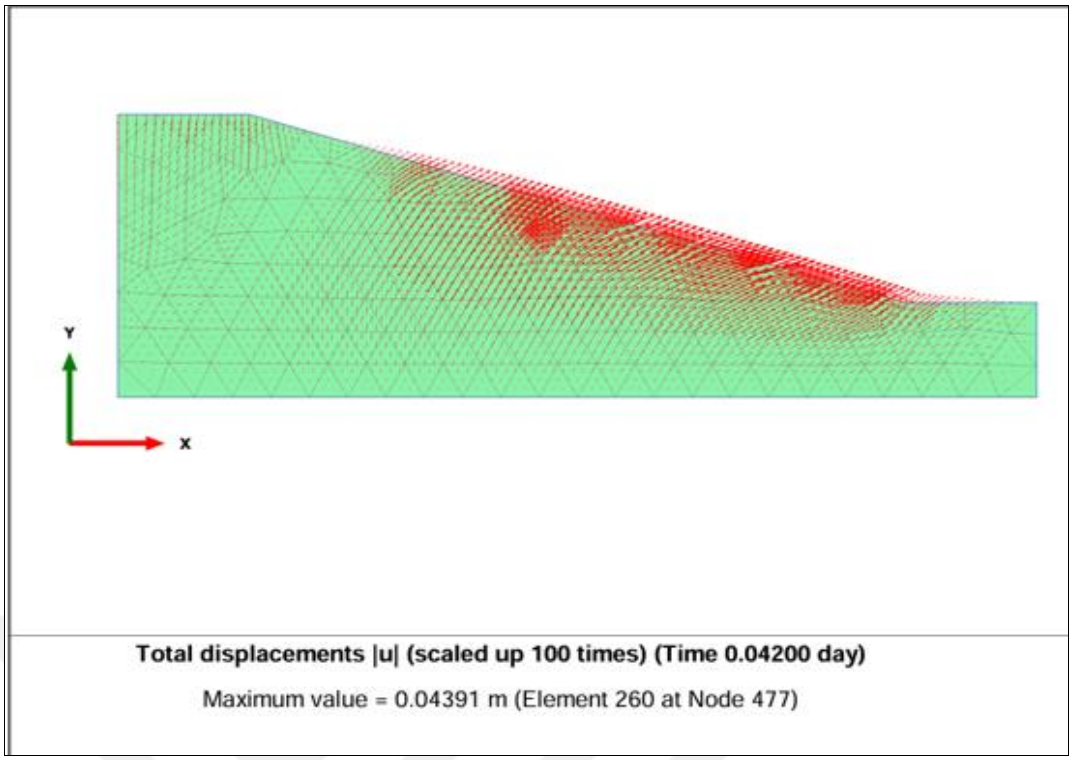

Figure 4.21: Total Displacement Arrows Presentation q= 28 mm/hr for HSM

Table 4.4: Slope Deformations with Different Rainfall Intensities HSM

Rainfall intensity (mm/hr)	Maximum displacement at crest slope (mm)	Maximum heave (upward movement) at mid of the slope (mm)
0	0.3	0.8
12	-17	19
21	-18.3	19.7
28	-17.9	20

*Negative sign means settlement (down ward movement) and the positive is upward movement (heave)

Table 4. 5: Table Comparison of Slope Deformations with Different Rainfall Intensities for MCM and HSM

Rainfall intensity (mm/hr)	MCM		HSM	
	Settlement at crest of a slope (mm)	heave at mid of slope(mm)	Settlement at crest slope (mm)	heave at mid of the slope (mm)
0	-0.02	0.015	0.3	0.8
12	-0.29	41	-17	19
21	-0.108	41	-18.3	19.7
28	-0.142	40	-17.9	20

4.7.2.2 Effect of rainfall duration on deformation by Using HSM

A model simulation was conducted across different rainfall intervals (1, 4, 8, 16, and 24 hours) with a consistent rainfall intensity of 21mm/hr. The slope soil was modelled using the Hardening Soil model. **Hata! Başvuru kaynağı bulunamadı.** shows the impact of rainfall on the total values of deformations. There was a noticeable settlement in the crest of the slope and a corresponding heave in the mid of the slope, While the findings obtained by modelling rainfall using the Mohr-Coulomb Model, as shown in

, show just an upward movement in the slope (crest and mid of the slope).

Table 4.6: Slope Deformations with Different Rainfall Time HSM

Rainfall time (h)	Maximum displacement at the crest of the slope (mm)	Maximum heave at mid of the slope(mm)
0	0.3	0.8
1	-17	19
4	-12	22
8	-14	20
16	-5	12
24	-12	32

Table 4.7: Comparison of Slope Deformations with Different Rainfall Durations for MCM and HSM

Rainfall time (h)	MCM		HSM	
	Maximum displacement at the crest of the slope (mm)	Maximum heave (upward movement) at a slope (mm)	Maximum displacement at the crest of the slope (mm)	Maximum heave at mid of the slope (mm)
0	-0.02	0.015	0.3	0.8
1	-0.108	41	-17	19
4	44	69	-12	22
8	44	72	-14	20
16	50	80	-5	12
24	55	85	-12	32

4.8 Comparison of the Effect of Rainfall on Safety factor Between Coarse, Very Fine Mesh and Fine Mesh By using the Hardening Soil Model (HSM)

4.8.1 Effect of rainfall intensities on safety factor by using HSM

The effect of rainfall was simulated by applying the hardening soil model for rainfall intensity of 12, 21, and 28 mm/ hr over a one-hour rain time using a coarse and very fine mesh. Figure 4.22 show the result of the safety factor for very fine mesh, and Figure 4.23 show the result of the safety factor for coarse mesh obtained. **Hata! Başvuru kaynağı bulunamadı.** shows the Comparison effect of rainfall on safety factors Between coarse, very fine mesh and fine mesh by using the Hardening Soil Model (HSM). Noted the convergence of the safety factor for fine and very fine mesh. However, the safety factor results for the course mesh are different from the fine mesh, as the rainfall did not affect the safety factor for the intensities (12 and 28) mm\hr. In contrast, the safety factor for the rain intensity (21) mm\hr decreased clearly and by 26%.

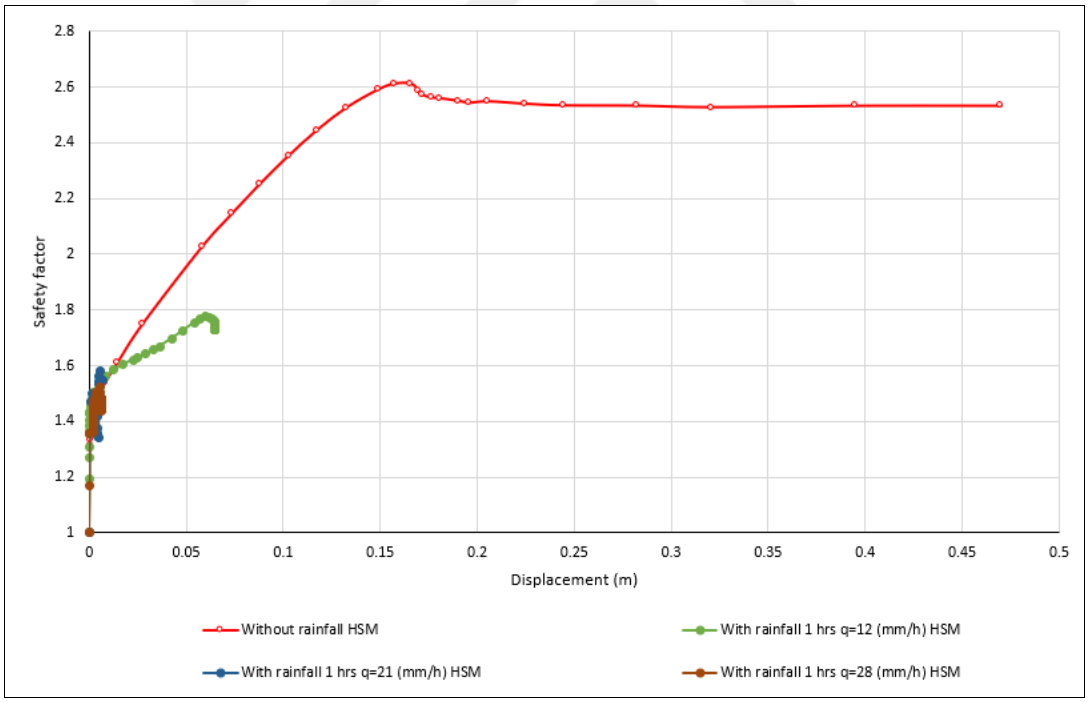

Figure 4.22: Safety Factor of Slope for Very Fine Mesh by using HSM

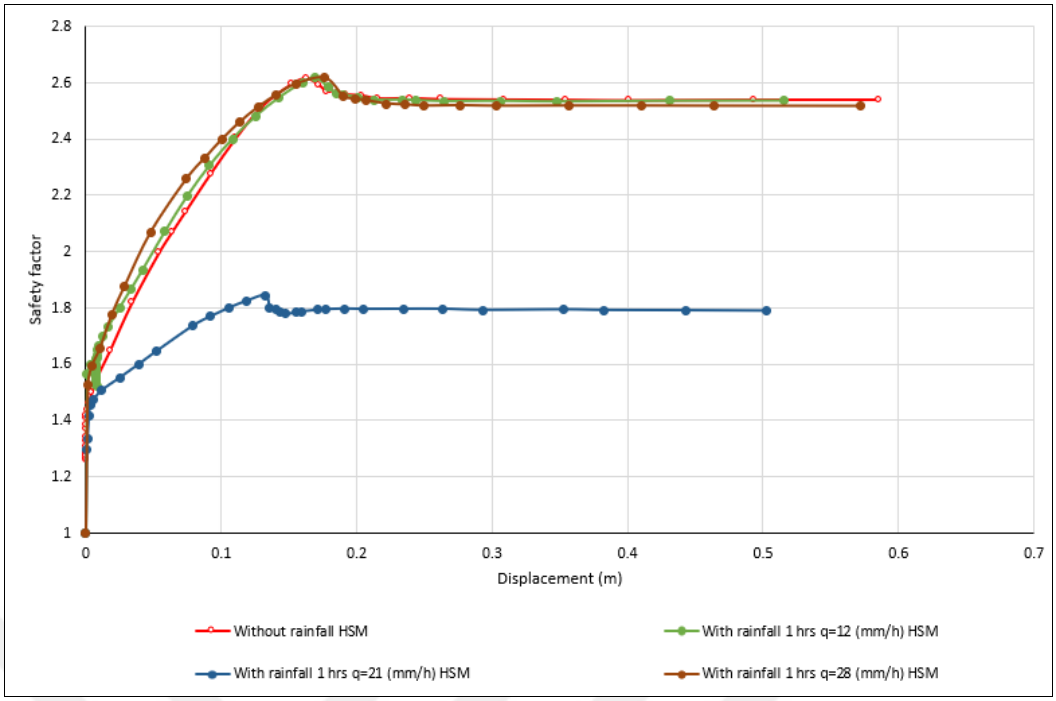

Figure 4.23: Safety Factor of Slope for Coarse Mesh by using HSM

Table 4.8: Comparison of the Effect of Rainfall on Safety Factors between Coarse, Very Fine and Fine Mesh using the Hardening Soil Model (HSM)

Rainfall intensity	Safety factor for fine mesh	Safety factor for very fine mesh	Safety factor for coarse mesh
0	2.54	2.53	2.53
Q= 12 mm\hr	1.66	1.73	2.53
Q=21mm\hr	1.63	1.58	1.87
Q=28mm\hr	1.5	1.52	2.51

4.8.2 Effect of rainfall duration on safety factor by using HSM

The effect of rainfall was simulated by applying the hardening soil model for rainfall intensity of 21 mm/ hr over (1, 4, 8, 16, and 24 hours) using a coarse and very fine mesh. Figure 4.24 show the result of the safety factor for Very fine mesh, and Figure 4.25 show the result for Coarse mesh obtained. By examining figure 4.15 which depicts the safety factor affected by rain for various durations using a Fine Mesh. It can be noted that the safety factor findings for the Coarse and Fine mesh are similar. The behavior of the very fine mesh is different, particularly under rainy one hour.

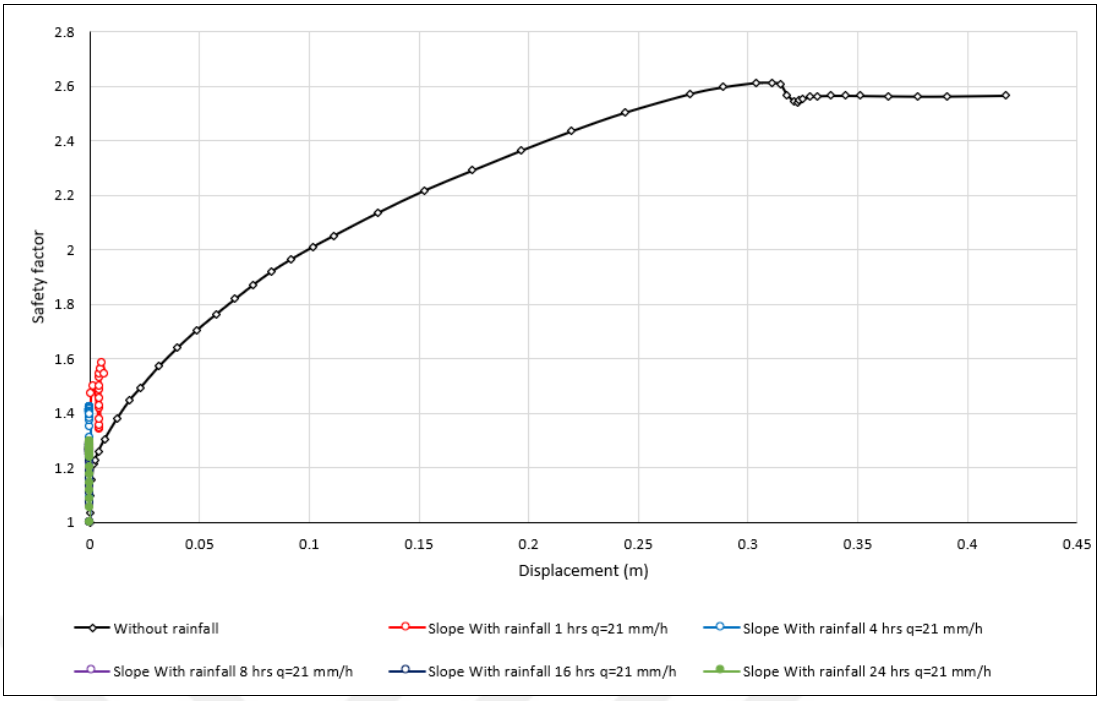

Figure 4.24: Safety Factor of Slope for Very Fine Mesh by using HSM

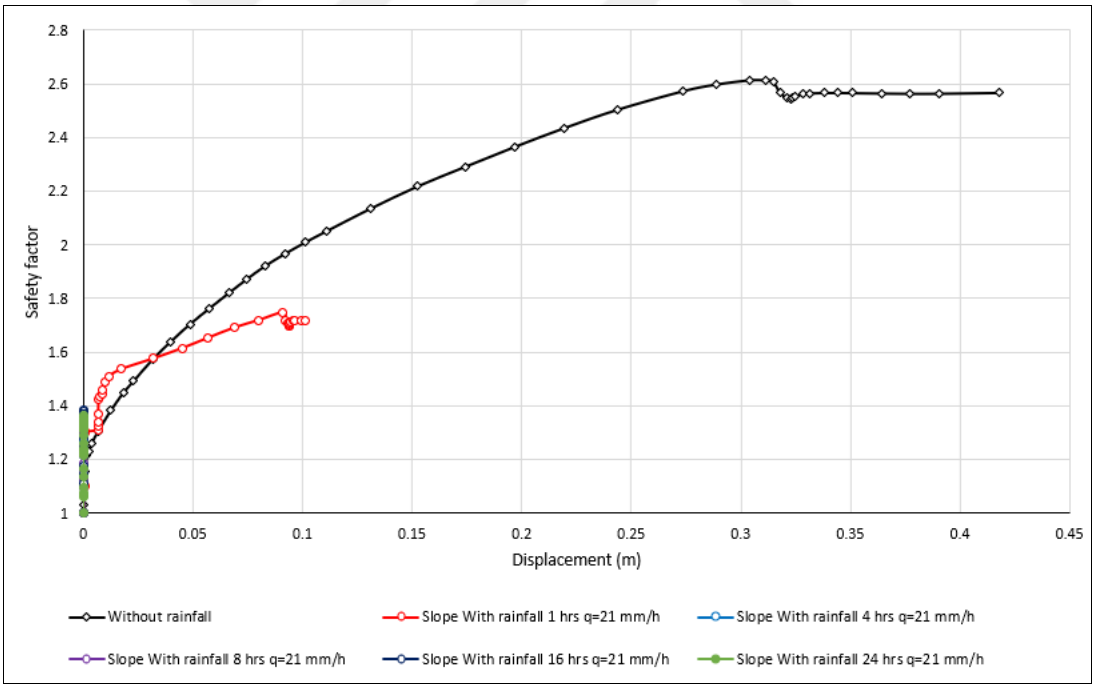

Figure 4.25: Safety Factor of Slope for Coarse Mesh by using HSM

5. CONCLUSION AND RECOMMENDATION

The finite element program PLAXIS 2D 2020 was employed in this study to analyze the effect of rainfall on the safety factor and the displacement of the slope. The PLAXIS 2D 2020 was verified with the models chosen for the study. A comparison was also made between the behavior of the Mohr-Coulomb model (MCM) and the Hardening Soil model (HSM) for simulating rainfall. The following sections summaries the main Conclusions of the study:

5.1Conclusions

1- The safety of the slope is affected by rainfall of different intensities, leading to same percentage 15% reduction at MCM soil model. response under the influence of rainfall, where the safety factor decreased by (15 %) for all rain intensities by the same percentage.

   The effect of rainfall intensity for different periods has a different impact on the safety factor at hardening soil model. The safety factor by application of HSM on the model decreased by (35%) for the rain intensity of 12 mm/hr. Approximately the same percentage for the rain intensity of 21 mm/hr, and the safety factor decreased by 40% for rainfall intensity of 28 mm/hr. Thus, it is confirmed that increasing the duration of rainfall leads to an increase in the decrease in the safety factor.

2- We conclude from this that the soil model affects the values of the safety factor under the influence of rain, as it was shown that the HSM shows sensitive response on the safety factor behavior in the event of rain.

3- The effect of rainfall intensity on the slope, when using the Mohr-Coulomb model for a fixed period and different rainfall intensities, led to deformations in the soil. An upward movement occurred in the mid of the slope area, and no noticeable deformation was observed in the crest of the slope. The upward movement occurs throughout the slope when exposed to rainfall for different periods.

4- The behavior of the Hardening soil model in analyzing the effect of rainfall with different rainfall intensities on the deformations is logical, as it showed the occurrence of settlement and upward movements in parts of the slope; the Mohr-Coulomb model did not show noticeable deformation in the slope top area, but it showed deformation in the mid of the slope.
5- The Hardening Soil model indicates the occurrence of up-and-down movements in the slope when rain falls at different periods. Meanwhile, the Mohr-Coulomb model indicates the occurrence of upward movements throughout the slope without mentioning the occurrence of downward movements.
6- The soil model affects the values of the safety factor under the influence of rainfall, as it was shown that the Hardening Soil model affects the response and behavior in the event of rain differently from MCM.
7- In the absence of rain, HSM behaves the same as the MCM, but there is a difference in the presence of rain.

8- The simulation of rainfall effects using the Hardening Soil Model (HSM) generated varying results depending on the intensity of rainfall and the mesh size used. The choice of mesh size impacts the simulation results, with finer meshes showing more consistent behavior under different rainfall intensities. In comparison, coarser meshes may produce different results, especially under moderate rainfall intensity.

5.2 Recommendations

Using the Hardening Soil Model (HSM) to study the effect of rainfall on the factor of safety and displacement in the PLAXIS 2D program. Earth dams should be analyzed with soil models not only with MCM but also with HSM model to check the settlements at the crest under rainy conditions.

5.3 Future studies

1. Study rainfall's effect on the safety factor and displacement with a structure on a slope.

2. A study on occurring earthquakes (dynamic analysis) after rainfall.
3. Changing the slope angle, studying soils of different types.

REFERENCES

[1] J. Kellett, A. Caravani, and F. Pichon, “Financing disaster risk reduction: Towards.” 2014.

[2] Mr. Digvijay P. Salunkhe, Assist. Prof. Guruprasd Chvan, Ms. Rupa N. Bartakke, and Ms. Pooja R Kothavale, “An Overview on Methods for Slope Stability Analysis,” Int. J. Eng. Res., vol. V6, no. 03, pp. 528–535, 2017, doi: 10.17577/ijertv6is030496.

[3] Y. C. Yang, H. G. Xing, X. G. Yang, J. W. Zhou, and M. Pastor, “Determining the critical slip surface of three-dimensional soil slopes from the stress fields solved using the finite element method,” Math. Probl. Eng., vol. 2016, 2016, doi: 10.1155/2016/7895615.

[4] X. Chen, Y. Wu, Y. Yu, J. Liu, X. F. Xu, and J. Ren, “A two-grid search scheme for large-scale 3-D finite element analyses of slope stability,” Comput. Geotech., vol. 62, pp. 203–215, 2014, doi: 10.1016/j.compgeo.2014.07.010.

[5] BRAJA M. DAS, Principles of Geotechnical Engineeringitle, Seventh Ed. USA, 2009.

[6] H. Kumsar, Ö. Aydan, and R. Ulusay, “Dynamic and static stability assessment of rock slopes against wedge failures,” Rock Mech. Rock Eng., vol. 33, no. 1, pp. 31–51, 2000, doi: 10.1007/s006030050003.

[7] L. Li and X. Chu, “Failure Mechanism and Factor of Safety for Spatially Variable Undrained Soil Slope,” Adv. Civ. Eng., vol. 2019, 2019, doi: 10.1155/2019/8575439.

[8] L. Li and X. Chu, “Risk assessment of slope failure by representative slip surfaces and response surface function,” KSCE J. Civ. Eng., vol. 20, no. 5, pp. 1783–1792, 2016, doi: 10.1007/s12205-015-2243-6.

[9] J. Huang, A. V. Lyamin, D. V. Griffiths, K. Krabbenhoft, and S. W. Sloan, “Quantitative risk assessment of landslide by limit analysis and random fields,” Comput. Geotech., vol. 53, pp. 60–67, 2013, doi: 10.1016/j.compgeo.2013.04.009.

[10] J. M. Duncan, S. G. Wright, and B. T. L, “Soil Strength and Slope Stability,” John Wiley Sons, vol. 2, no. 1, pp. 37–72, 2014.

[11] Rocscience, “Application of the Finite Element Method to Slope Stability,” Proc. Inst. Civ. Eng., no. 1, pp. 2001–2004, 2001.

[12] Y. H. Chok, “Modelling the Effects of Soil Variability and Vegetation on the Stability of Natural,” no. October, 2008.

[13] F. G. Bell and R. R. Maud, “Examples Of Landslıdes Assocıated Wıth The Natal Group And Pıetermarıtzburg Formatıon In The Greater Durban Area Of

Natal, South AfrıcA," Bull. Int. Assoc. Eng. Geol., pp. 11–20., 1996, doi: https://doi.org/10.1007/BF02594936.

[14] R. G. Singh, G. A. Botha, N. P. Richards, and T. S. McCarthy, "Holocene landslides in KwaZulu-Natal South Africa," South African J. Geol., vol. 111, no. 1, pp. 39–52, 2008, doi: 10.2113/gssajg.111.1.39.

[15] D. L. Webb and A. B. A. Brink, "Slope failure on shale of the Pietermaritzburg Shale Formation, Mayat Place, Durban," Eng. Geol. South. Africa, vol. 3, pp. 107–111, 1983.

[16] K. A. Johnson and N. Sitar, "Hydrologic conditions leading to debris-flow initiation," Can. Geotech. J., vol. 27, no. 6, pp. 789–801, 1990, doi: 10.1139/t90-092.

[17] D.-G. Fredlung and R. Rahardjo, "Soil Mechanics for Unsaturated Soils. A Wiley-Interscience Publication. John Wiley & Sons.," 1993.

[18] "Relationship_between_rainfall_and_landsl.pdf."

[19] T. T. Lim, H. Rahardjo, M. F. Chang, and D. G. Fredlund, "Effect of rainfall on matric suctions in a residual soil slope," Can. Geotech. J., vol. 33, no. 4, pp. 618–628, 1996, doi: 10.1139/cgj-33-4-618.

[20] C. W. W. Ng and Q. Shi, "Influence of rainfall intensity and duration on slope stability in unsaturated soils," Q. J. Eng. Geol., vol. 31, no. 2, pp. 105–113, 1998, doi: 10.1144/GSL.QJEG.1998.031.P2.04.

[21] P. Flentje, R. Chowdhury, and a S. Miner, "Periodic and continuous landslide monitoring to assess landslide frequency — selected Australian examples," vol. 2010, no. 2008, pp. 1863–1874, 2010.

[22] J. H. Zhu, M. M. Zaman, and S. A. Anderson, "Modelling of shearing behaviour of a residual soil with recurrent neural network," Int. J. Numer. Anal. Methods Geomech., vol. 22, no. 8, pp. 671–687, 1998, doi: 10.1002/(SICI)1096-9853(199808)22:8<671::AID-NAG939>3.0.CO;2-Y.

[23] A. Dai, K. E. Trenberth, and T. R. Karl, "Effects of clouds, soil moisture, precipitation, and water vapor on diurnal temperature range," J. Clim., vol. 12, no. 8 PART 2, pp. 2451–2473, 1999, doi: 10.1175/1520-0442(1999)012<2451:eocsmp>2.0.co;2.

[24] X. Zhang, L. A. Vincent, W. D. Hogg, and A. Niitsoo, "Temperature and precipitation trends in Canada during the 20th century," Atmos. - Ocean, vol. 38, no. 3, pp. 395–429, 2000, doi: 10.1080/07055900.2000.9649654.

[25] I. Tsaparas, H. Rahardjo, D. G. Toll, and E. C. Leong, "Infiltration characteristics of two instrumented residual soil slopes," Can. Geotech. J., vol. 40, no. 5, pp. 1012–1032, 2003, doi: 10.1139/t03-049.

[26] H. Rahardjo, K. J. Hritzuk, E. C. Leong, and R. B. Rezaur, "Effectiveness of horizontal drains for slope stability," Eng. Geol., vol. 69, no. 3–4, pp. 295–308, 2003, doi: 10.1016/S0013-7952(02)00288-0.

[27] D. G. Fredlund and H. Rahardjo, "Soil mechanics principles for highway engineering in arid regions," Transp. Res. Rec., vol. 1137, pp. 1–11, 1987.

[28] D. G. Fredlund and N. R. Morgenstern, "Stress state variables for unsaturated soils," J. Geotech. Eng. Div., vol. 103, no. 5, pp. 447–466, 1977.

[29] R. D. Holtz, W. D. Kovacs, and T. C. Sheahan, An introduction to geotechnical engineering, vol. 733. Prentice-Hall Englewood Cliffs, 1981.

[30] K. Terzaghi, R. B. Peck, and G. Mesri, Soil mechanics in engineering practice. John wiley & sons, 1996.

[31] D. G. Fredlund and H. Rahardjo, Soil mechanics for unsaturated soils. John Wiley & Sons, 1993.

[32] J. Krahn, "â€ œStability Modeling with SLOPE/Wâ€, GEOSLOPE/W International," Ltd. Canada, 2004.

[33] L. W. Abramson, H. M. Macdonald, T. S. L. Parsons, Q. & Douglas, S. Francisco, and G. M. B. Parsons, "SLOPE STABILITY AND STABILIZATION METHODS Second Edition," pp. 1–54, 2002.

[34] J. Lynn Peterson and J. Lynn, "Probability analysis of slope stability Probability analysis of slope stability Recommended Citation Recommended Citation," 1999, [Online]. Available: https://researchrepository.wvu.edu/etd

[35] S. S. Rao, The finite element method in engineering. Butterworth-heinemann, 2017.

[36] R. A. Sauer, T. X. Duong, K. K. Mandadapu, and D. J. Steigmann, "A stabilized finite element formulation for liquid shells and its application to lipid bilayers," J. Comput. Phys., vol. 330, pp. 436–466, 2017.

[37] G. A. (Eds. . Griffiths, D. V., & Fenton, Probabilistic methods in geotechnical engineering. 2007.

[38] J. M. Duncan, "State of the Art : Limit Equilmrium and Finite Element Analysis of Slopes," J. Geotech. Eng., no. July, pp. 577–596, 1996.

[39] D. V Griffiths and P. A. Lane, "Slope stability analysis by finite elements," Geotechnique, vol. 49, no. 3, pp. 387–403, 1999.

[40] R. E. Hammah, J. H. Curran, T. Yacoub, and B. Corkum, "Stability analysis of rock slopes using the finite element method," in Proceedings of the ISRM regional symposium EUROCK, 2004.

[41] R. . Yu, R. Salgado, W. Sloan, and J. M. Kim, "Limit_Analysis_versus_Limit_Equilibrium.pdf," J Geotech Geoenviron Eng ASCE, vol. 124. pp. 1–11, 1998.

[42] B. Zhang and H. Chen, "Analysis on abutment aseismatic stability by using finite element and rigid body limit equilibrium method," Chinese J. Rock Mech. Eng., vol. 20, no. 5, pp. 665–670, 2001.

[43] H. Cheng and X. Zhou, "A novel displacement-based rigorous limit equilibrium method for three-dimensional landslide stability analysis," Can. Geotech. J., vol. 52, no. 12, pp. 2055–2066, 2015.

[44] H. Khabbaz, B. Fatahi, and C. Nucifora, "Finite element methods against limit equilibrium approaches for slope stability analysis," in Australia New Zealand Conference on Geomechanics, Geomechanical Society and New Zealand Geotechnical Society, 2012.

[45] J. C. Reginald Hammah, Thamer Yacoub, Brent Corkum, “a Comparison of Finite Element Slope Stability Analysis With Conventional Limit-Equilibrium Investigation,” 2010.

[46] Y. M. Cheng, T. Lansivaara, and W. B. Wei, “Two-dimensional slope stability analysis by limit equilibrium and strength reduction methods,” Comput. Geotech., vol. 34, no. 3, pp. 137–150, 2007.

[47] J. M. Duncan and S. G. Wright, “Soil Strength and Slope Stability”. John Wiley and Sons. Inc. Hoboken. New Jersey 297p,” 2005.

[48] E. Bahsan, H. J. Liao, J. Ching, and S. W. Lee, “Statistics for the calculated safety factors of undrained failure slopes,” Eng. Geol., vol. 172, no. April, pp. 85–94, 2014, doi: 10.1016/j.enggeo.2014.01.005.

[49] J. E. Norris et al., Slope stability and erosion control: ecotechnological solutions. Springer Science & Business Media, 2008.

[50] A. W. Bishop, “First Technical Session : General Theory of Stability of Slopes The Use Of The Slıp Cırcle In The Stabılıty Analysıs Of SlopeS,” Géotechnique. pp. 7–16, 1955. [Online]. Available: https://www.icevirtuallibrary.com/doi/epdf/10.1680/geot.1955.5.1.7

[51] D. P. Deng, L. Li, and L. H. Zhao, “A new method of sliding surface searching for general stability of slope based on Janbu method,” Rock Soil Mech., vol. 32, no. 3, pp. 891–898, 2011.

[52] T. Bai, T. Qiu, X. Huang, and C. Li, “Locating global critical slip surface using the Morgenstern-Price method and optimization technique,” Int. J. Geomech., vol. 14, no. 2, pp. 319–325, 2014.

[53] J. K. Gilbert, C. Boulter, and M. Rutherford, “Models in explanations, Part 1: Horses for courses?,” Int. J. Sci. Educ., vol. 20, no. 1, pp. 83–97, 1998.

[54] M. J. Anderson and P. J. Whitcomb, RSM simplified: optimizing processes using response surface methods for design of experiments. Productivity press, 2016.

[55] W. Nie, D. Feng, W. Lohpaisankrit, C. Li, J. Yuan, and Y. Chen, “A dynamic Bayesian network-based model for evaluating rainfall-induced landslides,” Bull. Eng. Geol. Environ., vol. 78, no. 3, pp. 2069–2080, 2019, doi: 10.1007/s10064-017-1221-2.

[56] A. Zaki, M. Al-Qasi, A. Majid, and A. Al-Rammahi, “Seepage And Slope Stabılıty Analysıs Of Levees Subjected To Floodıng (Theorıtıcal Study),” J. Eng. Sustain. Dev., vol. 22, no. 03, 2018, doi: 10.31272/jeasd.2018.3.10.

[57] D. Bhattacherjee and B. V. S. Viswanadham, Use of Hybrid Geosynthetics in Mitigating Rainfall-Induced Slope Instability, vol. 28. Springer Singapore, 2019. doi: 10.1007/978-981-13-6701-4_45.

[58] L. Z. Mase, “Slope Stability and Erosion-Sedimentation Analyses Along Sub-watershed of Muara Bangkahulu River in Bengkulu City, Indonesia,” E3S Web Conf., vol. 148, 2020, doi: 10.1051/e3sconf/202014803002.

[59] H. F. Yeh and Y. J. Tsai, “Effect of variations in long-duration rainfall intensity on unsaturated slope stability,” Water (Switzerland), vol. 10, no. 4, 2018, doi: 10.3390/w10040479.

[60] S. Merat, L. Djerbal, and R. Bahar, Rainfall Effect on Slope Stability Using Numerical Analysis. Springer International Publishing, 2018. doi: 10.1007/978-3-030-01665-4_97.

[61] Y. Pan, G. Wu, Z. Zhao, and L. He, "Analysis of rock slope stability under rainfall conditions considering the water-induced weakening of rock," Comput. Geotech., vol. 128, no. 999, p. 103806, 2020, doi: 10.1016/j.compgeo.2020.103806.

[62] Z. Zhang, X. Fu, Q. Sheng, D. Yin, Y. Zhou, and J. Huang, "Effect of Rainfall Pattern and Crack on the Stability of a Red Bed Slope: A Case Study in Yunnan Province," Adv. Civ. Eng., vol. 2021, 2021, doi: 10.1155/2021/6658211.

[63] J. Qian, D. Sun, G. Li, and Y. Wu, "Study on the Influence of Various Rainfall Types on the Stability of High and Steep Slopes," Geofluids, vol. 2021, 2021, doi: 10.1155/2021/7906573.

[64] J. Nazrien Ng et al., "The Effect of Extreme Rainfall Events on Riverbank Slope Behaviour," Front. Environ. Sci., vol. 10, no. March, pp. 1–14, 2022, doi: 10.3389/fenvs.2022.859427.

[65] T. Bračko, B. Žlender, and P. Jelušič, "Implementation of Climate Change Effects on Slope Stability Analysis," Appl. Sci., vol. 12, no. 16, 2022, doi: 10.3390/app12168171.

[66] Z. Deng et al., "In Situ Experimental Study of Natural Diatomaceous Earth Slopes under Alternating Dry and Wet Conditions," Water (Switzerland), vol. 14, no. 5, 2022, doi: 10.3390/w14050831.

[67] J. S. Gidon and S. Sahoo, "Hydrological effects on Rainfall-Induced Slope instability: A Case Study," Res. Sq., pp. 1–27, 2023.

[68] S. Dandagawhal, "Settlement analysis of pile foundation using plaxis 2D," Int. J. Sci. Res., vol. 8, 2019.

[69] R. Manual, "Plaxis 2D reference manual," Plaxis Ref. Man., pp. 167–167, 2017.

[70] D. M. Potts, L. Zdravković, T. I. Addenbrooke, K. G. Higgins, and N. Kovačević, Finite element analysis in geotechnical engineering: application, vol. 2. Thomas Telford London, 2001.

[71] Z. Alsharifi, M. Shakir Mahmood, A. Akhtarpour, Numerical Evaluation of Slope Stability for Construction and Seismic Loads: Case Study, International Journal of Engineering, Transactions A: Basics Vol. 34, No. 7, (2021) 1602-1610.

[72] M. Budhu, Soil mechanics and foundations. John Wiley and Sons, 2010.

[73] I. F. Hasan and Y. N. Saeed, "Analysis of Rainfall Data-Iraq North.pdf," Al-Rafidain Eng. J., vol. 25, pp. 105–117.

APPENDICES

Appendix A: PLAXIS 2D 2020 Program Outputs

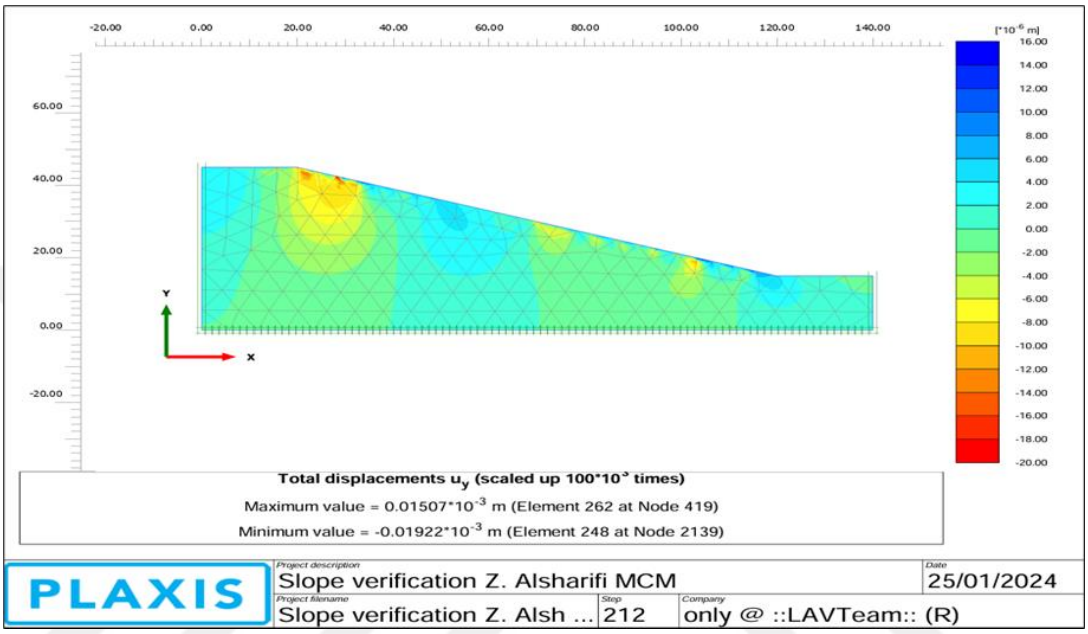

Figure A.1: PLAXIS 2D 2020 Program Outputs

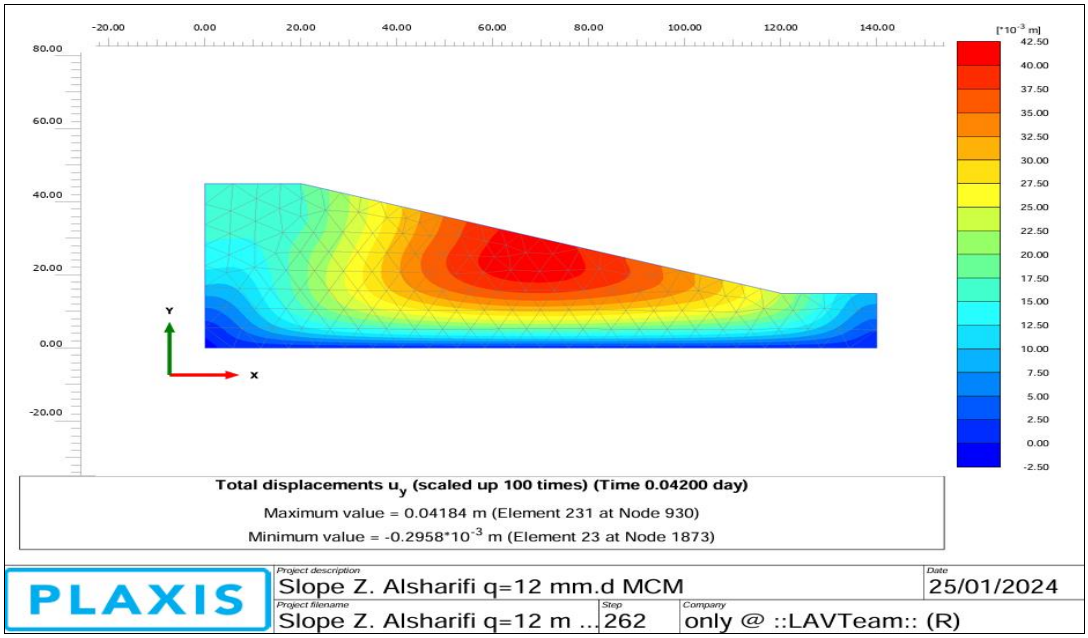

Figure A.1: (Cont.) PLAXIS 2D 2020 Program Outputs

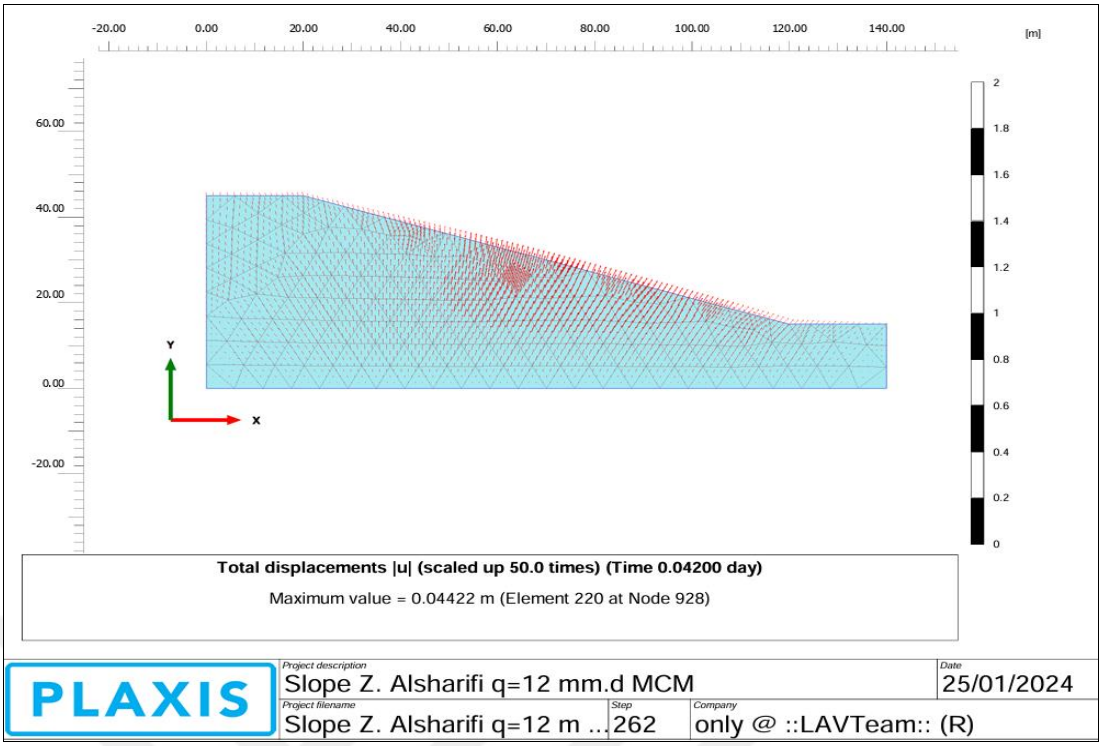

Figure A.1: (Cont.) PLAXIS 2D 2020 Program Outputs

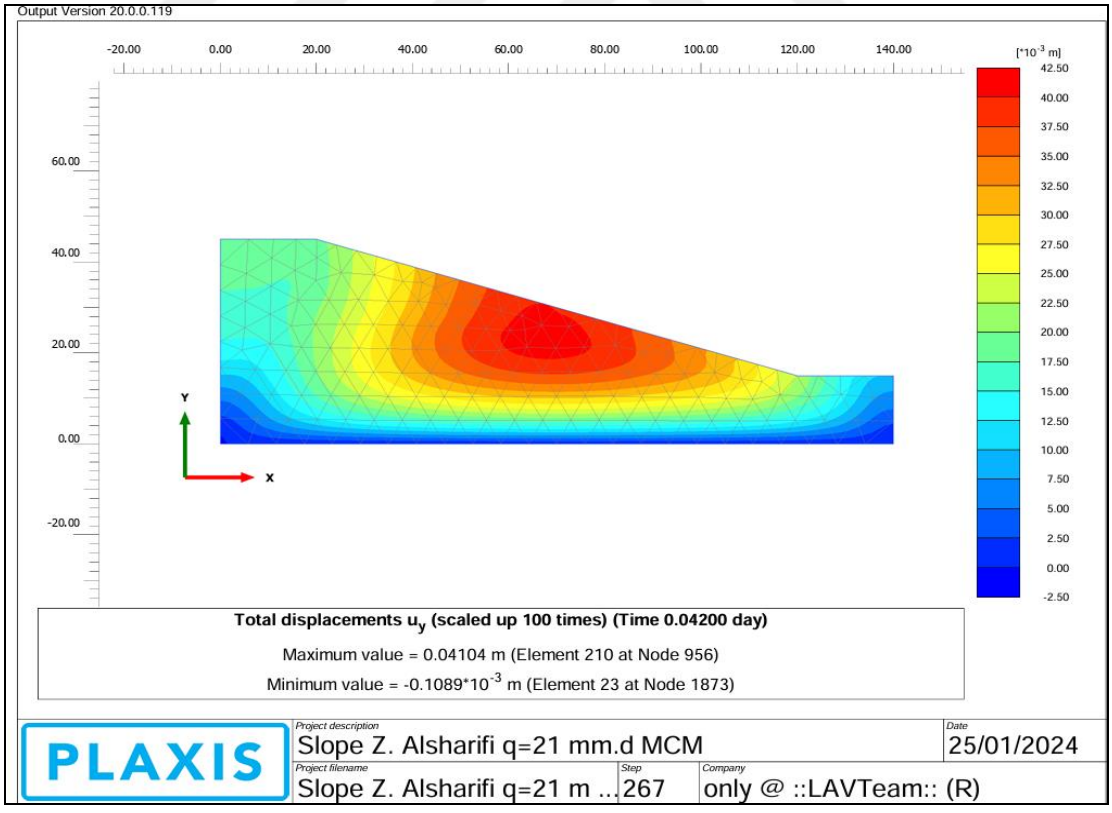

Figure A.1: (Cont.) PLAXIS 2D 2020 Program Outputs

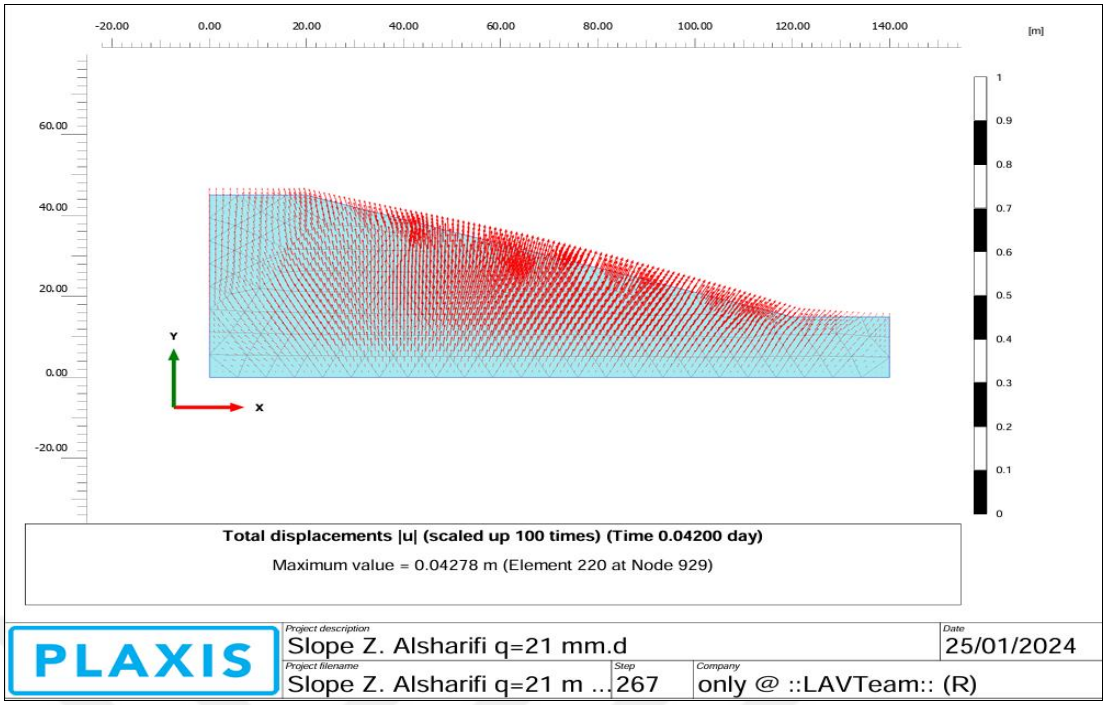

Figure A.1: (Cont.) PLAXIS 2D 2020 Program Outputs

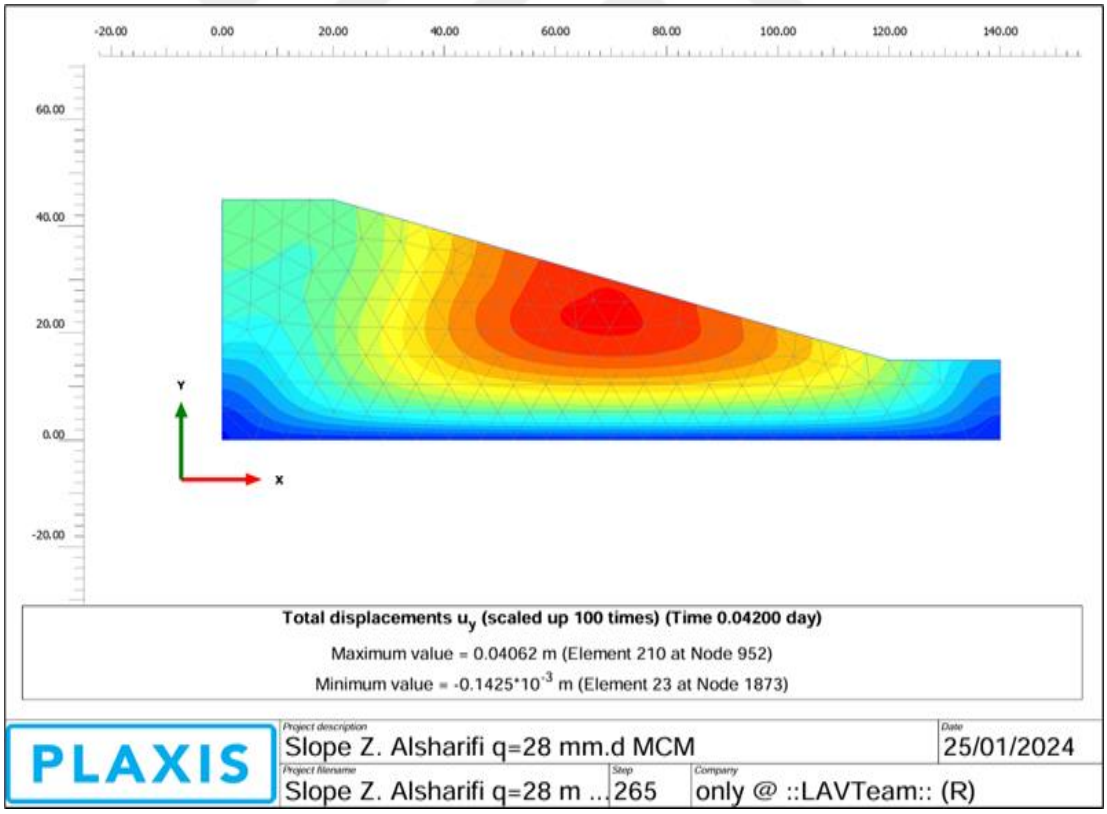

Figure A.1: (Cont.) PLAXIS 2D 2020 Program Outputs

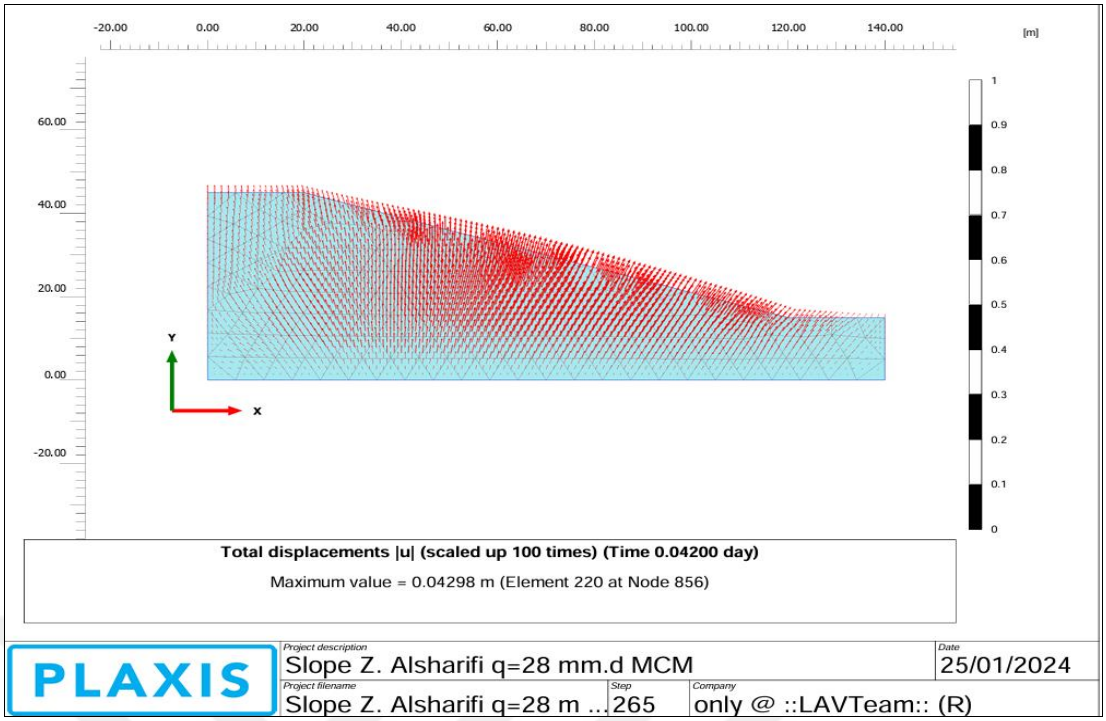

Figure A.1: (Cont.) PLAXIS 2D 2020 Program Outputs

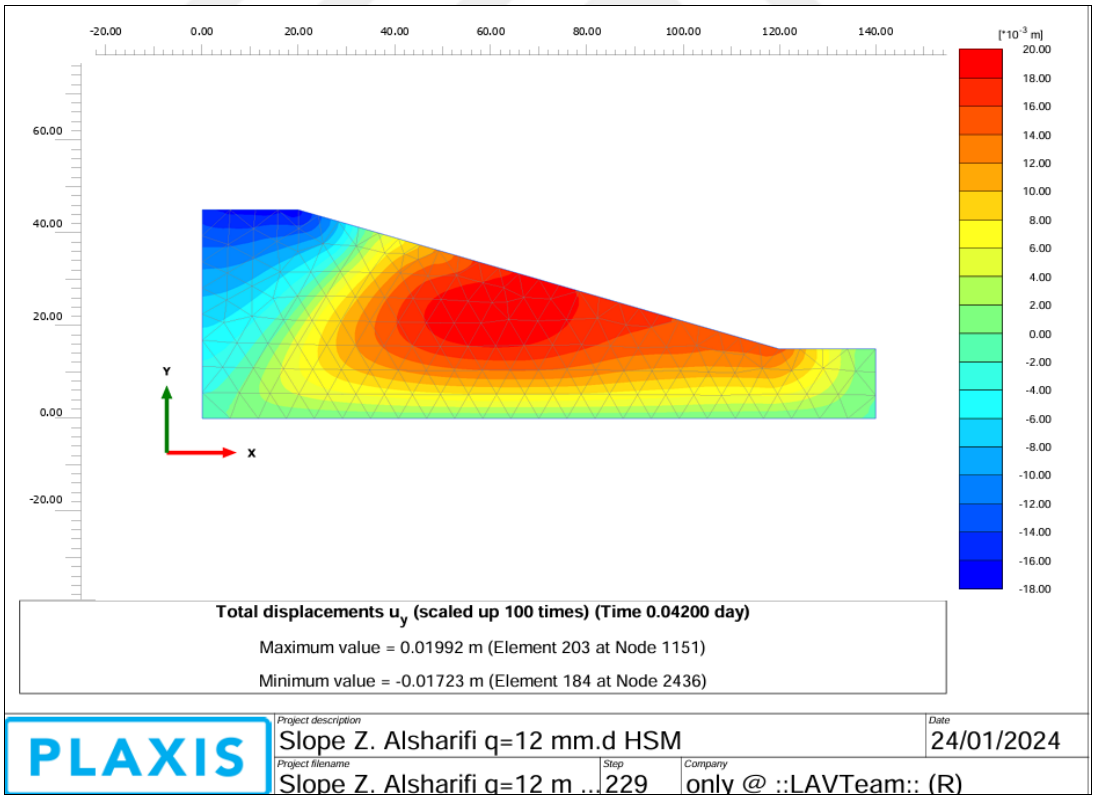

Figure A.1: (Cont.) PLAXIS 2D 2020 Program Outputs

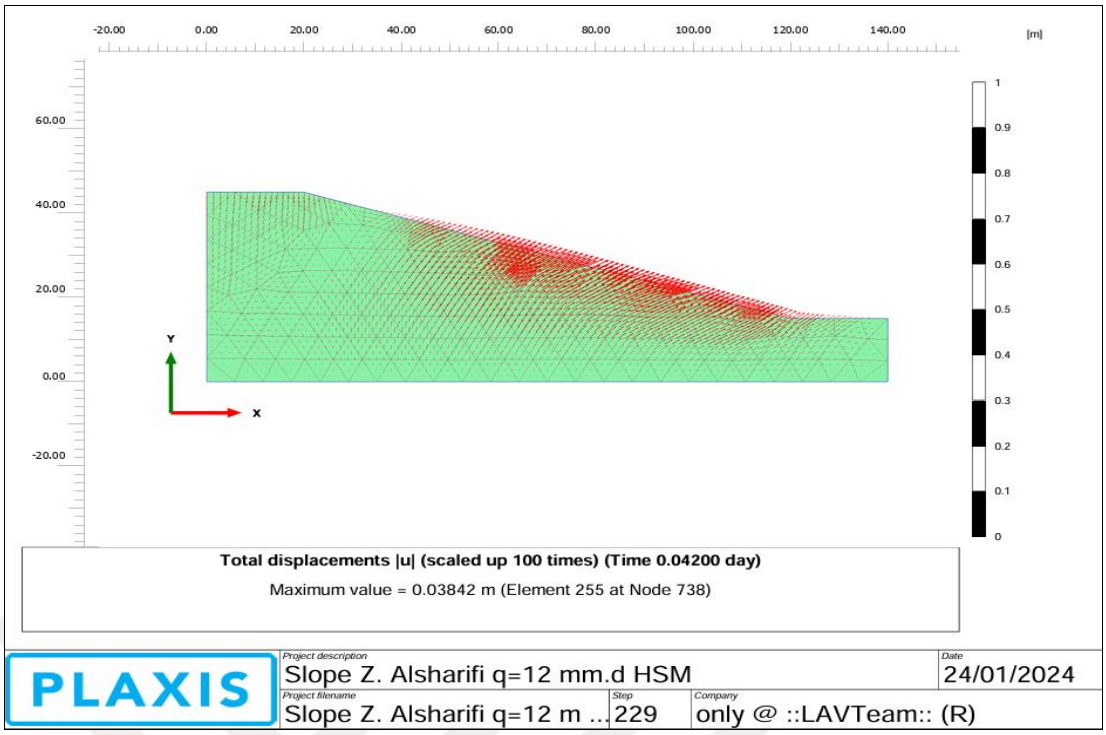

Figure A.1: (Cont.) PLAXIS 2D 2020 Program Outputs

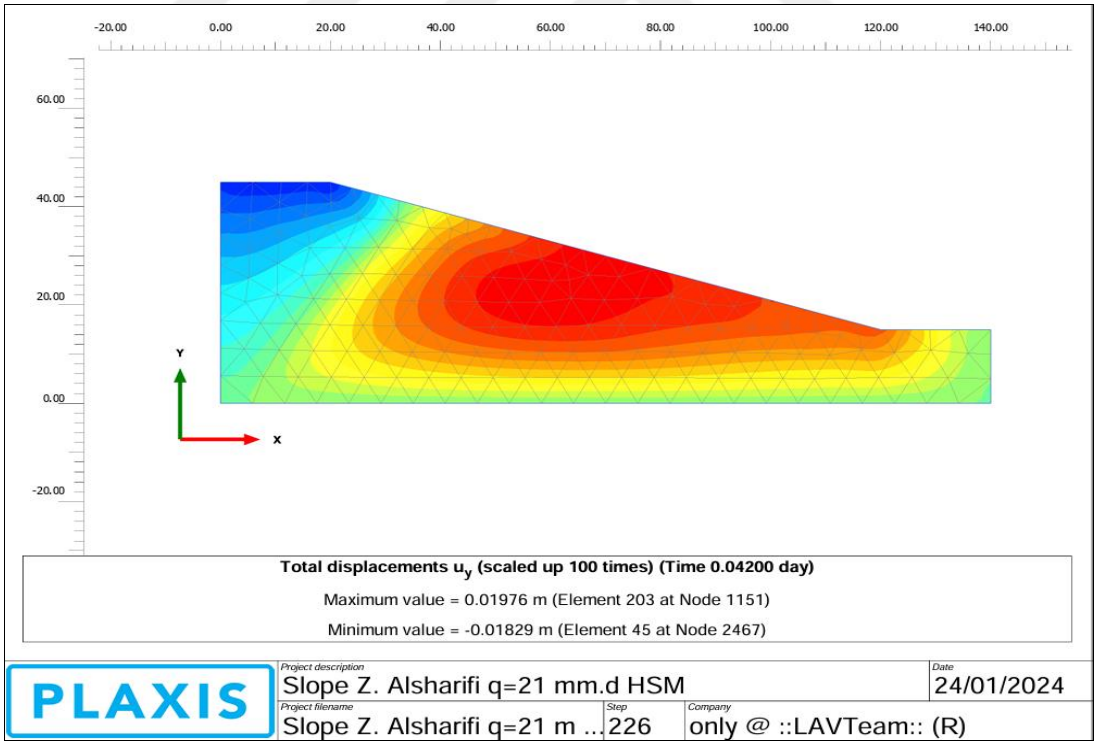

Figure A.1: (Cont.) PLAXIS 2D 2020 Program Outputs

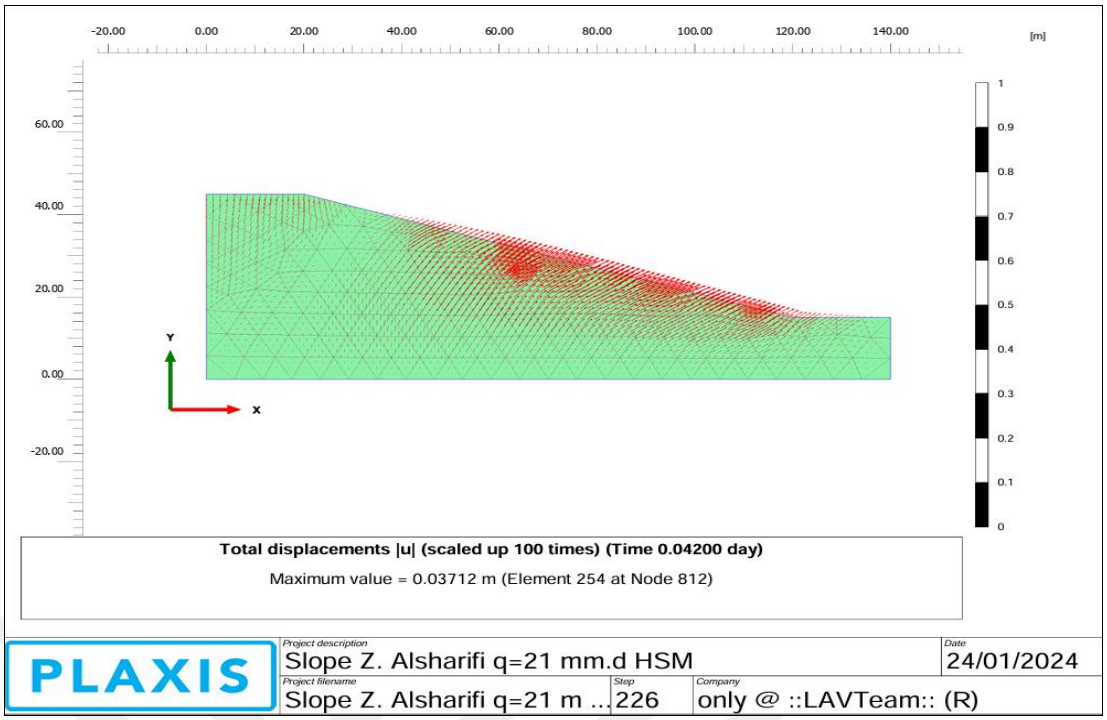

Figure A.1: (Cont.) PLAXIS 2D 2020 Program Outputs

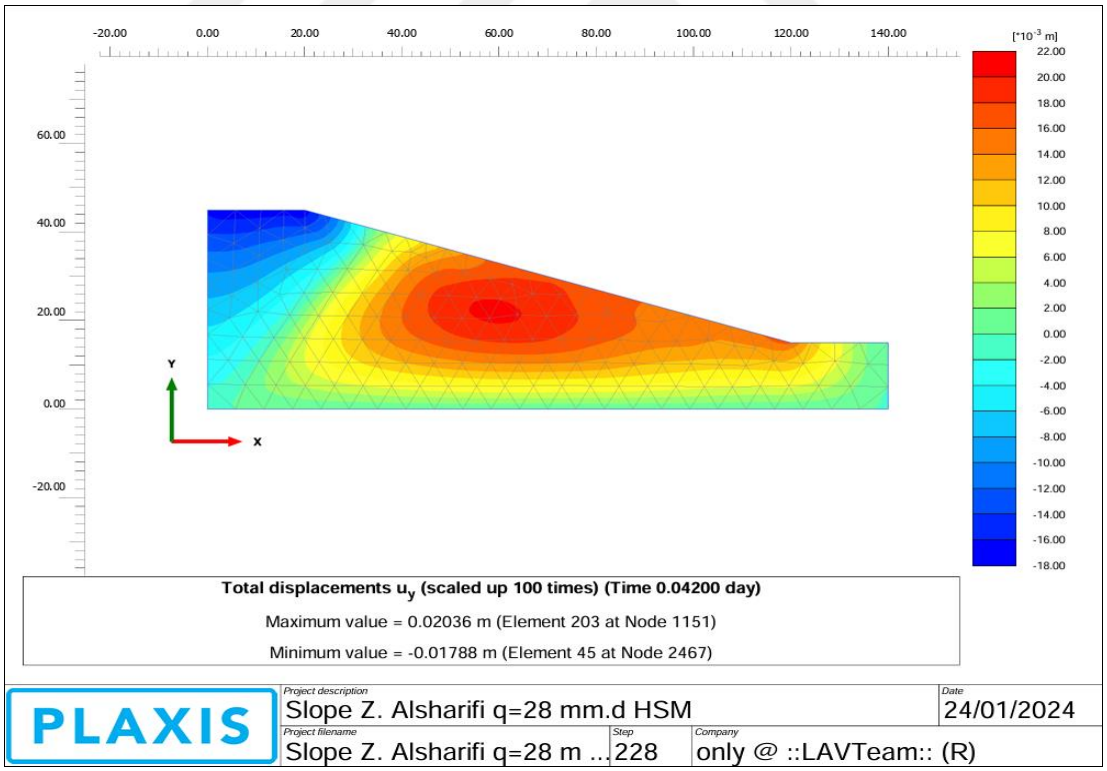

Figure A.1: (Cont.) PLAXIS 2D 2020 Program Outputs

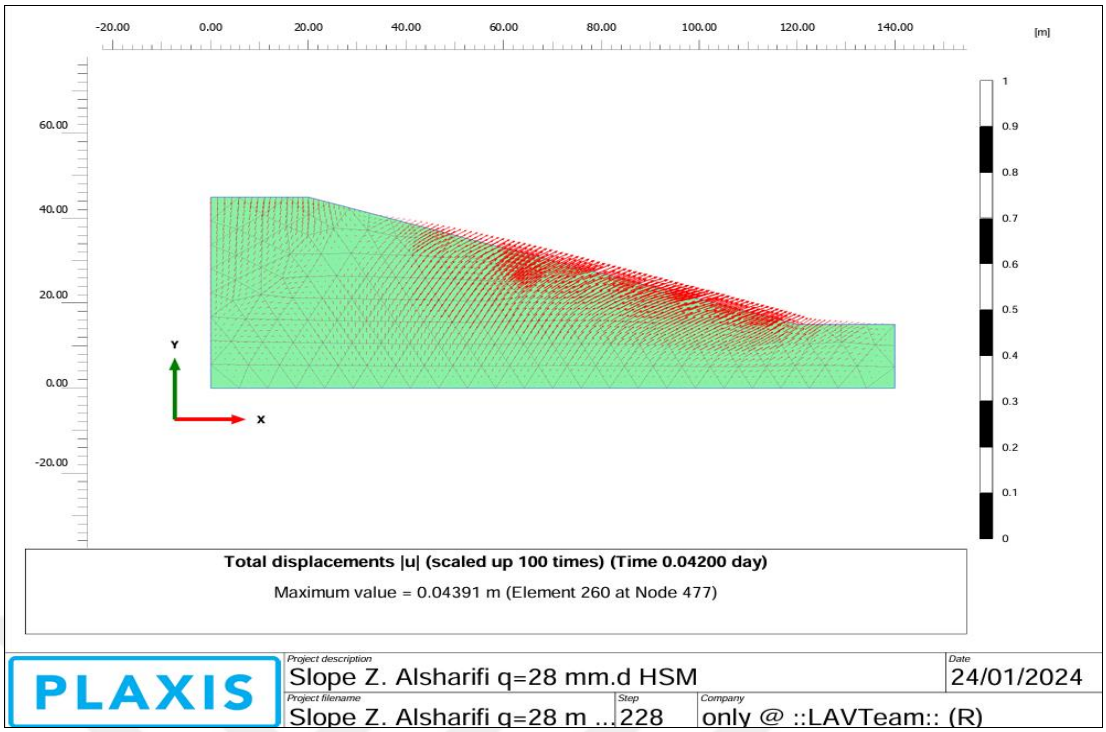

Figure A.1: (Cont.) PLAXIS 2D 2020 Program Outputs

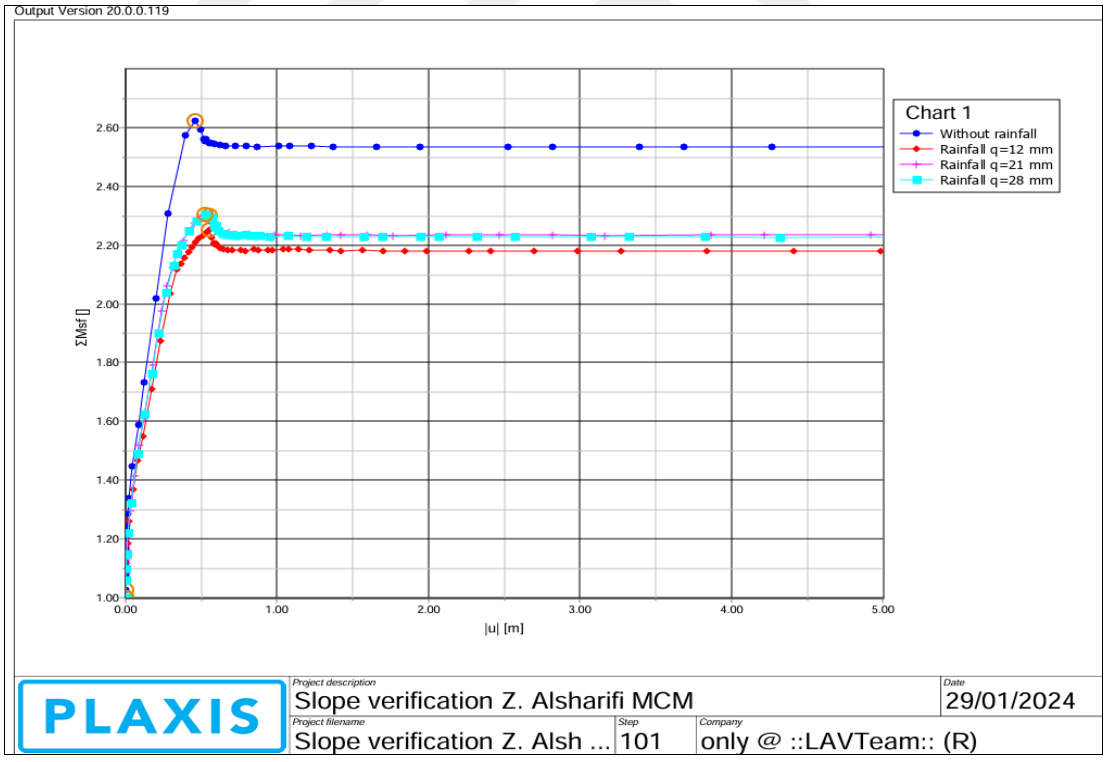

Figure A.1: (Cont.) PLAXIS 2D 2020 Program Outputs

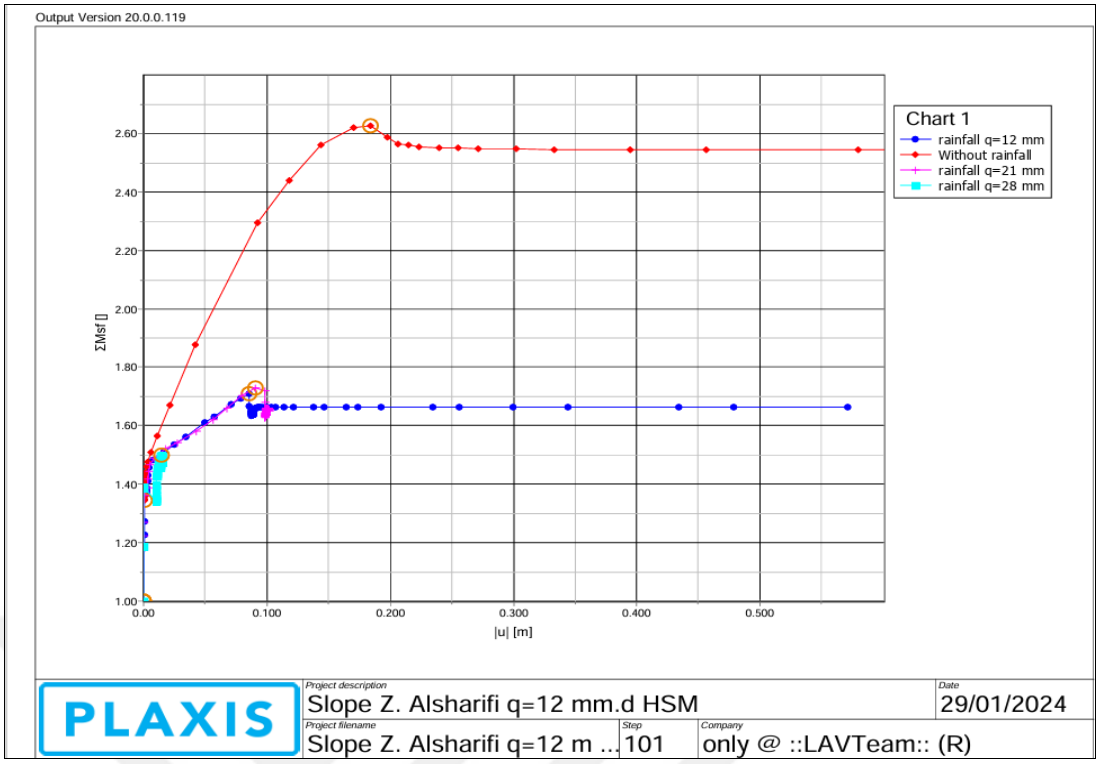

Figure A.1: (Cont.) PLAXIS 2D 2020 Program Outputs

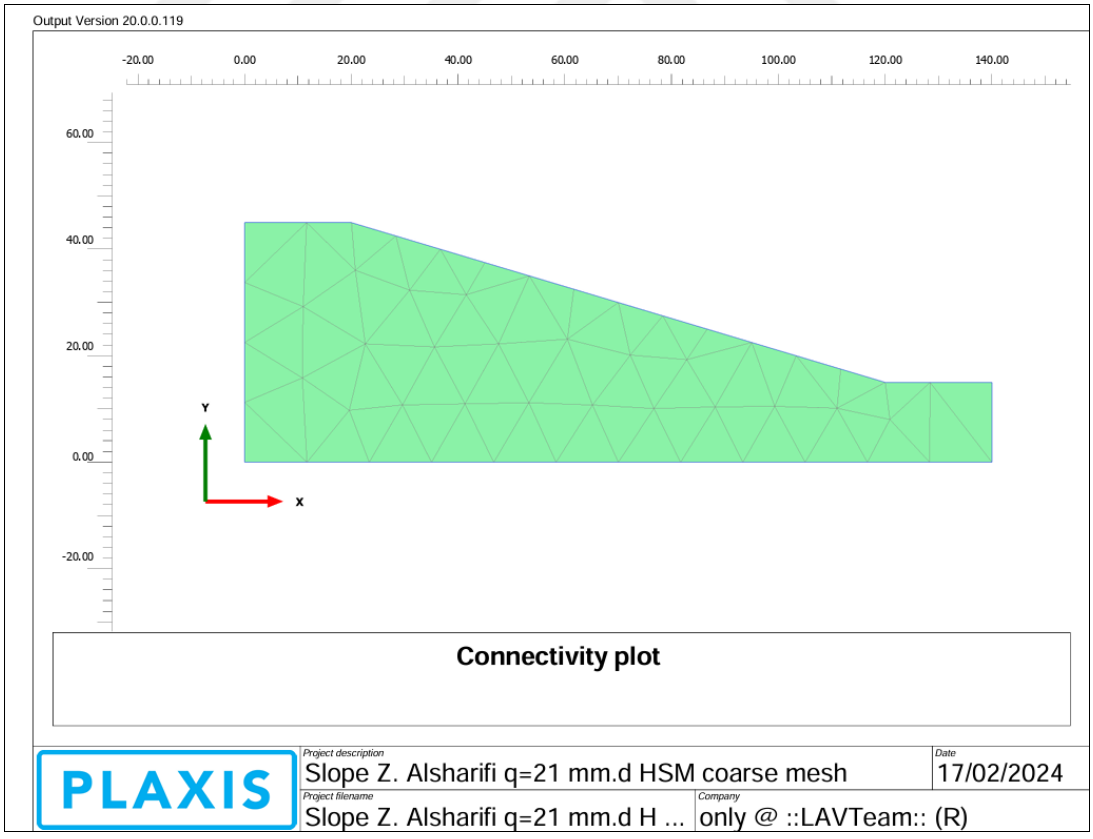

Figure A.1: (Cont.) PLAXIS 2D 2020 Program Outputs

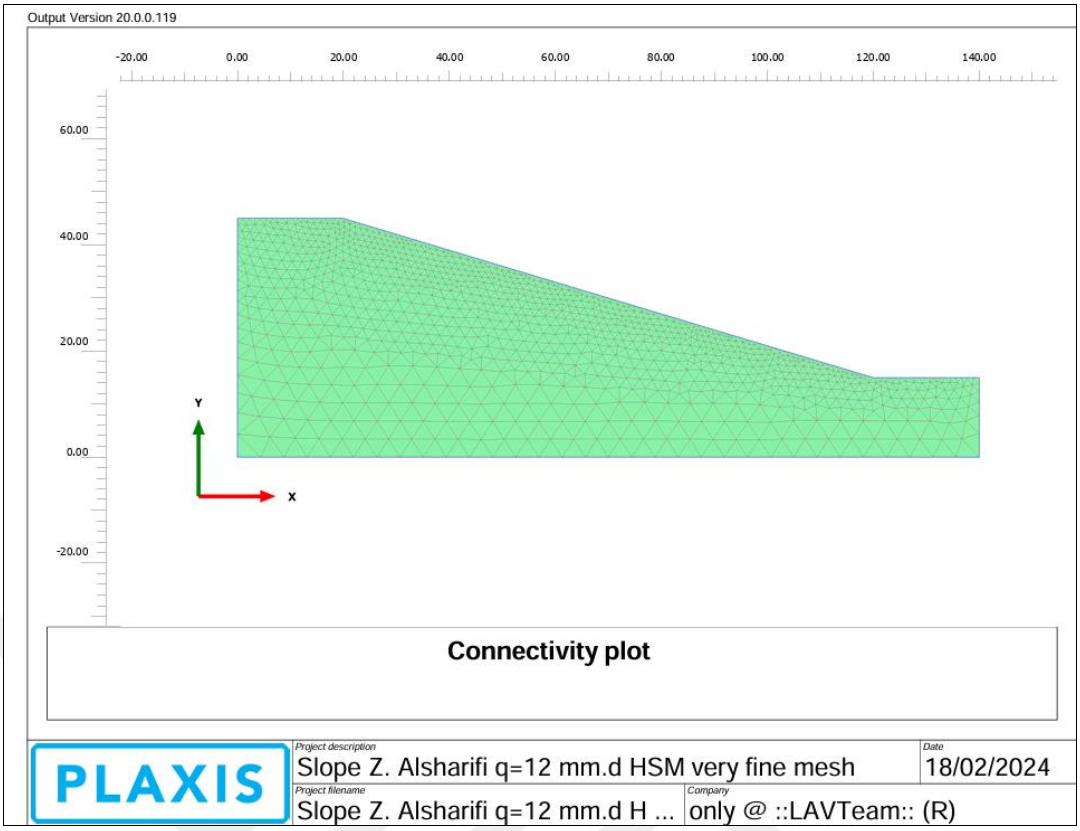

Figure A.1: (Cont.) PLAXIS 2D 2020 Program Outputs

RESUME

Sarah Galib Faraj AL-ISAWI

EDUCATION:

- High School: 2004 graduated from AL- Khansaa High School
- Bachelor: 2008 graduated from Baghdad University, Faculty of Engineering, Civil Engineering Department.

PROFESSIONAL EXPERIENCE AND REWARDS:

- Supervision on project (Fallujah university project site) (2009-2013).
- supervision on project (Ibn – Sina hospital) (2014-2017).